Université de Montréal

Uncovering parallel ribosome biogenesis pathways during pre-60S subunit maturation

Par
Lisbeth Carolina Aguilar

Département de biochimie et médecine moléculaire
Faculté de Médecine

Mémoire présenté à la Faculté des études supérieures
en vue de l'obtention du grade de maître ès Sciences
en biochimie
option génétique moléculaire

Janvier 2014

Abstract

Paralogs are present during ribosome biogenesis as well as in mature ribosomes in form of ribosomal proteins, and are commonly believed to play redundant functions within the cell. Two previously identified paralogs are the protein pair Ssf1 and Ssf2 (94% homologous). Ssf2 is believed to replace Ssf1 in case of its absence from cells, and depletion of both proteins leads to severely impaired cell growth. Results reveal that, under normal conditions, the Ssf paralogs associate with similar sets of proteins but with varying stabilities. Moreover, disruption of their pre-rRNP particles using high stringency buffers revealed that at least three proteins, possibly Dbp9, Drs1 and Nog1, are strongly associated with each Ssf protein under these conditions, and most likely represent a distinct subcomplex. In this study, depletion phenotypes obtained upon altering Nop7, Ssf1 and/or Ssf2 protein levels revealed that the Ssf paralogs cannot fully compensate for the depletion of one another because they are both, independently, required along parallel pathways that are dependent on the levels of availability of specific ribosome biogenesis proteins. Finally, this work provides evidence that, in yeast, Nop7 is genetically linked with both Ssf proteins.

Keywords: Ribosome biogenesis, parallel pathways, paralogs, Ssf, Ssf2, subcomplex, Nop7, genetic interactions

Résumé

Les paralogues sont présents lors de la biogenèse des ribosomes ainsi que dans les ribosomes matures sous forme de protéines ribosomiques, et sont généralement censées jouer des fonctions redondantes dans la cellule. Deux paralogues précédemment identifiées sont la paire de protéines Ssf1 et Ssf2 (94 % d'homologie). Ssf2 remplacerait Ssf1 en cas d'absence du dernier dans la cellule, et l'absence des deux protéines diminue la croissance cellulaire. Nos résultats révèlent que, dans des conditions normales, les paralogues Ssf s'associent à des ensembles de protéines similaires, mais avec différentes stabilités. De plus, la perturbation de leurs particules pré-rRNP à l'aide de tampons de haute stringence a révélé qu'au moins trois protéines, probablement Dbp9, Drs1 et Nog1, sont fortement associées à chaque protéine Ssf dans ces conditions, et très probablement représentent des sous-complexes distincts. Dans cette étude, les phénotypes cellulaires observés lors de la déplétion des protéines Nop7, Ssf1 et/ou Ssf2 ont révélé que les paralogues Ssf ne peuvent pas compenser entièrement pour la diminution de l'autre, car ils sont, indépendamment l'un de l'autre, nécessaires le long de voies de biogénèse ribosomale parallèles qui dépendent des niveaux de protéines impliqués dans la biogénèse des ribosomes disponibles. Enfin, ce travail fournit des preuves que, dans la levure, Nop7 est génétiquement lié aux deux protéines Ssf.

Mots-clés: Biogénèse ribosomale, voies parallèles, paralogues, Ssf, Ssf2, sous-complexe, Nop7, interactions génétiques

Table of content

List of tables

List of figures

List of abbreviations

DNA: desoxyribonucleic acid

UTR: untranslated region

mRNA: messenger ribonucleic acid

rRNA: ribosomal ribonucleic acid

snoRNA: small nucleolar ribonucleic acid

SSF2Δhph: SSF2 depleted mutant with hygromycin B resistance

Kb: kilobases

bp: base pair

V_{MAX}: maximum speed

EtOH: ethanol

Res: resistance

IPTG: isopropylthio-β-galactoside

kDa: kilodalton

ORF*:* open reading frame

MS: mass spectrometry

w/v: weight to volume ratio

SDS-PAGE: sodium dodecyl sulfate polyacrylamide gel electrophoresis

PVDF: polyvinylidene difluoride

NC: nitrocellulose

rpm: rotation per minute

Pol I: RNA polymerase I

SGD: saccharomyces genome database

LB: luria broth

SOC: super optimal broth with catabolic repression

Amp: ampicillin

Kan: kanamycin

CAM: chloramphenicol

YPD: yeast peptone dextrose

SC-Met-His: synthetic complete media without methionine and histidine

GRS-Met: synthetic complete media with galactose, raffinose, sucrose and without methionine

G418: geneticin

ClonNAT: noursethricine

RES: restriction enzyme site

ORF: open reading frame

μ: micro

α: anti

UTR: untranslated region

PrA: ProteinA

HA: human influenza hemagglutinin

His5: histidine gene

KanMX4: kanamycin resistance gene

KanMX6: kanamycin resistance gene optimized for yeast

Ph/Cl/IAA: phenol/chloroform/isoamyl alcohol

RiBi: ribosome biogenesis

LSU: large subunit

SSU: small subunit

μL: microliter

pmol: picomol

mg: milligram

qRT-PCR: quantitative reverse-transcriptase polymerase chain reaction

To my parents

Acknowledgements

I would like to thank Marlene Oeffinger for allowing me to be her first master student. It has been an honour and quite a life changing experience. Also, thank you for the yoga.

I would like to thank also the members of the lab. Katherine Cléroux, thank you for sharing lunch times and unforgettable 24-hour long experiments. Thank you to Pierre Zindy and Christian Trahan, the two post-docs of the lab. Your help saved me many times during troubleshooting and also many thanks for sharing your knowledge in general. I would like to thank Karen Wei for being present and sharing funny anecdotes. Thank you Matthew for sharing media and other lab stuff without asking too many questions. Thank you to Jordi (Ros Rodriguez) for the many Spanish conversations.

Thank you to Jacques Archambault and his students, especially Jennifer Orellana and Michael Lehoux, who were also of big help. Thank you to François Robert and Celia Jeronimo, for kindly sharing their lab utilities and equipment. A special thank you to Anne Helness, Pierre and the members of the technological platform (Odile Neyret, Agnès Dumont and Myriam Rondeau), who helped me set up the qRT-PCR experiments.

I would like to thank my family, husband and *belle-famille*: all of you have made many sacrifices and have contributed to my success. Thank you to my rottweilers, who were present throughout my university studies until very recently. I love you, I miss you. Finally, I would like to thank Gaby, my lil' sis', for the UdeS, the proof-reading and the rest. And last but not least, *thank you mama* for believing in my potential even when I didn't. We come from very far and this is thanks to you and dad. This is part of your vision.

1 Introduction

1.1 Ribosome biogenesis

It is known that ribosomes are essential to every growing cell from Archaea to Animalia, including *homo sapiens*. As for the yeast *Saccharomyces.cerevisiae*, cells have to meet a minimal size requirement before they are able to divide and this is intimately linked to the number of ribosomes available in the cell [1, 2]. Ribosomes are large ribonucleoprotein (RNP) machines made of a large and a small subunit (LSU and SSU), 78 ribosomal proteins (Rps) and four rRNAs (ribosomal RNAs), the active component of the ribosome that is responsible for mRNA (messenger RNA) translation. Making a ribosome involves ~200 trans-acting factors that mediate ribosome biogenesis (RiBi), which entails pre-rRNA processing and modification as well as its hierarchical, complex assembly with Rps.

1.1.1 Pre-rRNA processing

A single cell's genome has about 120 rDNA polycistronic tandem repeats in chromosome XII, a highly transcribed region (Fig 1.1) [3]. Each resulting polycistronic transcript contains 18S, 5.8S and 25S pre-rRNA which are flanked by external transcribed spacers I and II (ETS) and separated by internal transcribed spacers I and II (ITS).

The earliest event is ETS2 processing by the endoribonuclease Rnt1, a protein which dimerizes and recognises tetraloop structures [4]. Cleavage of the primary transcript at site B_0 by Rnt1 gives rise to the 35S pre-rRNA.

1.1.1.1 35S to 32S processing: ETS1 and ITS1

The ETS1 region is highly structured and requires stem loops for correct A_0 and A_1 endonucleolytic cleavages to occur [4]. The 33S pre-rRNA is obtained through A_0 processing, which can be performed by many endonucleases, including Rnt1 and RNase MRP [4-6]. The released 5'ETS portion of the transcript is degraded by the exosome (3'→5' exonuclease, Rrp6) or by Rat1/Rai1 (5'→3' exonuclease Rat1) [4]. A_1 endonucleolytic cleavage can be performed by various endonucleases, including RNase MRP, yields 32S pre-rRNA and the exosome degrades the A_0-A_1 fragment [4, 6].

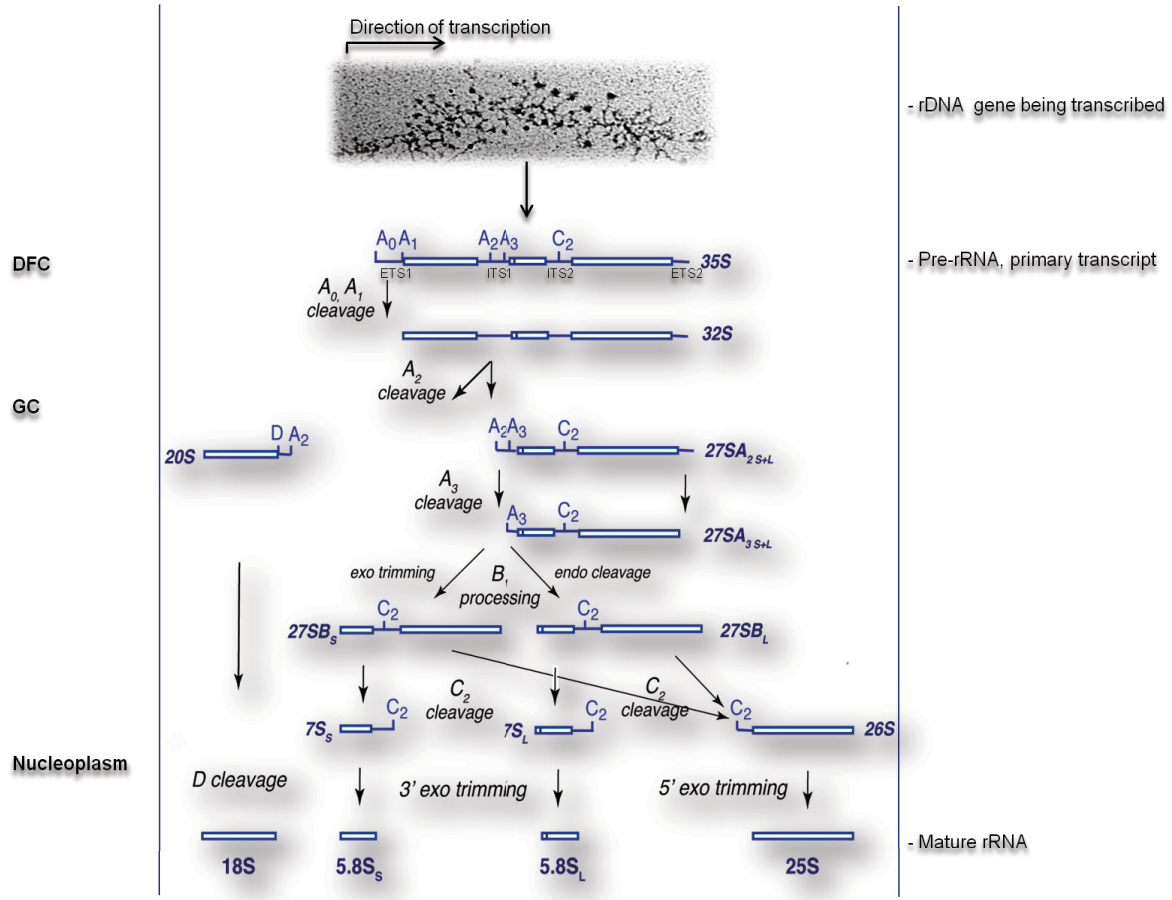

Figure 1.1 : The pre-rRNA processing pathway in yeast

In dividing cells, about half of the rDNA repeats are in an open chromatin state, ready for transcription. A single rDNA repeat is simultaneously transcribed by many RNA polymerase I, each resulting in a polycistronic primary transcript which is cotranscriptionnally processed by early RiBi factors. RiBi particles appear as decorations in an inverted Christmas tree, the base being rDNA associated with polymerases and the branches being the pre-rRNA transcripts. Each primary transcript contains 18S, 5.8S and 25S pre-rRNA flanked by transcribed spacers (External: ETS1, ETS2 and Internal: ITS1, ITS2) which are sequentially cleaved and processed. Detailed in section 1.1.1. Figure modified from (3, 7).

ITS1 processing occurs almost simultaneous to A_1 processing; A_2 endonucleolytic cleavage can be performed by Rcl1, RNase MRP or Rnt1 [4, 6, 8]. Interestingly, a delay A_0 and A_1 processing is not deleterious to the cell [4]. U3 snoRNA, is a special class of box C/D snoRNP believed to stabilise pre-rRNA and facilitate A_0, A_1 and A_2 processing by its RNA basepairing to the 5'ETS of 35S pre-rRNA (just upstream of cleavage site A_0), at least two regions within ITS1 and the 5' coding region of 18S [9].

1.1.1.2 Processing of 20S pre-rRNA in the cytoplasm

A predominant cleavage at site A_2 separates 20S from $27SA_2$ pre-rRNA processing, and thus maturation of 40S from that of 60S pre-ribosomal subunits. In a minor pathway, however, cleavage at site A_3 occurs prior to those at sites A_0, A_1 and A_2, which generates 23S pre-rRNA. This precursor is then sequentially processed at A_0 (A_0-A_3=22S), A_1 (A_1-A_3=21S) and A_2 (A_1-A_2=20S) by the usual processing factors [10]. In all cases, 20S pre-rRNA is already fully processed at its 5'. Its 3' will be partially trimmed (3'→5') by Xrn1 before the final maturation event through endoribonuclease cleavage by Nob1at site D in the cytoplasm [8].

1.1.1.3 27S precursor maturation: ITS1/ETS2 processing

At the stage of 27SA precursors, the 3'-end of ITS1 pairs with the 5'-end of 5.8S rRNA [11, 12]. Concomitantly, ETS2 is completely removed by B_0-B_2 processing through the action of a yet unidentified protein, generating the mature 3'-end of the 25S [4].

A_3-cleavage within ITS1 is performed endonucleolytically by RNase MRP, prior to exonucleolytic digest of the resulting A_2-A_3 fragment, as well as processing of $27SA_3$ pre-rRNA from site A_3 by the 5'→3' exonucleases Xrn1, Rat1 or Rrp17. This will generate the mature 5' end of $5.8S_S$ ($27SB_S$ pre-rRNA) [7, 13]. $27SB_L$ pre-rRNA is presumably obtained through an endonucleolytic cleavage after cleavage at A_3, however, the enzyme responsible for this event is still unknown [12].

Both 27SB pre-rRNAs are subsequently processed within ITS2 by apparently identical pathways to generate the mature 25S rRNA and the mature 3' ends of either $5.8S_S$ or $5.8S_L$

rRNAs. $5.8S_S$-containing ribosomes are five times more abundant than $5.8S_L$-containing ribosomes.

1.1.1.4 Processing events within ITS2

After ITS1 removal, the pre-rRNA adopts another intermediate structure in which the 5' of 25S interacts with the 3' of the 5.8S rRNA and forms a stem loop structure that is critical for processing and which is conserved in the mature ribosome [14]. During its processing, ITS2 switches from an open 'ring' to a closed hairpin structure [14]. The closed hairpin structure can form spontaneously and its formation is prevented by RiBi factors [12].

Unlike ITS1, ITS2 sequences are not recognised by RiBi proteins of distantly related organisms [15]. However, the secondary structures adopted by the pre-rRNAs are similar and the important nucleotides required for correct processing are conserved [15]. It has been proposed that correct ITS2 processing requires RiBi factors recognising specific secondary structures, specific sequences, or both [14].

Cleavage at site C_2 by an unidentified endonuclease within ITS2 generates the 7S and 26S pre-rRNAs. Following C_2 cleavage, the 3' of 7S pre-rRNA is exonucleolytically processed, first by the exosome followed by fine trimming through Rrp6, Rex1 or Rex2 to first generate a stable precursor, the 6S, and then finally the mature 5.8S rRNA.

The 5' processing of 26S pre-rRNA is performed by Xrn1, Rat1 or Rrp17 and generates first 25S' (C_2 to $C_{1'}$ processing), and then, after further fine trimming, mature 25S rRNA.

1.1.2 Assembly with ribosomal proteins

As pre-rRNA is processed in the compartments of the nucleolus, some RiBi factors will mediate its assembly with ribosomal proteins of the large subunit (Rpl). This is the case with the ribosomal-like proteins (Rlp), which interact with RiBi factors and are believe to mimic the structure of Rpls, inducing proper folding and conformational changes of the pre-rRNA structure prior to the entry of the corresponding Rpl protein [16]. For instance, Rlp7 has been reported to bind to two regions. It binds to the ITS2, very close to the 5.8S coding region

and also to the 5' of the 25S coding region, a region forming the proximal stem loop where Rpl7 is found in the mature ribosome [16]. Therefore, some RiBi proteins are required to correctly fold pre-rRNA so that accommodation of the Rpl protein is possible, while other RiBi factors are required to recruit the Rpl proteins into the pre-rRNP particle. In the case of Rpl5 and Rpl11, they are recruited along with 5S rRNA as a module through interactions with LSU RiBi factors Rpf2 and Rrs1 [17]. The import of ribosomal proteins into the nucleus is predominantly mediated by Kap123, an importin [18].

1.1.3 The RiBi pathway

Most RiBi proteins have been identified and are highly conserved in higher eukaryotes. They can be classified according to their function or to their entrance into the maturing pre-RNP particle (early, intermediate or late factors). However, even if most of their roles can be predicted, their exact function(s), substrates and physical interactions within the dynamic pre-rRNP particles remain elusive.

In the dense fibrillar compartment (DFC) of the nucleolus, ribosome biogenesis is dependent on chromatin remodelling and RNA polymerase (pol) I regulation [19-23]. Co-transcriptionally, snoRNPs will modify pre-rRNA (2'-O-ribose methylation and pseudourydilation) and early RiBi factors will be recruited onto the nascent transcript to form the pre-90S particle [3, 24, 25]. As the particle transitions towards the granular compartment (GC) of the nucleolus, the primary transcript is separated in two by the A_2 cleavage and distinct RiBi factors bind pre-rRNA, forming pre-60S and pre-40S particles. Within pre-60S maturation, several LSU RiBi proteins are required to ensure ribosome biogenesis, including Nop7 and the paralog pair Ssf1 and Ssf2 (Fig. 1.2).

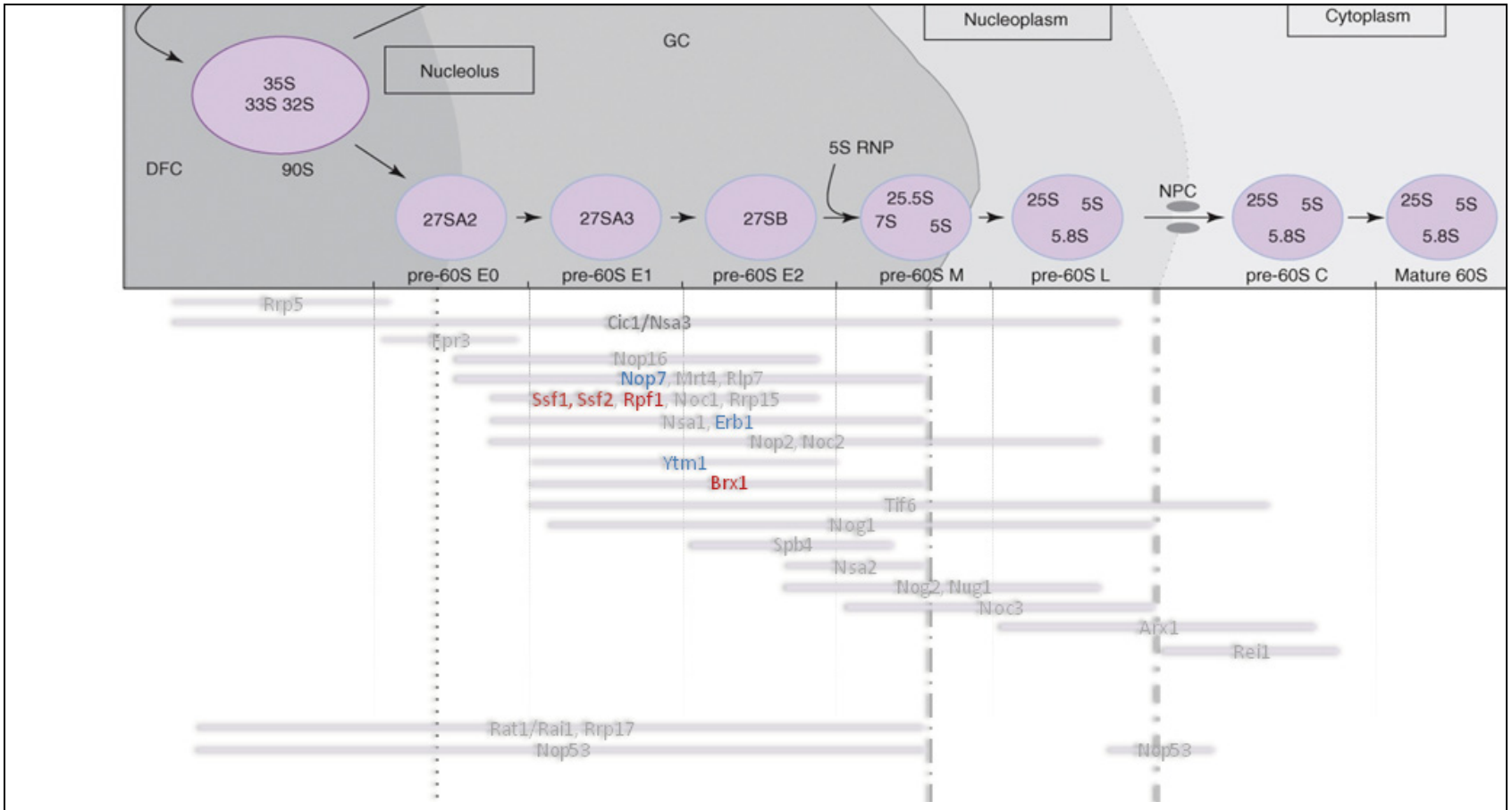

Figure 1.2: RiBi pathway of the LSU

Ribosome biogenesis involves 200 non-ribosomal proteins (RiBi) that modify, cleave, fold and correctly associates pre-rRNA with the ribosomal proteins (Rps). As the LSU matures, it moves from the dense fibrillar compartment (DFC) and granular compartment (GC) of the nucleolus to the nucleoplasm and its maturation is completed once it is in the cytoplasm. Here, the estimated time of entry and of exit of some RiBi proteins involved in the LSU maturation are shown. In red: some of the Brix/Imp superfamily members. In blue: trimeric complex Nop7, Erb1 and Ytm1. Information and figure adapted from (2, 7).

1.2 Parallel pathways during pre-60S maturation and specialized ribosomes

In the field, most of the RiBi proteins involved in ribosome biogenesis are now characterised. Although the presence of multiple parallel pathways during yeast ribosome biogenesis has been highly debated, it is now an accepted concept and several groups are now working to uncover them [2]. The presence of parallel/alternative pathways ensuring ribosome biogenesis is further supported by the presence of different pools of mature ribosomes within the cell under normal conditions and the emergence of specialized ribosomes under specific cellular stress (26-29). In any case, substantial work still need to be performed in order to define the players involved in these parallel pathways, which is aided by the significant advances in proteomics.

1.2.1 Hierarchies of processing factors

1.2.1.1 Loss of essential RiBi factors does not result in cell death

Although most RiBi factors are said to be essential, their depletion results in impaired or slowed cell growth, rather than cell death, while mature ribosomes are still produced. This emphasizes the presence of alternative maturation within the cell as an adaptive response to maintain the essential translation machinery and thus secure cell survival. Some work has been performed to elucidate some of these pathways during pre-90S maturation in which it has been shown that ribosome biogenesis first requires the t-UTP complex (Utp4, Utp5, Utp8, Utp9, Utp10, Utp15 and Nan1) and can then continue via at least three alternative pathways involving i) the RiBi protein Rrp5 and then the UTP-C complex (Utp22, Rrp7 and Cka1); ii) the U3-snoRNP complex; iii) the UTP-B complex (Pwp2, Dlp2, Utp21, Utp13, Utp18 and Utp6) [25, 30, 31]. The association of either the U3-snoRNP or the UTP-B complexes allows the incorporation of Bms1, a GTPase required for U3 snoRNA pairing with the pre-90S that is found associated to a lesser extent with Rcl1 [25, 30]. Since U3 sno-RNAcan be involved in A_0, A_1 and A_2 processing, this data suggests that in one pathway, Bms1 stabilizes the U3-snoRNP complex which is responsible for A_0, A_1 and A_2 processing [9]. In the pathway in which UTP-B enters the pre-90S particle, Bms1 possibly enters as a heterodimer with Rcl1, which

performs the A_2 cleavage while other endonucleases perform A_0 and A_1 cleavages. Following Bms1 binding, two alternative pathways ensure ribosome biogenesis. In one case, Kre33 enters the particle and in the other, Utp20 binding will allow the association of either the Mpp10 complex (Mpp10 and Imp4) or the protein Enp2 [25].

However, several components of the pre-90S have still not been associated with this pathway, and imply that other alternative pathways exist but remain to be elucidated.

Moreover, it has been shown that some proteins can enter as preformed modules (e.g. Rcl1/Bms1) or alone (e.g. Bms1), depending on the cellular context, which further adds to the complexity of elucidating these pathways. There is also some evidence of parallel pathways during pre-60S maturation, where the Nop7 and Nug1 associated particles share nearly identical pre-rRNA content, indicating that they are involved in the same pre-rRNA processing events, and yet they have only a 25% overlap in RiBi protein content [32].

1.2.1.2 RiBi protein paralogs

In the past, protein paralogs were believed to have redundant functions. This, however, is not the case for at least some of the ribosomal proteins (Section 1.2.2.2). Some RiBi factors were also shown to have paralogs, as in the case of the Ssf1/Ssf2 and Fpr3/Fpr4 paralogs. Their potential role in the context of alternative pathways has never been investigated.

Structural studies of the pre-rRNP particles are now elucidating part of the structural rearrangements required for its remodelling and those mainly involve stearic hindrance constraints. This could explain why a protein can enter the pre-rRNP particle alone (e.g. Bms1) or in a subcomplex (e.g. Bms1/Rcl1), depending on the previous RiBi proteins that associated with the pre-90S particle around its binding site [25, 30]. As paralogs have subtle amino acid changes and are compacted in the pre-rRNPs, in close contact with other RiBi proteins, it is valid to ask whether these changes are sufficient to trigger alternative pathways. Unlike what was previously assumed, an extensive comparison of the Ssf1 and Ssf2 interactors suggest that these paralogs have in fact non-redundant functions within the cell, a feature that has never been explored in the context of ribosome biogenesis (Section 1.3.2).

1.2.2 Specialized ribosomes

1.2.2.1 Two types of ribosomes containing $5.8S_S$ or $5.8S_L$ rRNA

Most evidently, there exist two types of ribosomes, containing either $5.8S_S$ (80%) or $5.8S_L$ (20%) rRNA. Their divergence during ribosome maturation is clear because they generate two types of precursors from $27SA_3$ exonucleolytic or endonucleolytic processing, resulting in either $27SB_L$ or $27SB_S$. However, the trans-acting factors involved in generating the minor pathway ($27SB_L$) have not yet been reported and its cellular significance is still poorly understood. To this date, no clear assays have been performed to verify if these ribosomes have different affinities with different subsets of mRNAs or if they react differently when submitted to ribosomal stress as it has been shown for hypo-pseudourydilated ribosomes, which are more susceptible to frame shift errors and show decreased IRES-dependent translation rate upon specific cellular stress [4, 26, 29, 33].

1.2.2.2 Ribosomal proteins: paralogs with different functions

Of the 78 ribosomal proteins, 59 have a paralog (A or B) [4]. Two ribosomal pools, each containing one of the two paralogs, can be spatially separated within the cytoplasm suggesting that the ribosomes containing ribosomal protein paralogs could have distinct functions within the cell [28]. Furthermore, to this day, it is unclear how assembly of these ribosomal protein paralogs onto the maturing ribosome occurs and whether it is achieved through parallel RiBi pathways.

One specific function was demonstrated for three ribosomal proteins of the large subunit (Rpl7A, Rpl12B, and Rpl22A) and one of the small subunit (Rps18B). These ribosomal proteins were shown to have a role in the correct localisation and translation of ASH1 mRNA, while their paralogs do not [28]. Interestingly, upon depletion of the LSU RiBi factors Loc1 or Puf6, the ribosomes carrying these particular ribosomal proteins are still generated yet mislocalized within the cytoplasm altering ASH1 mRNA transport and translation [28].

1.2.2.3 Ribosomal proteins and ribosome types

More and more evidence pointing towards specialized ribosomes, that are also different in composition, are emerging. It has been reported recently that a retroviral and oncogenic protein, *V-erbA*, can alter ribosome biogenesis such that a second pool of ribosomes, which does not contain the ribosomal protein Rpl11, is generated [27]. It has been suggested that these Rpl11-depleted ribosomes can have a higher translational affinity with certain types of mRNA [27]. Given the fact that Rpl11 plays an important role in the activation of both tumor suppressors c-myc and p53, this mechanism by *V-erbA* appears to be an appropriate adaptive response to inhibit the cellular response upon infection. Another such examples is found in *E. coli*, where in order to survive the presence of the antibiotic kasugamycin, the bacteria generates functional ribosomes lacking at least six ribosomal proteins, two of which are essential [34]. Because this antibiotic mimics mRNA structure between the P and E sites of the ribosome, loss of these ribosomal proteins most likely changes the ribosomal structure at this region such that the antibiotic is no longer able to block the ribosome during translation.

1.3 Specific RiBi proteins

1.3.1 Nucleolar protein 7 (Nop7)

Pes1 was originally discovered as *pescadillo* in zebrafish, where it was shown to be important for eye development [35]. Moreover, its mouse homolog Pes1 was shown to interact with the p53 suppressor Mdm2 in mouse astrocytes [35]. In yeast, the NOP7 (*Nucleolar Protein 7*) gene is located in chromosome VII and its cellular protein abundance is ~ 4530 molecules per cell according to SGD [30]. Nop7 (also called Yeast pescadillo homolog 1) links ribosome biogenesis to cell cycle progression and DNA repair [1, 36]. The protein has two coil-coil regions one of which is in its C-terminal and contains a nuclear localisation signal (NLS, Fig. 1.3).

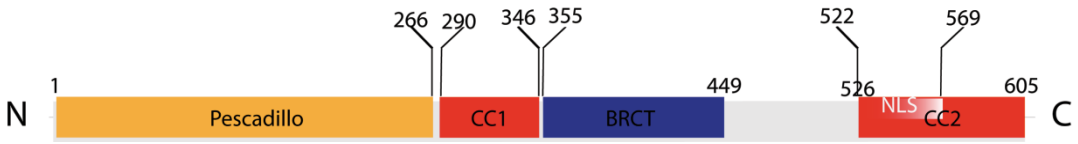

Figure 1.3: Nop7 protein and its domains

Nop7 is composed of four main domains: *pescadillo,* a conserved region required for ribosome biogenesis; BRCT, a domain required for cell cycle and DNA damage responses; CC1 and CC2, two coil-coil regions, CC2 containing a nuclear localisation signal (NLS) which can be cleaved. For further details refer to main text. Image constructed according to information from (1).

The C-terminal region needs to be truncated for some cellular functions since a shorter form of Nop7 was detected using an antibody against the N-terminus of the protein [(1)]. This C-terminus-truncated form of Nop7 is cytoplasmic and co-sediments with polysomes [(1)]. However, details on how this modification is triggered and why it is needed remain elusive to this date and do not seem to be linked to its function during ribosome biogenesis [(1)].

In the following sections, only functions of full-length Nop7 will be discussed, as the affinity purifications isolated the interactors of C-terminally tagged Nop7 cells in log (Nop7-PrA, Fig. 1.4A) and lag phase (Nop7-TAP, Fig. 1.4B) [(37, 38)]. The lag phase interactors were identified in a high-throughput study and are therefore more likely to contain false positives. However, Nop7 particles during log phase also contain proteins involved in similar processes, and at least its interaction with ORC complexes has been confirmed in complementary immunoprecipitations assays (IPs, e.g. ORC2) [(1)]. It is therefore possible that Nop7 has other functions in processes other than ribosome biogenesis, ensuring fine-tuning between these processes.

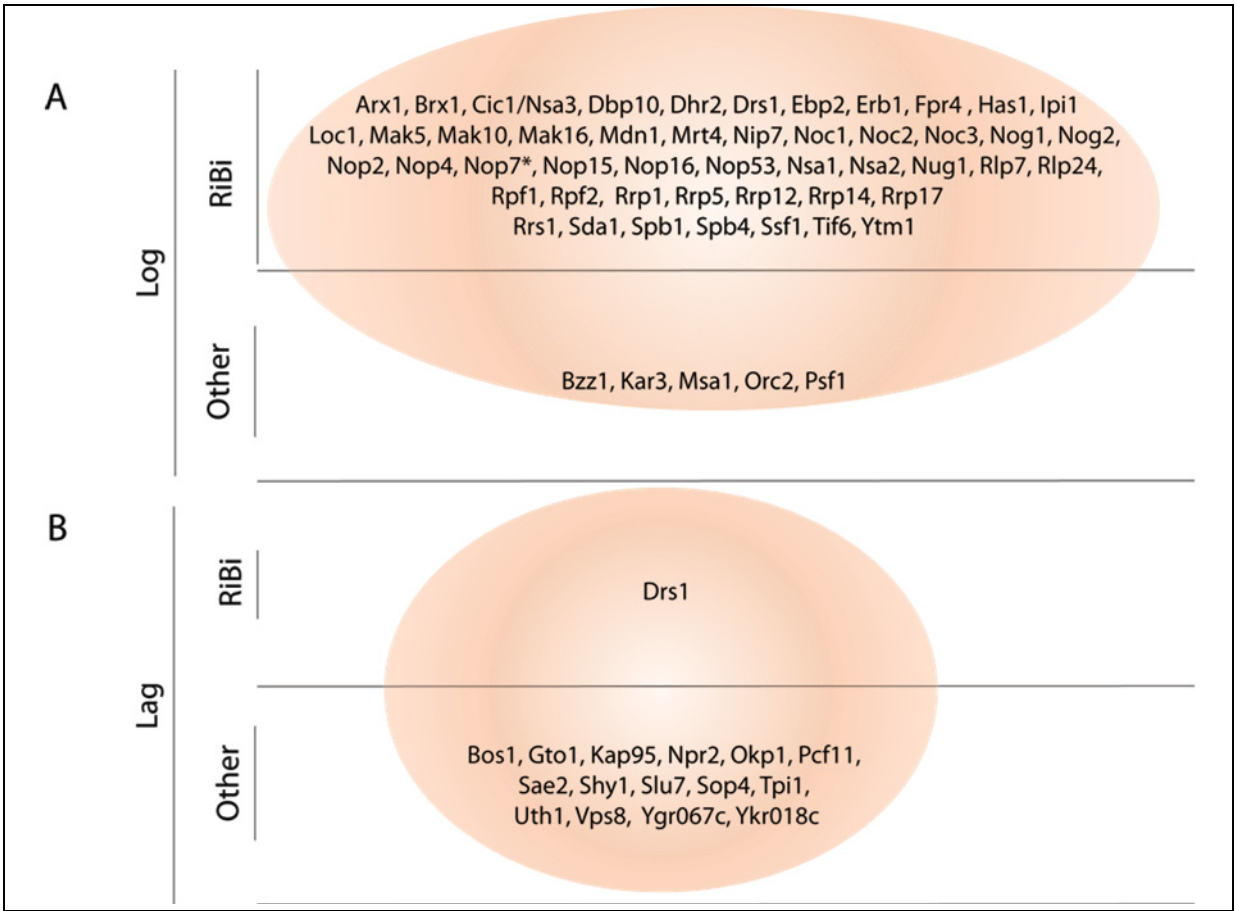

Figure 1.4: Nop7 interactors during log and lag phase

(**A**) During log phase, Nop7-PrA is mostly associated with pre-60S RiBi proteins but is also associated with five proteins involved in other cellular processes. According to information from (37). (**B**) During lag phase, when ribosome biogenesis is shut down, Nop7-TAP is mostly associated with proteins which are involved in other cellular functions but is still associated with one RiBi protein. According to information from (38).

1.3.1.1 Nop7 and ribosome biogenesis

Through its evolutionary conserved *pescadillo* domain, nucleolar Nop7 enters early during ribosome biogenesis and is found in pre-90S and early pre-60S particles. During this stage it is most likely a scaffold protein as it is present in at least three distinct RNP particles during pre-60S maturation (Fig. 1.5) [36]. It binds the C-terminal tail of Erb1 and forms a highly stable trimeric complex with Ytm1 [39]. This trimeric complex is required for correct processing of $27SA_3$ pre-rRNA to 27SB through exonucleolytic trimming (step * of figure 1.5) [1, 39]. Nop7 can also bind directly to pre-rRNA, possibly through its BRCT domain [12].

Its interaction with RNA was determined using a crosslinking technique and was pinpointed to helix H54 within the 5'coding region of 25S rRNA [12]. Nop7 appears to travel with the pre-60S subunit from the nucleolus to nuclear rim, and has been proposed to have different functions, processing, assembly and lastly quality control of export-competent subunits, depending on its subnuclear localisation [36].

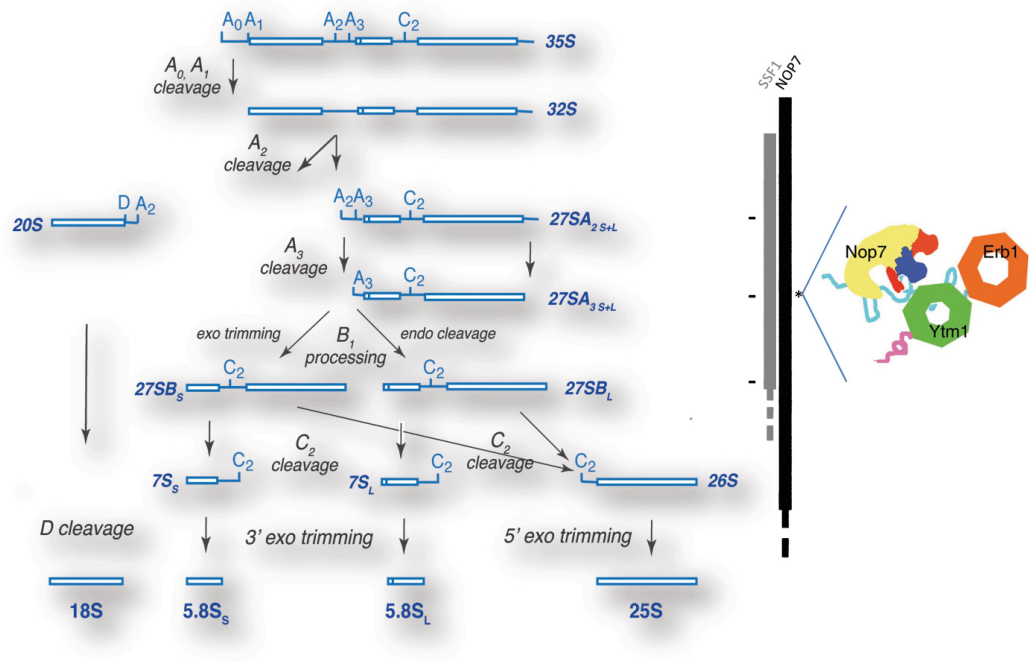

Figure 1.5: Ssf1 and Nop7 are involved in the LSU pathway
Ssf1 and Nop7 have been found in three distinct particles of the LSU maturation pathway containing either $27SA_2$, $27SA_3$ and $27SB_S$ pre-rRNA. Nop7 is known to form a trimeric complex necessary for exonucleolytic trimming of $27SA_3$. Adapted from (2, 7, 39).

1.3.1.2 Nop7 depletion phenotype

Upon depletion of Nop7, cell growth is severely delayed and is at least in part caused by delayed ribosome biogenesis, as the Dt roughly doubles and Nop7-depleted cells arrest longer in G2 [1, 36]. However, even if cell growth was affected, depletion of Nop7 did not lead to cell death, which suggests that alternative mechanisms are still present to ensure ribosomal production. The proteins involved in these pathways however have never been investigated. What is known, is that whole cell extracts of Nop7-depleted showed a general decrease in

Ytm1 and Erb1 protein levels, which was not the case for other RiBi proteins that were not directly interacting with Nop7 [39]. This suggests that formation of the trimeric complex is necessary for these proteins to be involved in ribosome biogenesis and that depletion of one of these proteins likely leads to a cellular down-regulation of the other two proteins by yet to be determined mechanisms. Interestingly, Nop7 also seems to have a synergistic interaction with Rpl25, however, in what capacity is still unclear. This assumption is due to the synthetic lethal phenotype observed upon Nop7 depletion in an Rpl25 *temperature-sensitive* strain in restrictive conditions (glucose-containing medium at 37°C) [36].

Upon Nop7 depletion, pre-rRNA processing is also affected, as previously demonstrated by Northern blot, primer extension and pulse-chase analysis [36]. Nop7 depletion profoundly affects LSU maturation: absence of Nop7 causes processing of $27SA_3$ pre-rRNA into $27SB_L$ through endonucleolytic cleavage and a switch to the minor pathway producing $5.8S_L$-containing ribosomes [36]. Moreover, after 24 hours of depletion, slight accumulation of primary transcript 35S was observed with a reduction in 27SB, 7S and 6S precursors [36]. Only mature 25S and $5.8S_S$ rRNA decreased and an aberrant precursor was observed (23S), which indicated a delay in A_0, A_1 and A_2 processing [36]. Interestingly, Nop7-containing particles contain Drs1 both during log and lag phase although they do not directly interact with each other according to a yeast-two hybrid assay and although Drs1-depleted cells are also deficient in 25S and 5.8S pre-rRNA maturation [38, 40]. This suggests that Nop7 and Drs1 are involved in similar pathways during ribosome biogenesis and are also associated with at least another common protein not involved in ribosome biogenesis during lag phase. Finally, an accumulation of aberrant pre-rRNA generated by premature C_2 cleavage was also observed in Nop7-depleted cells by primer extension analysis from a probe annealing within ITS2 [36, 40].

1.3.1.3 Nop7, cell cycle, DNA replication and DNA repair

Nop7 is a member of the BRCT domain-containing family of proteins, which play an important function in human cells in the development of breast and colorectal cancer [41-44]. This may explain some functions of PES1, the human Nop7 homolog, and its interactions with Mdm2 [36]. The BRCT domain is located in between the two coil-coil regions and is also common to proteins involved during cell cycle progression and DNA repair, such as BRCA1, RAD9, DPB11 and ECT2 (Fig. 1.3) [45].

During log phase, Nop7 particles affinity purify (AP) with Msa1, a protein required to initiate transcription of G1-specific genes [30]. A mechanism by which Nop7 is involved in regulating Msa1 activity is possible, as it has previously been shown that Nop7-depleted cells arrest longer in G1[1].

During log phase, Nop7 has a role in DNA replication through associations with ORC complexes and Psf1, a protein involved in DNA replication machinery assembly [1]. Consistent with Nop7 having a role in regulating DNA replication, very few Nop7-depleted cells arrest in S phase [1, 36]. It is possible that Nop7 remains associated with proteins involved in inhibiting DNA replication during lag phase as it is likely associated with an uncharacterized protein (Ykr018c) whose cellular levels are increased upon DNA replication stress [1, 30].

In addition, the tubulin content of Nop7 depleted cells decreases in S phase cells [1]. Consistent with Nop7 having a possible role in tubulin maintenance and remodelling, Nop7-associated complexes were found to contain proteins involved in microtubule maintenance during both log (e.g. Kar3) and lag phase (e.g. Okp1). Kar3 is a microtubule motor required for spindle pole body formation during mitosis and meiosis, and Okp1 is a protein of unknown function required during kinetochore-microtubule assembly [30]. Moreover, during log phase, it is known that Nop7 directly binds to Ytm1, a RiBi protein known to directly interact with tubulin and required to G1/S transition [46].

1.3.1.4 Nop7 and protein paralogs

Another interesting feature of Nop7, that is still unexplained, is that it interacts with proteins that have paralogs, both during log and lag phase. During log phase, Nop7-associated complexes contain Ssf1, Fpr4 (LSU RiBi factors, paralogs: Ssf2 and Fpr3 respectively) and Msa1 (cell cycle initiation, paralog: Msa2), during lag phase, Ykr018c (mitochondrial protein increased upon DNA replication stress, paralog: Iml2) and Uth1 (required for mitochondria biogenesis, paralogs: Nca3). Since Nop7 seems to be involved in several cellular processes together along ribosome biogenesis and the cell cycle (G1, S and G2), it is possible that it triggers slightly different cascades through interactions with both or just one of these

paralogs. Further investigation will be necessary to determine if Nop7-associated particles during lag phase really include Ykr018c and Uth1 or are false positives.

1.3.1.5 Nop7 orthologs in higher eukaryotes

As mentioned above, several Nop7 orthologs exist in higher eukaryotes, such as zebrafish, *Xenopus laevis, mouse and humans*. During embryogenesis, *Pes* mRNA has been found in several developing organs of different embryos. In mouse, the protein is found throughout developing brain structures; in *Xenopus laevis*, it is found in early eye structures, the neural crest, and pronephros development, while in zebrafish it is found in the eye, brain, and skeletal muscle structures [36, 47]. Pes1 was also found to be upregulated in p53-/- cells as well as in some breast cancer tumors [36, 47]. In higher eukaryotes, *pescadillo* protein can be sumoylated at two regions of its BRCT domain [1]. Similar to yeast, it forms a trimeric complex with WD12 and Bop1, the human homologs of yeast Ytm1 and Erb1, that is required for progression into S phase and LSU biogenesis [48]. Pes1 also has functions independent of ribosome biogenesis during *Xenopus laevis* pronephros development [47].

1.3.2 Suppressor of Ste4 paralogs 1 and 2 (Ssf1/2)

In the presence of pheromones, the two proteins Ssf1 and Ssf2 were found to suppress Ste4, allowing bud formation during the mating response [49, 50]. This is how the Ssf proteins were discovered and named although the mechanisms for this regulation are still elusive to this date. This finding however shows that the Ssf proteins can function in other cellular processes.

1.3.2.1 Ssf paralogs can bind RNA

The Ssf proteins belong to the Brix/Imp superfamilly of proteins, which is further composed of LSU RiBi proteins Brx1, Rpf1, Rpf2, and pre-90S RiBi protein Imp4 [51, 52]. The shared Brix domain contains a σ70-like motif and confers to this superfamily the capacity to bind RNA. This has been demonstrated for Imp4, Rpf1 and Rpf2, which can all bind single-

stranded (ss) RNA, but with different affinities [53]. Wehner *et al* not only demonstrated the capacity of σ70-like motif to bind RNA but also studied the depletion phenotypes for each of these proteins using pulse-chase and analyzed the rRNA precursors co-isolated during affinity purification of each of the proteins. From these analyses, the RNA binding site of the Ssf paralogs was suggested to be located within the ITS1, between cleavage site A_3 and the 5' coding region of mature 18S rRNA [52-54]. Another study of the Imp/Brix superfamilly proposed that the family members closely interact with one other functionally [51].

1.3.2.2 Differences between the Ssf proteins

The Ssf1 and Ssf2 proteins are believed to have arisen from genome duplication. Their genes are located in different chromosomes and are not expressed at the same levels under normal growth conditions [30]. SSF1 is located on chromosome VIII and its protein abundance is ~8150 molecules per cell, while SSF2 is located on chromosome IV and its protein abundance is ~1350 molecules per cell [30].

The two proteins share a 94% sequence homology, and, with a few exceptions, most of the non-homologous sequence regions contain amino acids with equivalent charge (exceptions in red, Fig. 1.6) [30, 52, 54]. They share the Brix/σ70-like motif and a predicted homo/heterobinding domain (HBD).

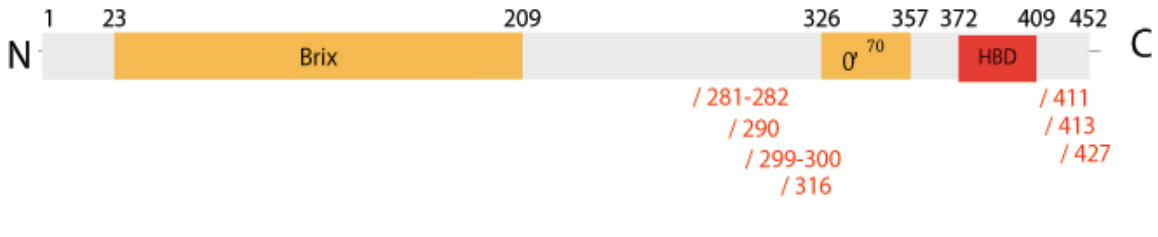

Figure 1.6: Ssf1/2 proteins and their domains
The Ssf paralogs share an RNA binding domain. In red are indicated the amino acids that do not have the same charge. According to information taken from (30, 52, 54) and Blastp alignment.

1.3.2.3 Ssf-protein depletion phenotype

Depletion of either of the paralogs has not been reported to affect ribosome biogenesis, yet depletion of both proteins simultaneously for 12 hours did affect pre-rRNA processing [54]. The primary transcript, 35S pre-rRNA, accumulated along with aberrant precursors 23S, 5'ETS-D and A_2-C_2 [54]. The presence of these aberrant precursors indicated that A_0, A_1 and A_2 processing was delayed and that C_2 cleavage occurred prematurely. Concomitantly, precursors normally found in wild-type cells were no longer detected: $27SA_2$, 27SB, 20S, 7S and 6S pre-RNAs [54]. Fatica *et al* also reported an overall reduction in mature rRNAs, including 5S rRNA [54]. 5S rRNA is transcribed by RNA polymerase III in the nucleolus. It is processed and assembled with Rpl5 and then enters into the pre-60S particle after C_2 cleavage in the nucleus, also associated with other RiBi proteins (Rpf2, Rrs1 and Rpl11) [17]. Part of the drop in 5S rRNA could alternatively be explained by changes in the chromatin state caused by a drop in Ssf1 and Ssf2, as both proteins have been found to interact with histones modifiers. However, the paralogs are unexpectedly associated with proteins of opposite function (Fig. 1.7 A and B). Ssf2 has been found associated with histone deacetylases Rpd3 and Hda1, while Ssf1 has been found to be associated with a histone 3 methylase (Sdc1); a component of a complex that exchanges H2AZ to H2A (Swr1); and an acetylase of the N terminal tails of H4 and H2A (Eaf7) [38, 55, 56]. Although these associations come from high-throughput data, which is background prone, those interactions could at least partially be accounted for the drop in overall transcription observed. During lag phase, Ssf1 was also found associated with histones 3 (Hht1 and Hht2) and 4 (Hhf1 and Hhf2) [55, 56].

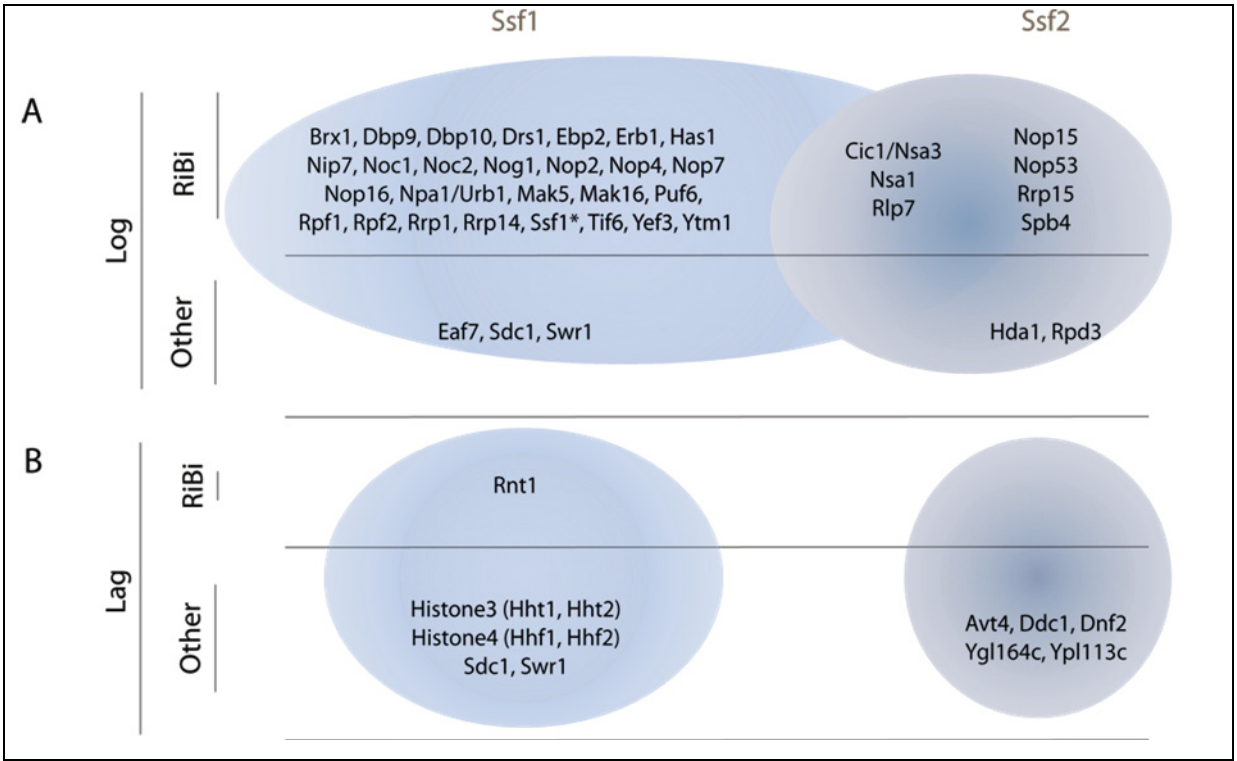

Figure 1.7: Proteins associated with Ssf1 and Ssf2

(**A**) During log phase, most of the RiBi proteins associated with Ssf1 are not associated with Ssf2. Both Ssf proteins have also been linked to proteins not involved in ribosome biogenesis during log and (**B**) lag phase, suggesting that they are involved in non-overlapping cellular functions. According to information taken from (38, 54-56).

1.3.2.4 The Ssf paralogs can form complexes with different proteins

To verify if the Ssf proteins can form similar complexes, reported affinity purification results were compared during lag and log phase.

Cells in lag phase have not been extensively studied, but it is known that cells are no longer dividing, ribosome biogenesis is shut-off and cells survive with the existing pool of ribosome [57, 58]. However, as many RiBi proteins have been found to be involved in other cellular processes during log phase (e.g. Nop7 and Ytm1). If RiBi proteins are present during lag phase, then they likely function as sensors for energetic changes within the cell. Data retrieved from (high throughput) lag phase affinity purifications suggest that both Ssf proteins are part of distinct complexes. Ssf1 AP during lag phase has not been performed but it was found as part of the Rnt1 particle [38]. Rnt1, an endonuclease, is an early RiBi factor required for rDNA transcription which has a role in closing rDNA repeats and increasing rDNA

transcription by physically interacting with RNA polymerase (pol) I [30, 59]. If Ssf1 and Rnt1 belong to common particle during lag phase, then Ssf1 could inhibit Rnt1 activity and thereby be indirectly involved in repressing rDNA transcription. Ssf2, on the other hand, was found to associate with proteins involved in amino acid synthesis (Ypl113c and Avt4), cell polarity (Dnf2) and the DNA damage response (Cdc1). If these interactions are real, then Ssf2 likely serves as a sensor of energy changes and DNA integrity. In addition to these proteins, Ssf2 was also linked to a RanGTP of unknown function (Ygl164c) and Avt4, a protein belonging to the family of transporters required in the brain and CNS for release of neurotransmitters GABA-glycine. If these associations are real then Ssf2 and its higher eukaryote orthologs share an evolutionary conserved interaction that seems to be useful for HIV viral infection in higher eukaryotes (Fig. 1.7 and Section 1.3.2.5).

During log phase, the Ssf1 particle contains several RiBi proteins, including Nop7 but excluding Ssf2, that have been associated to A_3 and $B1_{S+L}$ processing (Dbp9, Nop7, Nop15, Npa1/Urb1, Nsa1 and Rlp7; Fig. 1.7A). The Ssf2 particle has never been analyzed in log phase cells. A search for its interactors revealed that it has been reported in very few RiBi particles. In accordance with its role in these steps, it is present in particles required for A_3 processing and $B1_{S+L}$ processing (Nop15, Nsa1, Rlp7) [55]. Unexpectedly, Ssf2 interacts with Rrp15 and Nop53 using a coiled-coil motif (yeast two hybrid), whilst these proteins are absent from the Ssf1 particle [55, 60]. Interestingly, Rrp15 is also absent from the Nop7 particle which suggests that both Ssf2 and Rrp15 are required in a processing pre-rRNP particle that is independent of the main pre-60S maturation pathway. Together, these data are consistent with the Ssf1 and Ssf2 proteins performing a non-redundant function during ribosome biogenesis.

1.3.2.5 Ssf1/2 orthologs in higher eukaryotes

Interestingly, the need of a paralog for Ssf1 seems to be conserved in *Xenopus laevis (Peter pan-b*, *Ppan-b*) and even in humans, where Ppan2 is generated by alternative splicing events. In higher eukaryotes, *Ppan* is constitutively expressed in human cells of adults but, at least in *Xenopus laevis,* its expression is more regulated during embryogenesis [47, 61]. *Ppan* mRNA is expressed in nuclei and mitochondria of cells during eye development, neural crest, craniofacial cartilage and pronephros development, and appears to be always associated with

regions rich in microtubule structures [47, 62]. Tecza and collaborators depleted *Ppan* mRNA using a morpholino (MO) targeting both paralogs (verified by *nBlast*) and demonstrated that, during pronephros development, the essential *Ppan* pair is needed for embryogenesis, a function independent of ribosome biogenesis [47]. Another study from the same group involved the use of the same MO and also of MO2, which targeted mRNA of *Ppan-b* only (verified by *Blastn*), with the same results, indicating that *Ppan-b* depletion is sufficient to affect early eye and cranial cartilage formation [62].

In humans, the Ssf1 homolog Ppan, is always co-transcribed with the $P2Y_{11}$ gene, an ATP receptor required during granulocytic differentiation, and up-regulation of both *PPAN* and $P2Y_{11}$ genes has been linked to a specific type of leukemia [63]. In HeLa extracts, up-regulation of Ppan and Ppan-$P2Y_{11}$ proteins has been observed as a response to the presence of HIV-1 *Rev* protein and Ran-GTP [64]. The viral mRNA contains RRE sequences that are recognised by the *Rev* protein and complexes with Ran-GTP to transport the viral mRNA to the cytoplasm, where it is translated by ribosomes [65]. Upregulation of *PPAN* is therefore a mechanism for forcing an increase in ribosome biogenesis.

1.4 Ssf1, Ssf2 and Nop7

1.4.1 Ssf1 and Nop7

Isolated Ssf1-TAP complexes were previously reported to show tremendous overlap with Nop7-PrA ones (Fig. 1.8). This is not surprising, as both proteins assemble onto pre-60S particles during the same time, and both play a role during $27SA_2$, $27SA_3$ and 27SB processing. However, some RiBi proteins have been found distinctly only in the Ssf1-TAP complexes: Puf6, a repressor of ASH1 mRNA translation; Dbp9, a RNA helicase involved in 27S pre-rRNA processing (S and L) and Yef3, γ-subunit of elongation factor3 [30, 66]. This suggests that Ssf1 might also belong to particles that do not contain Nop7. The Nop7 particle entails several very early and late factors, as it enters the pre-90S particle and is released at the nuclear rim. However, the Nop7 complex also contains proteins required for ETS1, ITS1

and ITS2 processing that are not part of the Ssf1 particle (Loc1, Nop15, Sda1, Mak10, Dhr2 and Nop53), which suggests that it can form particles lacking Ssf1.

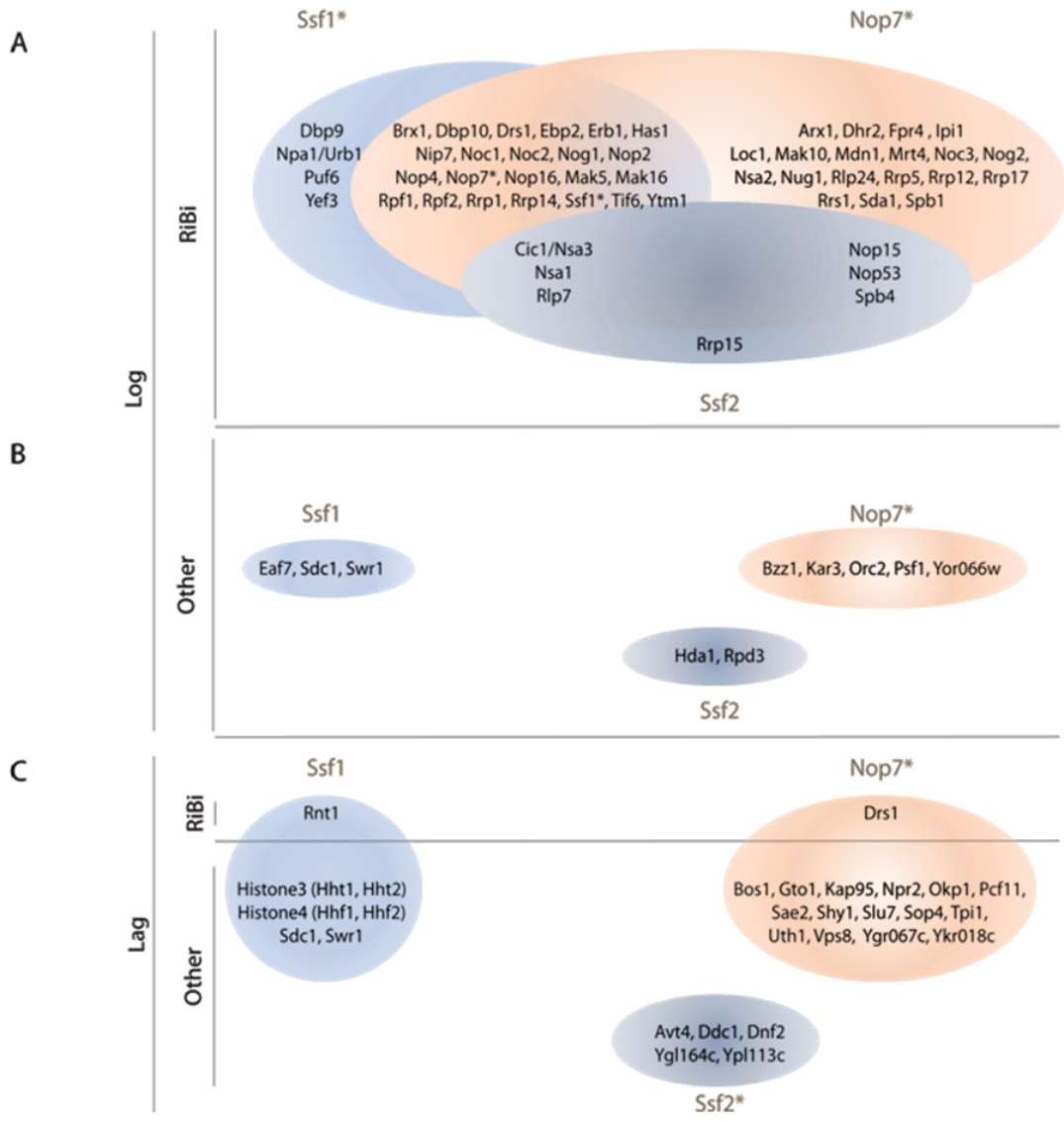

Figure 1.8: Proteins associated with Ssf1, Ssf2 and Nop7

According to already published data, (**A**) most of the RiBi proteins associated with Ssf1 are also Nop7-associated during log phase while Ssf2 has been found with proteins mostly Nop7-associated. Ssf1, Ssf2 and Nop7 have also been linked to other proteins, suggesting that they are involved in other cellular functions both during (**B**) log and (**C**) lag phase. An asterix (*) indicates whenever a tagged version of Ssf1, Nop7 or Ssf2 was used as bait. Built according to information from M. Oeffinger, unpublished data, (38, 54-56, 60, 67-71).

1.4.2 Ssf2 is most likely involved in a parallel pathway

Ssf1 and Ssf2 paralogs have been predicted to heterodimerize and yet Ssf2 is absent in the Ssf1 particle (Fig. 1.8). Data analysis of high-throughput studies, have revealed that it belongs to the Cic1/Nsa3, Nsa1 and Rlp7 particles, like Ssf1. However, it also co-precipitates with RiBi proteins belonging to the Nop7 particle but not with Nop7. Moreover, it also directly associates with Rrp15 and Nop53, which are not part of the Ssf1 particle. As Ssf2 compensates for the loss of Ssf1, it is likely that the compensation phenotype observed during ribosome biogenesis in ensured through an as yet uncharacterized alternative pathway. Thus studying the functions of Ssf1 and Ssf2 during ribosome biogenesis is relevant to the overall picture of ribosome assembly and maturation.

1.5 Research project

The potential distinct and overlapping functions of the Ssf1 and Ssf2 paralogs have not yet been determined. Although the two proteins share 94% of their amino acids, they are able form complexes with histone modifiers of opposite function and with different protein sets during lag phase; this also seems to be the case during ribosome biogenesis in log phase (Fig. 1.8) [38, 55, 56, 60]. Both proteins have been predicted to bind to ITS1 pre-rRNA and play a role in preventing premature cleavage at site C_2, which is located within ITS2 (Table I and Fig. 1.9) [53, 54].

Table I: Summary of what is known about Ssf1/2 and Nop7

	Nop7	**Ssf1**	**Ssf2 (94%identical to Ssf1)**
Cellular distribution	Nucleolar, punctuated at nuclear rim [36]	Nucleolar [50, 54]	
abundance (molec/cell)	4530 [30]	8150 [30]	1350 [30]
Known subcomplexes formed	Ytm1/Erb1/Nop7 [39]	N/D	
Direct interactions	C term tail of Erb1 [39]	N/D	- Rrp15 [60] - Nop53 [60]
	Nop7/Ssf1 in *Xenopus laevis* [47]		N/D
Binds pre-rRNA?	5' of 25S [12]	Predicted to bind ITS1 near the 5' of 5.8S [53]	
Function during pre-rRNA maturation	Scaffold protein [36]	N/D	
Depletion phenotype	- Accumulation of 35S [36] - Aberrant 23S, premature C_2 cleavage [36] - Pre-rRNA reduction of 27SB, 7S, 6S [36] - Mature rRNA reduction: 25S, $5.8S_S$ [36, 40] - Switch to $5.8S_L$- ribosome production [36]	- Accumulation of 35S [54] - Reduction of $27SA_2$, 27SB, 20S, 7S, 6S [54] - Reduction of all mature rRNAs, including 5S [54] - Accumulation of aberrant 23S, 5'ETS-D, A_2-C_2 [54] - Premature C_2 cleavage [54] - Reduction of all mature rRNAs [54]	
Known	- required for exit from G_0 - DNA replication	- necessary for yeast budding [49, 50]	

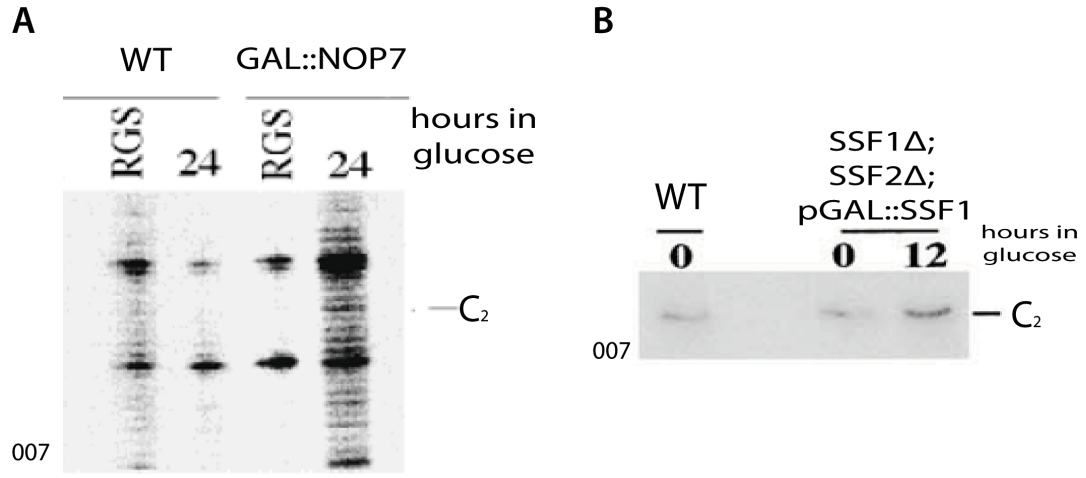

Figure 1.9: Similar to Ssf1/Ssf2 depletion, Nop7 depletion results in premature C_2 cleavage.

Primer extension performed from probe 007 and resolved on 6% polyacrylamide gel showed that **(A)** Nop7 depleted cells accumulate 26S pre-rRNA (as demonstrated by a stop at site C_2), which is also observed upon **(B)** Ssf1 and Ssf2 depletion. Adapted from [36] and [54].

Nop7 is a protein predicted to have several functions, as it is found in at least three distinct sub-nuclear compartments and associated with changing pre-ribosomal complexes [36]. The protein interacts with the 5' coding region of 25S rRNA and its depletion causes a mild pre-mature C_2 cleavage phenotype (Fig. 1.9) [12, 36]. The trimeric Nop7-Erb1-Ytm1 complex has been extensively studied; the complex is only found in one of the pre-ribosomal complexes Nop7 can be found in during ribosome biogenesis, which is at the stage of $27SA_3$ processing to $27SB_S$ [39]. Nop7 is a major player in the main LSU maturation route that generates $5.8S_S$-containing ribosomes.

Recent evidence reported a direct interaction between Ssf1 and Nop7 in *Xenopus laevis* during pronephros development, an interaction independent of the proteins function in ribosome biogenesis [47]. Similar information has already been used to identify a set of proteins that enter the pre-rRNP particle as a subcomplex during ribosome biogenesis, like the Rpf2 module required for 5S rRNA incorporation into the pre-60S particle following C_2 cleavage [17]. A comparison of Ssf1 and Nop7 particles has revealed that both have many RiBi

proteins in common yet also contain distinct RiBi proteins specifically involved in A_3 and B_1 processing, which suggests that Ssf1 and Nop7 are involved in common as well as overlapping pre-60S maturation pathways (Fig. 1.8). On the other hand, Ssf2-associated particles have never been characterized, and this protein is not found in either Ssf1and Nop7 particles but with RiBi proteins involved in 27S processing, suggesting that it has a non-redundant function to Ssf1 during ribosome biogenesis.

Further investigation of Ssf1 and Nop7 interactions during ribosome biogenesis and the better understanding of the role of Ssf2 during ribosome biogenesis and other cellular processes therefore become relevant.

The aim of this project is to uncover the presence of parallel pathways during ribosome biogenesis that may involve different paralogs of known ribosome biogenesis factors, namely Ssf1 and Ssf2.

My main hypotheses are:

1. Ssf1 and Ssf2 associate with distinct pre-rRNP particles and subcomplexes.
2. Nop7 and Ssf1 are genetically linked and function along the main LSU maturation pathway.
3. Nop7 and Ssf2 are not genetically linked.
4. Ssf2 functions along an alternative parallel LSU maturation pathway, independent of Ssf1 and Nop7.

To validate my hypotheses, I will:

1. Use a PCR-based (polymerase chain reaction) strategy to generate yeast strains to study Nop7/Ssf1/Ssf2 interactions.
2. Use ssAP (single step affinity purification) to compare Ssf1 and Ssf2 complexes and identify potential subcomplexes.
3. Use the generated strains to modulate one or two of the target proteins (SSf1, Ssf2 and/or Nop7) in order to uncover the presence of parallel pathways by monitoring changes in
    i. cell growth
    ii. total protein levels for the target factors
    iii. pre-rRNA processing
    iv. mRNA levels of the target proteins

As both Ssf1 and Ssf2 can form homo or heterodimers, bind pre-rRNA and, potentially, also bind Nop7, I will also generate the necessary tools to validate these interactions *in vitro*.

Hence I will:

4. Use recombinant Ssf1, Ssf2 and Nop7 for *in vitro* interaction studies.

2 Material and methods

2.1 General recipes and protocols

2.1.1 Media composition

Here is the media composition list used when manipulating bacterial and yeast strains. For agar plate preparation, the media was supplemented with 2% agar before autoclaving.

2.1.1.1 For bacterial manipulation

LB-Luria Broth: 1%(W/V) Bacto-tryptone, 0.5%(W/V) yeast extract, 1%(W/V) NaCl. Autoclaved.
For agar plate preparation, the media was supplemented with 2% agar before autoclaving.

SOC-Super optimal broth with catabolic repression: 2%(W/V) vegetal peptone, 0.5%(W/V) yeast extract, 10mM NaCl, 2.5mM KCl, 10mM $MgCl_2$, 10mM $MgSO_4$, 20mM glucose. Autoclaved.

Table II : List of the antibiotics used when manipulating bacteria

Antibiotic	Abbreviation	Solubilised in	1000X stock (mg/mL)
Ampicillin	*Amp*	*50%EtOH*	*50*
Kanamycin	*Kan*	*Water*	*50*
Chloramphenicol	*CAM*	*100%EtOH*	*35*

2.1.1.2 For yeast manipulation

YPD: 1%(w/v) yeast extract, 2%(w/v) peptone, 2%(w/v) glucose. Autoclaved.
YPGRS: 1%(w/v) yeast extract, 2%(w/v) peptone, 2%(w/v) galactose, 2%(w/v) raffinose, 2%(w/v) sucrose. Autoclaved.

Drop-out media: 1.5%(w/v) yeast nitrogen base (amino acid and ammonium sulfate free), 5%(w/v) ammonium sulfate, 1X amino acids except methionine and/or histidine, 2% of each sugar needed. Filter sterilized. The media was prepared with freshly autoclaved water.

D*rop-out media with antibiotics*, ammonium sulfate was replaced with 0.1%(w/v) of monosodium glutamate.

2.1.2 Whole cell lysis - protein extraction [72]

The protocol used for whole cell lysis was taken from (72). Approximately 2.5 OD_{600} (optical density) of cells were incubated for 5min (minutes) at RT (room temperature) with 200µL of 0.1M NaOH. The pellet was then resuspended in 50µL of modified Laemmli SDS sample buffer (detailed below) and stored at -20°C. Prior to loading, the samples were boiled for 3min at 95°C and spun. A 20µL volume of supernatant ($1OD_{600}$ of cells) was loaded on a pre-cast 4-12% Bis-Tris gel.

The modified Laemmli SDS sample buffer is a mixture of 0.06M Tris-HCl pH6.8, 5% glycerol, 2%SDS 4% β-mercaptoethanol and 0.0025% bromophenol blue, as described in (72).

2.1.3 Western blot (WB)

Bis-Tris gels (4-12%) were run at 185V for approximately 45min in a Tris-Tricine buffer. Protein transfer to nitrocellulose (NC) membrane or activated polyvinylidene difluoride (PVDF) membrane was performed for 2 hours (60V, 4°C) or overnight (30V, 4°C) in Towbin buffer. For WB analysis of yeast strains, antibodies PAP (α-PrA-HRP), α-HA (mouse), α-Nop7 (rabbit) and α-β-actin (mouse) were used (Table VIII). For recombinant protein purification, α-GST-HRP and α-HIS (mouse) antibodies were used (Table III).

The membranes were blocked in 1XTBST and 5% non-fat milk or BSA rocking for 20 min to 1hour at RT. The probing with antibody was usually performed rocking for 1hr at RT. If a secondary antibody was needed (α-mouse or α-rabbit), the membrane was washed twice in 1XTBST (5min, rocking) before probing the secondary antibody (30min, RT). Three washes in 1XTBST (5min, rocking) were performed prior to detection.

To minimize background when probing secondary antibodies on PVDF membranes, the solution was supplemented with SDS and Tween 20 to a final concentration of 0.01% and 0.1% respectively.

Table III : List of antibodies used

Antibody	Animal	Provider	Method of detection	Concentration used	Diluted in
PAP (α-PrA-HRP)	Rabbit	Sigma	ECL	1:7500	TBST/milk
α-HA	Mouse	Genscript	α-mouse	1:5000	TBST/milk
α-GST-HRP	Rabbit	Genscript	ECL	1:3000	TBST/milk
α-HIS	Mouse	Sigma	α-mouse	1:7500	TBST/milk
α-Nop7	Rabbit	[39]	α-rabbit	1:7500	TBST/milk
α-β-actin	Mouse	Abcam	α-mouse	1:7500	TBST
α-mouse Cy600 or Cy800	Llama	LI-COR	Odyssey*	1:20000	TBST/milk
α-rabbit Cy600 or Cy800	Llama	LI-COR	Odyssey*	1:10000	TBST/milk

*Odyssey: Infrared imaging system (LI-COR Biosciences)

10X TBST, 1L: 24.2g Tris, 80g NaCl, 21mL Tween20 brought to pH 7.6 with HCl

Tris glycine buffer, 1L: 3.03g Tris, 14.4g Glycine, 1g SDS

Tris-trycine buffer, 1L: 3.63g Tris, 3.59g Trycine, 0.5g SDS

Towbin buffer, 1L: 100mL MeOH, 3.03g Tris, 14.4g Glycine

For PVDF membrane activation, the membrane was washed with MeOH and equilibrated in towbin buffer.

2.1.4 Casting homemade gels – BioRad's Mini protean

To make home-made tris-glycine gels BioRad's Mini protean's system was used. The percentage of the gel varied depending on the size of the protein being analysed.

Table IV : Volume (mL) of components needed to make resolving and stacking gels

Components	Resolving gel (10mL)			Stacking gel (5mL)
	6%	**8%**	**10%**	**5%**
Water	*5.3*	*4.6*	*4.0*	*3.4*
30% acrylamide mix	*2.0*	*2.7*	*3.3*	*0.83*
Tris solution*	*2.5*	*2.5*	*2.5*	*0.63*
10% SDS	*0.1*	*0.1*	*0.1*	*0.05*
10% ammonium persulfate (APS)	*0.1*	*0.1*	*0.1*	*0.05*
TEMED	*0.008*	*0.006*	*0.004*	*0.005*
Protein size (kDa)	***180-200***	***150***	***50-100***	**-**

*: For resolving gels, the Tris solution is 1.5M Tris-Cl pH 8.8. For stacking gels, it is 1M Tris-Cl pH6.8.

2.1.5 chDNA purification and DNA purification

2.1.5.1 chDNA purification

About 2.5ODs of cells were recovered from an o/n culture or from a plate and resuspended in 100µL of ultrapure water. The cells were treated with 100µL of breaking buffer (200mM NaOH, 2.5% SDS, 500mM NaCl, 2mM EDTA) for 5min at RT. Neutralisation was performed with 300µL of 0.5M Tris-HCl pH 6.8 and briefly vortex mixed to then add 500µL of a Phenol/Chloroform/Isoamyl alcohol (Ph/Cl/IAA corresponding ratio of 25:24:1). After thoroughly vortexing the sample at V_{MAX} for 1min, the sample was spun at V_{MAX} for 10minutes. The supernatant was then mixed to 2volumes of cold 100% EtOH and spun at V_{MAX} for 10minutes at 4°C. The resulting pellet was then washed with 500µL of 70% cold EtOH, spun at V_{MAX} for 3minutes at 4°C and air dried. The pellet was then resuspended in 50µL of ultrapure water, nanodrop quantified and the chDNA (chromosomal desoxyribonucleic acid) was adjusted to a final concentration of 250ng/µL for diagnostic PCRs (polymerase chain reaction) and of 100ng/µL cassette amplifications from chDNA. All DNA samples were stored at -20°C.

2.1.5.2 DNA purification

Gel extraction and column purification were performed during molecular cloning. *E.Z.N.A Gel Extraction Kit* from Omega bio-tech was used as described by the supplier.

2.1.5.3 Gel extraction

For DNA extraction of digested vector or insert from an agarose gel, the DNA was first migrated on a 0.5 or 1% agarose gel. The DNA band corresponding to the right molecular size was excised from the gel, weighted and melted at 55°C with a 1µL/µg volume ratio of *binding buffer (XP2)* supplied in the kit. The mix was passed through a *HiBind DNA Mini Column* by centrifuging for 1min at 10 000x*g*. The column was then washed once with 300µL of *XP2 buffer* and twice with 700µL *SPW Wash Buffer*, each time centrifuging for

1min at 13 000x*g*. A final centrifugation of the column alone (2min, 13 000x*g*) was performed to completely remove the EtOH (from the wash buffer) prior to elution. The insert was then eluted in 30µL of a 50mM Tris-Cl pH8.5 solution provided in the kit.

2.1.5.4 Column purification

Column purification of DNA was performed to remove buffers and enzymes no longer needed. The protocol was the same as for *gel extraction* except that an equal volume of *XP2 binding buffer* was added in the first step and no heating was necessary. Also, an additional washing with 700µL *SPW Wash Buffer* was performed.

2.1.6 RNA extraction [73] and purification

RNA extraction form yeast samples were performed using Trizol (Invitrogen) as described in (73). A total of 17-26 OD_{600} of cells (2.5-5.0x10^8cells) were pelleted and washed three times with water. The pelleted cells were resuspended in 500µL Trizol and 200µL of DEPC treated glass beads (0.4-0.5mm diameter). Cell walls were disrupted by vortexing (at least 6min, 4°C). The mixture was then incubated at 70°C (5 min) and at RT (3min). To separate the aqueous phase, 200µL of chloroform, mixed (vortexing for 15 sec), let stand at RT (3min) and centrifuged (V_{MAX}, 15min, 4°C). Most of the aqueous phase (350µL) was transferred into a new tube containing 500µL of isopropanol. RNA precipitated at RT for 10min and was pelleted by centrifugation (V_{MAX}, 15min, 4°C). The pellet was washed once with 70% EtOH (1mL), centrifuged (V_{MAX}, 5min, 4°C), air dried and resuspended in RNAse-free water or formamide. The RNA was quantified (nanodrop) and stored at -80°C.

For primer extension and qRT-PCR analysis, the RNA in water was DNAse treated using RNeasyMini-Kit (QIAGEN) as described by the manufacturer and quantified.

2.1.7 Northern blot

For northern blot analysis of high molecular weight pre-rRNA, 10µg of total RNA was resolved in a 1% agarose/1.25% formaldehyde gel (11X14cm) in 30mM tricine, 30mM triethanolamine, as described in (74). Passive transfer of the RNA onto HyBond-N+ nylon membrane was performed overnight in 10X SSC. To resolve low molecular weight species, 10µg of total RNA was run in an 8% polyacrylamide/ 7M urea gel in 1X TBE as described in

(36). RNA transfer onto HyBond-N+ nylon membrane was performed overnight in 0.5X TBE buffer (12V). Following transfer, RNA was cross-linked to the nylon membrane (stratalinker, 1200J/m^2, 254nm) and probed at 37°C essentially as described in (36) but using fluorescently labelled probes (labelling protocol is detailed below). Briefly, the membrane was pre-hybridized with pre-hybridization buffer (6XSSPE, 5X Denhardt's, 2% Fish Sperm DNA, 0.2% SDS) pre-heated to 65°C and let cool to 37°C for 15minutes. The membrane was incubated with the fluorescent probe (20pmol) for at least 1 hour and washed once with 6X SSPE (15min, 37°C) and scanned using Odyssey infrared imaging system (LI-COR Biosciences). The approximate locations of the probes used in this study are schematised in the following figure:

A

001: 5'-CCAGTTACGAAAATTCTTG; **002**: 5'-GCTCTTTGCTCTTGCC;
003: 5'-TGTTACCTCTGGGCCC; **005**: 5'- ATGAAAACTCCACAGTG
006: 5'-AGATTAGCCGCAGTTGG; **007**: 5'-CTCCGCTTATTGATATGC;
008: 5'-CATGGCTTAATCTTTGAGAC; **017**: 5'-GCGTTGTTCATCGATGC;
020: 5'-TGAGAAGGAAATGACGCT; **041**: 5'- CTACTCGGTCAGGCTC.

B

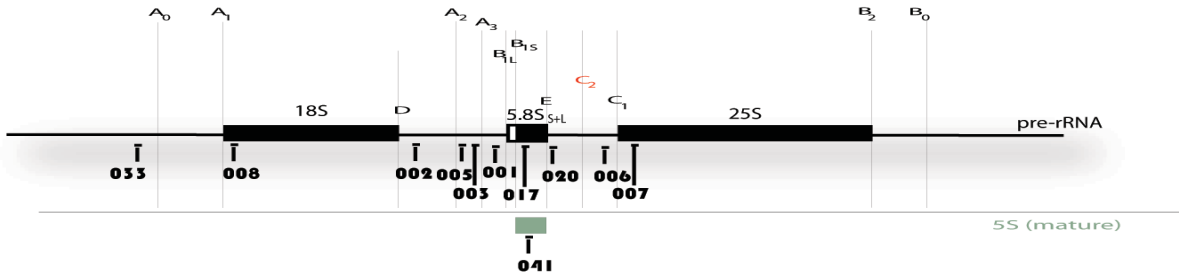

Figure 2.1: Probe sequences and approximate target location in the pre-rRNA

(A) The probes sequences and **(B)** the approximate location they target in the pre-rRNA were constructed according to data from (36, 54).

10X TBE, 500mL: 54g Tris, 27.5g Boric acid, 20mL 0.5M EDTA pH8.

2.1.7.1 Probe labelling

For northern blot (NB) detection of pre-rRNA species, probes were ordered from IDT with a 5' and 3' amine. For fluorescent primer extension, the primer order had only one amine (5'). The following protocol was used for probe labelling. 20µg of probe was resuspended in 20µL of 100mM $NaCO_3$ pH 9 buffer and incubated (no light, overnight RT) with 50µg of Dylight NHS ester 800 (Thermo Scientific). The following day, a nucleotide removal kit (Quiagen) was used as described by the supplier. The eluted labelled probe was quantified (nanodrop) and 20pmol of probe was used for NB detection and 10pmol of probe was used for each primer extension reaction.

2.1.8 Reverse transcription and primer extension

For both reverse transcription and primer extension, SuperScript II reverse transcriptase (RT from Invitrogen) was used.

The reverse transcription reaction was performed as described by the supplier using random hexamers (Operon). Briefly, 1µg or RNA was mixed to 100ng of random primers and 1µL of dNTP mix (each 10mM) in a final volume of 13µL. This mix was incubated at 70°C for 5 minutes and then let on ice for 1 minute. 4µL of 5X first strand buffer and 2µL of 0.1M DTT (both supplied in the kit) were added and the new mix was incubated at room temperature (RT) for 2 minutes, after which 1µL of the enzyme was added for total volume of 20µL. This mix was incubated at RT for 10 minutes and then at 42°C for 50 minutes. To inactivate the enzyme, the reaction mix was incubated at 70°C for 15 minutes. The cDNAs obtained were used for quantitative real-time PCR (qRT-PCR). As negative controls for the qRT-PCR reaction (RT-), an additional µg of total RNA per sample was prepared in parallel but water was added instead of the enzyme.

Primer extension analysis was performed using 1µg of total RNA per sample essentially as described in (75). Briefly, a 13µL mix of total RNA, 10pmol of fluorescently 5'-labelled probe 007 and 1µL of 10mM dNTP mix was incubated at 95°C for 1 minute and slowly let cool to 42°C for 3minutes. Then, 4µL of 5X standard buffer and 2µL of 0.1M DTT was added and incubated at 42°C for 2min. 1µL of enzyme was added and the reaction was performed at 42°C for 50 min, after which 2µL of 3M NaOAc pH 5.2 and 40µL of 100%

EtOH were used to stop the reaction. After centrifugation, the pellet was resuspended in 10µL of loading dye (7M urea, 1X TBE, bromophenol blue). 1.5µL of this mix was separated on an 8% polyacrylamide gel and detected using Odyssey infrared imaging system.

2.1.9 Plasmid purification

For plasmid purifications, *Wizard Plus SV Minipreps DNA purification system* from Promega was used. At each step during cell lysis, mixing by ups and downs or inversion was preferred to vortexing. All centrifugation steps involving the column were performed at V_{MAX} (13.2 Krpm) and RT.

Essentially, cells from 5mL of o/n grown cultures were pelleted and resuspended in 250µL of *Cell resuspension buffer*, lysed by adding 250µL of *Cell Lysis Solution* and 10µL of *alkaline protease solution* and incubating for 5min at RT. To neutralize the solution, 350µL of *neutralization solution* was added and then the lysed cells were centrifuged at top speed for 10min at RT. The supernatant was passed through the supplied *spin column* by centrifugation for 1min. The column was then washed with 750µL and then with 250µL of *wash solution* by centrifugation for 1min. Remaining EtOH was removed from the column with an additional centrifugation step (2min) and then the plasmid was eluted in 50µL of *nuclease free water.* The plasmid was quantified (Nanodrop), brought to a final concentration of 100ng/µL and visualised on a 0.5% agarose gel. Plasmids were stored at -20°C.

2.1.10 Bacterial transformation

For plasmids transformed in NEB turbo cells (Table X), NEB's protocol was used. In summary, the competent cells were thawed on ice and 50µL of cells were gently mixed and then incubated on ice for 30minutes with 100ng of plasmid. The cells were then heat shocked for 30sec at 42°C then let stand on ice for 5min. After adding 950uL of SOC media to each tube, the cells were incubated for 1hr at 37°C at 500rpm. The cells were then pelleted and resuspended in 100µL of SOC media for spreading onto an LB+Res plate (antibiotic depends on the plasmid that was transformed) and incubated for 16hrs at 30°C.

For transformations in pLYS and RipL cells (Table V), the protocol varied slightly: LB media was used instead of SOC and the 5min incubation on ice following the heat shock was not performed. These cells were incubated at 37°C o/n.

Table V: List of bacterial cells used for plasmid preparation and expression of recombinant protein

Purpose	ID	Strain	Genotype	Antibiotic resistance
Plasmid preparation	NEB Turbo	NEB Turbo competent E. coli (High Efficiency)	*F′ proA^{+}B^{+} lacI^{q} Δ lacZ M15/ fhuA2 Δ(lac-proAB) glnV gal R(zgb-210::Tn10)*Tet^{S} *endA1 thi-1 Δ(hsdS-mcrB)5*	-
Expression vector	RIPL	BL21-CodonPlus (DE3)-RIPL competent cells	*E. coli B F^{-} ompT hsdS($r_B^{-}m_B^{-}$) dcm^{+}Tet^{r} galλ(DE3) endA Hte [argU proL Cam^{r}] [argU ileY leuW Strep/Spec^{r}]*	*Tet^{r} Cam^{r} Strep/Spe^{r}*
	pLys	BL21-Gold(DE3)pLysS competent cells	*E. coli B F^{-} ompT hsdS($r_B^{-}m_B^{-}$) dcm^{+}Tet^{r} galλ(DE3) endA Hte [pLYS Cam^{r}]*	*Tet^{r} Cam^{r}*

2.2 Molecular cloning

To ensure the proper directionality of the insert, primers were designed so that BamHI and Xho1 restriction enzyme sites flanked the gene's ORF at its N and C terminal respectively during molecular cloning. For N-terminal GST-TEV tagging, the pGEX4T1 vector was used. For N-terminal His6-TEV tagging, the pET28 MHL GS vector was used. This vector is the pET28-MHL vector in which a BamH1 site (GS) was added in house between the TEV cleavage site and Nde1 restriction enzyme site.

Table VI: Plasmids used for molecular cloning

Plasmid	Plasmid size (bp)	Resistance	Type of N-term tagging	RES position in plasmid (bp)		Expected length of vector after RE treatment (bp)	Reference
				BamH1	Xho1		
pGEX4T1	*4969*	*Amp*	*GST-TEV*	*930*	*954*	*4786*	*GE Healthcare*
pET28-MHL GS	*7331*	*Kan*	*His6-TEV*	*5125*	*7166*	*5287*	*Oeffinger lab*

The plasmids above were cut using BamH1 and Xho1. Of the digestion products, the one with the expected length (Table VI) was gel purified and the ends were treated with

Antarctic Phosphatase to change the phosphate group into an OH and prevent re-ligation of the vector.

The following table shows the primers used to create the inserts for molecular cloning (Table VII). All primers were designed to have 6 random nucleotides at their 5', followed by a restriction enzyme site (RES), a start (for forward primer) or stop codon (for reverse primer) and 27nts complementary to the beginning of the gene (after the start) or its end (before the stop codon). For the 3' primers used with the pET28-MHLGS vector, 2 additional stop codons were added, as recommended in the pET28-MHL parental vector specifications sheet.

Table VII: Primers used for molecular cloning

#	Primer name	used with		primer sequence					Salt adjusted Tm (°C)
		pGEX4T1	pET28-MHLGS			Random	RES	Gene ORF	
1	5'_BamH1_Start_NOP7	√	√	Fwd	5`	aaa ccc	gga tcc	ATG AGA ATC AAG AAG AAA AAC ACC AGA GGT	71
2	5'_BamH1_Start_SSF1	√	√	Fwd	5`	aaa ccc	gga tcc	ATG GCC AAG AGA AGA CAA AAG AAA AGA ACA	71
3	5'_BamH1_Start_SSF2	√	√	Fwd	5`	aga aga	gga tcc	ATG GCT AAA AGA AGG CAG AAA AAG AGA ACG	71
4	3'_Xho1_Stop_NOP7	√		Rev	5`	tca tca	ctc gag	CTA TTT CTT GGA ATC TAG TTT ATT CAG TTT	67
5	3'_Xho1_Stop_SSF1	√		Rev	5`	tcg tcg	ctc gag	TTA TTC GAC CTC ACT AAA TAA GTC ACT ATC	71
6	3'_Xho1_Stop_SSF2	√		Rev	5`	ccc tcc	ctc gag	TTA TTC TAC TTC ACT GAA TAA GTC ACT ATC	71
7	3'_Xho1_3Stop_SSF1		√	Rev	5`	tcg tcg	ctc gag	TCATCATTATTC GAC CTC ACT AAA TAA GTC ACT ATC	72
8	3'_Xho1_3Stop_SSF2		√	Rev	5`	ccc tcc	ctc gag	TCATCATTATTC TAC TTC ACT GAA TAA GTC ACT ATC	72

RES= restriction enzyme site; ORF= open reading frame; start and stop codons are underligned.

2.2.1 Insert preparation

The expected size of the insert depended on the length of the target gene listed in table VIII + 30 to 36nt. The target gene ORF was amplified by PCR from purified W303a chDNA using the primers listed in table VII. The annealing temperature corresponded to the lowest salt-adjusted T_m value minus 3°C (Table IX). The PCR recipe and program were used are the following:

PCR mix final concentrations: iProof buffer 1X, 5'and 3' primers 0.5pmol/ul, 200µM of each dNTP, 2% DMSO, 1ng/uL chDNA, 0.25U/uL Taq.

Table VIII: Size of genes selected for molecular cloning

Gene	*SSF1*	*SSF2*	*NOP7*
gene length (nt)	*1362*	*1362*	*1818*

Table IX: PCR program used to amplify the insert from chDNA

Temperature (°C)		Time (min:sec)	Number of cycles
98		0:30	1X
98		0:05	30X
SSF1/2: 66	NOP7:63	0:10	
72		0:30	
72		5:00	1X
4		Forever	

The insert was then purified form a 1% agarose gel using the *gel extraction* protocol detailed in section 2.1.5.3 and then digested in parallel with the parental vector.

2.2.2 Restriction enzyme digestion

Because both BamH1-HF and Xho1 restriction enzymes (RE, from BioLabs) are compatible with the same buffer, the digestion of both the insert and vector using these enzymes could be performed simultaneously. The inserts and the vectors were each treated with both restriction enzymes for 1hr to o/n at 37°C in a total volume of 50µL. The reaction mix contained final concentrations of 1X Buffer4, 0.5µg/µL BSA, 3µg of vector or 30µL of purified insert and 1.5(U/µL) active units of each enzyme. The insert was then cleaned following the *enzymatic clean-up protocol* (Section 2.1.5.4) and then Nanodrop quantified and visualised for purity in a 1% agarose gel.

To make sure it did not re-ligate itself, the vector was treated with Antarctic Phosphatase. To do so, the RE-treated vector was run on a 1% agarose gel and the band corresponding to the expected size of the digested vector (Table VI) was extracted from the gel (Section 2.1.5.3). The eluted vector was treated with Antarctic Phosphatase for 15-30min at 37°C in a total reaction volume of 50µL containing 30µL purified vector, Antarctic Phosphatase 1X buffer, Antarctic Phosphatase 0.1U/µL. The reaction mix was incubated at

65°C for 5min to fully inactivate the enzyme and then let for 5min on ice. The vector was quantified using the Nanodrop and visualised for purity in a 1% agarose gel prior to ligation.

2.2.3 Verification of relative abundance of V and I and plasmid ligation

To efficiently ligate the vector with the insert, the ratio of insert to plasmid had to be of 3:1. At the end of the procedure, 100ng of plasmid was needed to transform into the rapid-growing bacterial NEB turbo cells. To ensure proper ratio, the following calculation was performed. This calculation allowed us to take into account the size of the linearized vector and of the insert to ensure that the ratio was of 3.

$$q_{insert} = \frac{(\text{cohesive} = 3, \text{blunt} = 10) \times \mathrm{L_{insert(bp)}} \times \mathrm{q_{plasmid(ng)}}}{\mathrm{L_{plasmid(bp)}}}$$

$$ng_{insert} = \frac{3 \times \mathrm{L_{insert(bp)}} \times \mathrm{100ng_{plasmid}}}{\mathrm{L_{plasmid(bp)}}}$$

Prior to ligation, a final verification on agarose gel was performed with 50ng of insert and digested/antarctic phosphatase-treated plasmid. The amount of insert calculated was incubated with 100ng of vector 1hr at 16°C, using the smallest volume possible (eg. 10µL). The reaction-mix contained 1X T4 DNA ligase buffer, *100ng* of plasmid, calculated amount of insert, 1µL T4 DNA ligase.

The plasmids were transformed into NEB turbo cells and grown for 8 hours at 37°C and then 15-20 single colonies were selected from the transformation plate. These transformants were grown in 500µL LB+Res at 37°C for 2-3hours while shaking at 500rpm. Then, 500µL of Ph/Ch/IAA was added and thoroughly vortexed, then spun at V_{MAX}, 56µL of 10X buffer was added and 5µL of the top layer was loaded on a 0.5% agarose gel to compare the clone's plasmid to the parental vector. Because the plasmid is now different in size, it will migrate differently in its supercoiled and circular forms (Fig. 2.2).

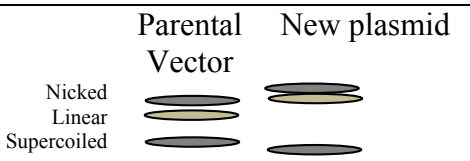

Figure 2.2: Expected bands when screening for positive plasmid transformants

As the new plasmid is expected to be of higher molecular weight that the parental plasmid, the nicked, linear and supercoiled forms of the new plasmid are expected to migrate differently on gel.

From this preliminary analysis, 5-6 potentially positive clones per plasmid were grown in liquid LB+resistance (3-5mL) o/n at 30°C, plasmids were purified and quantified using Nanodrop. To test for positive plasmids, a restriction enzyme digestion was performed using 500ng of plasmid in a total volume of 10 to 20µL of RE digestion reaction using restriction enzymes BamHI and XhoI (detailed above). The bands were resolved on 1% agarose gel. Three positive clones per plasmid were sent for sequencing using T7 promoter, T7 terminator and the primer internal for the ORF of the gene. The internal primer was chosen about 500np after the start of the gene (Table X).

Table X: Primers used to sequence-validate the plasmids

#	Primer name	pGEX4T1 derived	pET28-MHLGS derived	Sequence			Salt adjusted T_m (°C)
1	*5'_500bpSeqSSF1*	√	√	*Fwd*	*5`*	*TCT ATG TTT CAG AAT ATT TTC*	*50*
2	*5'_500bpSeqSSF2*	√	√	*Fwd*	*5`*	*TCC ATG TTC CAG AAT ATT TTC*	*54*
3	*5'_500bpSeqNop7*	√		*Fwd*	*5`*	*TTA GCC TAT GTT GCC AAG GAA*	*57*
4	*T7 Promoter*	√	√	*Fwd*	*5`*	*TAA TAC GAC TCA CTA TAG GG*	*48*
5	*T7 terminator*	√	√	*Rev*	*5`*	*GCT AGT TAT TGC TCA GCG G*	*54*

2.3 Recombinant protein

2.3.1 Recombinant protein expression

Once the clones were confirmed by sequencing, the plasmids were transformed in pLYS and RipL cells because they were available in the lab (Table X). Recombinant protein expression was assayed for each transformant using varying amounts of IPTG (0.5 or 1mM) and different temperatures (16°C, 25°C and 37°C). A 300µL aliquot was taken at time-points 0, 2, 4 and o/n. Then the best induction conditions were selected for large-scale inductions (Table XI).

Table XI: List of plasmids generated and optimized conditions for optimal protein expression

Plasmid name	Plasmid size (bp)	Background	Resistance	N-term tag	Optimized induction conditions	Reference
GST-TEV-NOP7	*6763*	*pGEX4T1*	*Amp*	*GST-TEV*	*pLYS, 1mM IPTG, 16°C o/n*	*This study*
GST-TEV-SSF1	*6307*	*pGEX4T1*	*Amp*	*GST-TEV*	*RipL, 0.5mM IPTG, 16°C, o/n*	*This study*
GST-TEV-SSF2	*6307*	*pGEX4T1*	*Amp*	*GST-TEV*	*pLYS, 1mM IPTG, 16°C o/n*	*This study*
HIS6-TEV-SSF1	*6649*	*pET28 MHL GS*	*Kan*	*His6-TEV*	*pLYS, 1mM IPTG, 16°C o/n*	*This study*
HIS6-TEV-SSF2	*6649*	*pET28 MHL GS*	*Kan*	*His6-TEV*	*RipL, 1mM IPTG, 16°C o/n*	*This study*

2.3.1.1 Small-scale optimisation

Each plasmid was transformed in pLYS cells. A single colony was streaked and then grown o/n in 5mL of LB+CAM+Res at 37°C (Tables VII, X and XVI). The following day, 300µL of the o/n culture was grown for 2hrs in 6ml of fresh LB+CAM+Res (37°C), resulting in an OD_{600} between 0.6-0.8. The cells were then divided in two 3mL aliquots and induced with 0.5 or 1mM IPTG. The 3mL aliquots were then divided into three aliquots of 1mL and shifted to 16°C, 25°C or 37°C. At each time-point (0, 2, 4hrs and o/n), a 300µL aliquot of culture was sampled for whole cell lysis treatment followed by WB analysis. The gels were run on a 10% Tris-glycine SDS-PAGE (Table IX) and blotted in activated PVDF membranes for immunodetection. To visualize the relative abundance of the protein, the membranes were stained for 1min with coomassie and destained with several washes in a destaining solution containing 25% ethanol.

The same procedure was performed for each plasmid when transformed in RipL cells. Once the best protein induction conditions were determined, large scale inductions were performed from each plasmid.

2.3.1.2 Recombinant protein expression

Each plasmid was transformed into the expression vector chosen from the optimization trials. The cells were streaked from glycerol stock onto LB +CAM +Res plates at 37°C, 150rpm, o/n. The following day, the clones were each grown over-day up to an OD_{600}~0.6 at 37°C, 150rpm (pre-culture). For each liter of induced culture, 50mL of pre-culture was prepared. The cells were let at 4°C o/n. The following day, the pelleted pre-culture cells were resuspended into 1L of LB media+CAM+Res and grown up to a final OD_{600} of 0.6. Then, the media was spiked with IPTG and shifted to the induction temperature determined during the optimisation step. The following day, the cells were pelleted at 4°C, 4000rpm for 20min. The pellet was weighed, flash-frozen with liquid nitrogen, and kept at -80°C for recombinant protein purification.

2.3.2 Recombinant protein purification

2.3.2.1 His_6-tagged proteins

For each gram of pellet, 7mL of binding buffer (100mM HEPES pH7.4/500mM NaCl/20mM imidazole/10 µg/mL antipain/2 µg/mL leupeptin/1 µg/mL pepstatine/2 µg/mL aprotinine/1 mM PMSF/70KU lysozyme) was used. The thawed sample was vortex resuspended, homogenized on ice (polytron, 1min) and incubated for 30min at 4°C on a rotating wheel, to let the lysozyme break down the cell walls. After 30min of incubation, the cells were sonicated using 5 cycles of 1min sonication, 1min on ice. DNA was broken by passing the mix several times through a syringe. The SN obtained after centrifugation (16 000g, 20min, 4°C) was filtered (0.22µm), de-gazed and passed into a HP His-Trap 1mL column HP from GE healthcare (FPLC). The column was washed with a volume of wash buffer (100mM HEPES pH7.4/500mM NaCl/50mM imidazole) equivalent to the injected sample and the proteins bound to the column were eluted in 4mL fractions of elution buffer

with increasing imidazole concentrations (100mM HEPES pH7.4/500mM NaCl with 75, 100, 300 or 500mM imidazole).

For analysis, 60µL of every fraction was recovered, mixed with 12µL of 6Xloading dye, and boiled (95°C, 5min). To validate the fractions to pool for the following steps, $1/500^{th}$ of each fraction were resolved on two 10% Tris-glycine SDS-PAGE gels. One of them was Coomassie stained (Fig. 2.3 A) and the other was transferred on a NC membrane and blotted with α-HIS antibody (Fig. 2.3 B). The fractions containing the protein were dialyzed against a 100mM Hepes pH8.0/ 10mM KCl/ 10mM $MgCl_2$/ 150mM NaCl/ 20% glycerol buffer and concentrated on a PALL concentrator with a MWCO of 30kDa as specified by the supplier. To verify the amount of recombinant protein obtained and potentially lost, a 37^{th} of input, retention and filtrate samples were resolved on a 4-12% Bis-Tris gel together with BSA samples of varying concentrations, later used as a standard curve. The resolved samples were transferred to a PVDF membrane and detected using α-his (mouse) as the primary antibody and α-mouse Cy800 as secondary antibody for detection of the tag (Odyssey). The PVDF membrane was then Coomassie-stained to approximate the amounts of purified protein from the BSA standard curve.

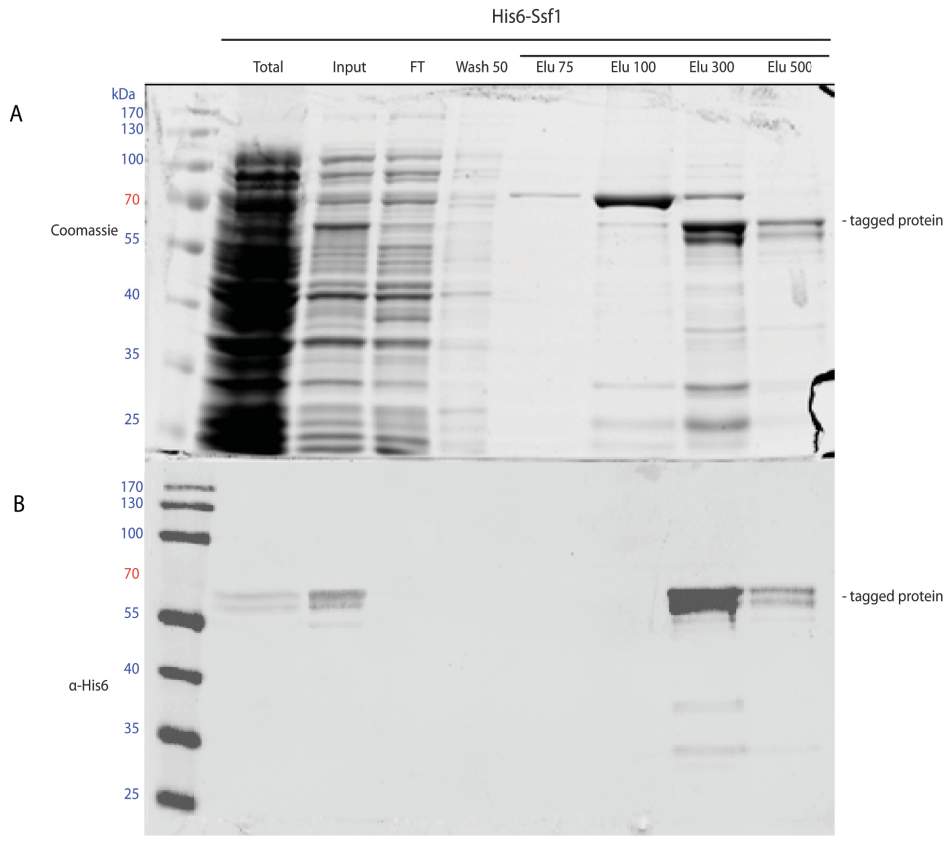

Figure 2.3: FPLC purification

His6-Ssf1 recombinant protein was purified by FPLC. A 500th of each purification step was resolved on a 10% SDS-PAGE gel and either **(A)** Coomassie stained or **(B)** transferred to a NC membrane and blotted with α-His. For further information, refer to text.

2.3.2.2 GST-tagged proteins

The frozen pellet was vortex resuspended in 10mL of binding buffer (1XPBS, 70KU lysozyme), homogenized on ice (polytron, 1min) and incubated for 30min at 4°C on a rotating wheel for lysozyme treatment. The cells were then sonicated 5 for cycles of 1min sonication, 1min on ice. DNA was further broken by passing the mix several times through a syringe. The SN obtained after centrifugation (16 000g, 20min, 4°C) was incubated for 1hr, 4°C, gentle agitation with a 750uL aliquot of homogenous 'Glutathione Sepharose 4 fast flow' resin from GE Healthcare pre-washed with binding buffer. The beads were then recovered by

centrifugation (1200rpm, 2min, 4°C) and washed three to four times with wash buffer (1XPBS). The recombinant protein was then eluted three times in 375uL of elution buffer (50mM Tris-Cl/10mM reduced glutathione pH8.0, 10min, RT). To validate the fractions to pool for the following steps $1/50^{th}$ of the eluates were run on a 10% Tris-glycine SDS-PAGE, transferred on PVDF membrane. Eluates in which recombinant protein was detected using anti-GST-HRP antibody (home-made ECL detection) were pooled, the eluates were concentrated and switched to 100mM Hepes pH8.0/ 150mM NaCl/ 0.5mM EDTA/ 10% glycerol/ 0.1% triton/1mM DTT buffer by passing them on a PALL concentrator with a MWCO of 30kDa as specified by the supplier (Fig. 2.4). To verify the amount of recombinant protein loss and the efficacy of cleaning, a 37^{th} of input, retention and filtrate samples were taken each time the MWCO column was used. These samples were resolved on a 10% tris-glycine SDS-PAGE gel next to BSA samples of varying concentrations, latter used as a standard curve. The resolved samples were transferred to a PVDF membrane and blotted using α-GST-HRP antibody for detection of the tag. The PVDF membrane was then Coomassie-stained to approximate the amounts of purified protein from the BSA standard curve.

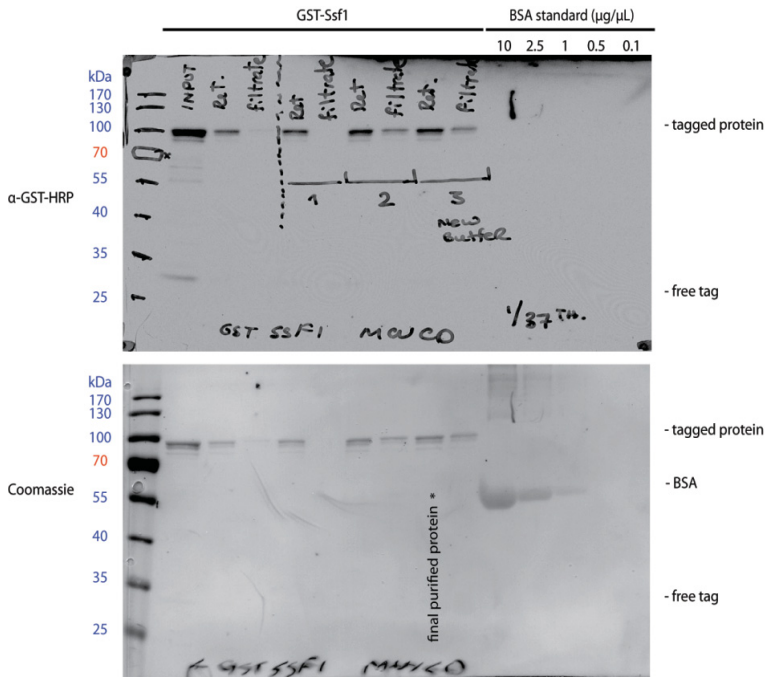

Figure 2.4: Molecular weight cut-off

The buffer was exchanged and the recombinant protein was separated from free tag using a molecular weight cut-off column of 30kDa. Free-tag and tagged protein were detected with α-GST-HRP antibody and the final concentration of purified protein was approximated using a BSA standard curve (µg/µL) and Coomassie staining. Here, a 37th of each purification step for GST-Ssf1 was resolved on a 10% SDS-PAGE gel and transferred on a PVDF membrane.

2.4 Construction of yeast strains

Two different haploid baker's yeast strains (*Saccharomyces cerevisiae*) were tested as parental: CML476a and W303a. Due to a growth defect detected in the CML476a strain, W303a was chosen as suitable background strain for all experiments in this project.

2.4.1 Endogenous modifications in yeast

The modifications performed were essentially I) insertion of a regulatable promoter in front of the gene of interest, II) deletion of the gene of interest, and III) C-terminal tagging of the gene of interest. In all cases, the procedure was based on the same principle: (Fig. 2.5) primers (Table XII) with a 5' region (45-66nts) targeting the gene of interest and followed by 18-20nts annealing with a plasmid containing the modification were designed. They were used to amplify a 1840-2236nt long cassette from a plasmid containing the modification (Table XIII) by PCR (Table XIV). The purified cassette was then transformed into the haploid background strain where it integrated into the genome by recombinant homology. A selection marker within the cassette allowed the survival of positive transformants in the presence of an antibiotic (Gal1 promoter: G418; Met25 promoter: ClonNAT, gene deletion: hygromycin B - hph), or the absence of an essential amino acid (C-terminal PrA tags: histidine plated directly onto media lacking histidine). In the case of drug-resistance cassettes, all cells were first grown in permissive media (YPD or SD-methionine) to form colonies. Then, positive transformants were selected by replica plating the colonies onto fresh, permissive media supplemented with the corresponding antibiotic (drug concentrations: Table XV). In the case of G418 resistant cassettes, a first selection was performed in 200µg active units of G418 per mL of replica plate and then a second replica plate was performed with a higher concentration of G418 (600µg of active units/mL). All transformants were tested by diagnostic PCR. The control primers are listed in Table XVI. The primer pairs used and their expected PCR product sizes indicating positive or negative transformants are listed in Table XVII. The standardized diagnostic PCR program is described in Table XVIII.

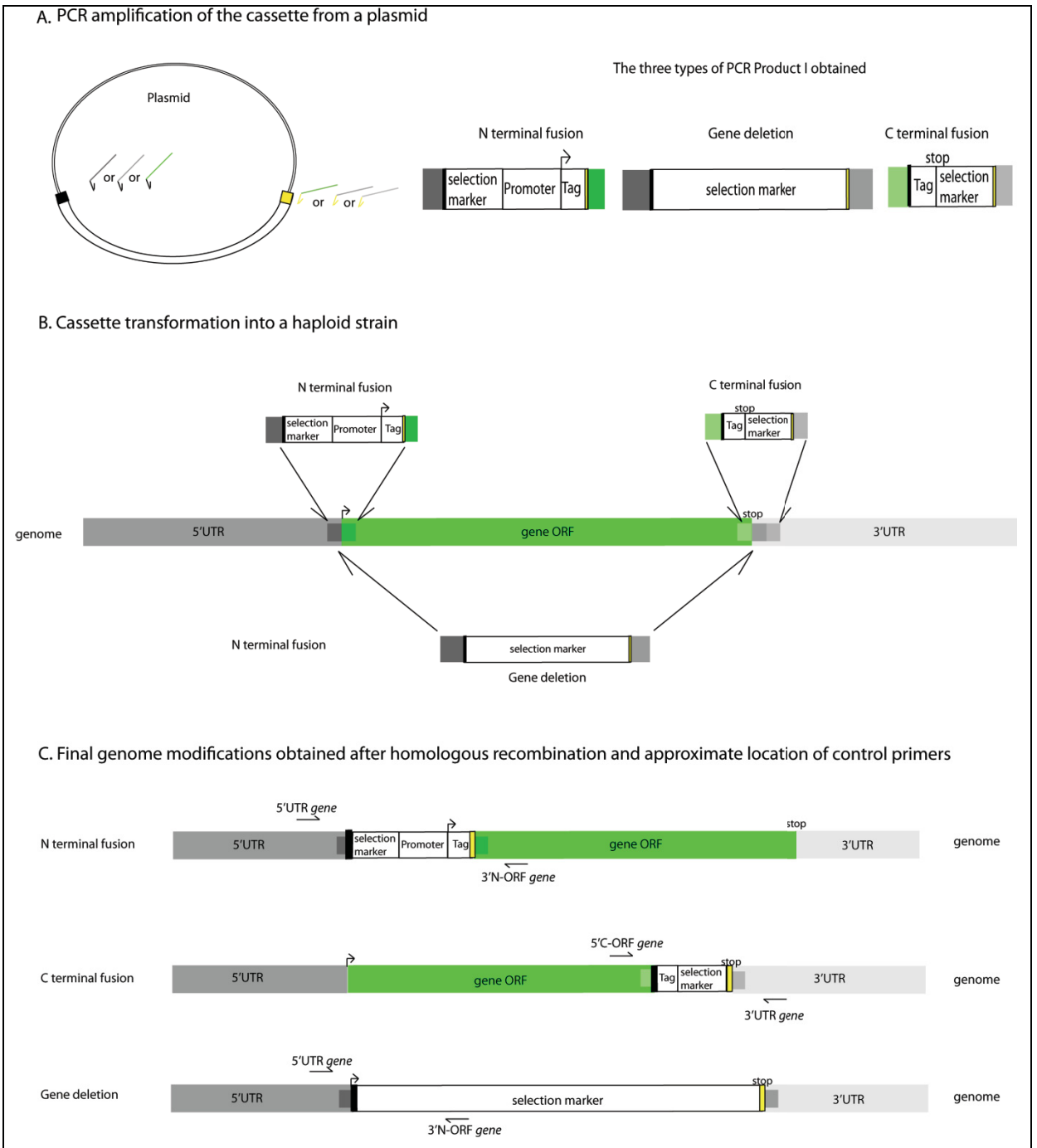

Figure 2.5: Types of modifications performed to yeast cells.

(A) Using primers that can anneal with a plasmid and recognise a specific region in the genome, the cassette was amplified by PCR and cleaned. **(B)** The cassettes were then transformed into haploid cells where **(C)** the cassettes integrated into the genome by recombinant homology. Positive transformants were validated by diagnostic PCR using control primers whose approximate locations are schematized here.

Table XII: List of primers used for yeast transformations

Purpose	Name	Direction	Sequence*	Used with plasmid
pGal insertion	*5'pGal1::NOP7*	*Fwd*	*5' AAA AAT TTT GGA AGG TTA ATT AGA GAT GTG TAG TAA ATC CTG CTG GTG GAA TAC ATT TTA* ***GAA TTC GAG CTC GTT TAA AC***	1
	3'pGal1::NOP7	*Rev*	*5' AGC TTG AGA TCT GGT AAT AAA GTT TCT TGC GTT ACC TCT GGT GTT TTT CTT CTT GAT TCT* ***GCA CTG AGC AGC GTA ATC TG***	1
pMet25 insertion	*5'pMet25::SSF1*	*Fwd*	*5' AAA AGA GTA TAA TCC AGA TAT AGC AGA CAA TAA AAT TTC AAG ATG* ***CGT ACG CTG CAG GTC GAC***	2
	3'pMet25::SSF1	*Rev*	*5' AGG TGT AAG CTG TGC ATG TGT TCT TTT CTT TTG TCT TCT CTT* ***GGC CAT CGA TGA ATT CTC TGT CG***	2
Gene deletion	*5'HphDelSsf2*	*Fwd*	*5' TAA TAT TCG ACT AAA TTG CAG CTG CTA GGT CAC CAT CCC GCA CAT ACC TTA GAT ATT TTG GAA CTA ATG* ***CGT ACG CTG CAG GTC GAC***	3
	3'HphDelSsf2	*Rev*	*5' ATC GGA GTC ATG GCT ACT ATA TGG ATA GTG ATG TTA CGT ACG GAG GAT ATA TAT ACA TAT CGT GCA TAA* ***ATC GAT GAA TTC GAG CTC G***	3
Cterm PrA	*5'Cic1PrACterm*	*Fwd*	*5' GAA AAA GAA TCT AGC GAG TCA GAA GCT GTC AAG AAG GCT AAA AGT* ***GGT GAA GCT CAA AAA CTT AAT***	4
	3'Cic1PrACterm	*Rev*	*5' GCA CCG CAC TCT ATG AAA TTC AAA TTT TTT TCT TCA CAA GAA AAA* ***GTC GAC GGT ATC GAT AAG CTT***	4
	5'Ssf1PrACterm	*Fwd*	*5' AGT GAC AGC GAA CAT TAT GGT AGC GTA CCA GAG GAT CTA GAT AGT GAC TTA TTT AGT GAG GTC GAA****GGT GAA GCT CAA AAA CTT AAT***	4
	3'Ssf1PrACterm	*Rev*	*5' TAT ATG TAT CAA GTA TGC AAT TTA TCT AAA GTG AAG AAG TAT ACG TGC GTT GGT GGA TAG CCA GGC* ***GTC GAC GGT ATC GAT AAG CTT***	4
	5'Ssf2PrACterm	*Fwd*	*5' GAT GTA CCA GAG GAT TTG GAT AGT GAC TTA TTC AGT GAA GTA GAA* ***GGT GAA GCT CAA AAA CTT AAT***	4
	3'Ssf2PrACterm	*Rev*	*5' TAT GAA TAA ACA GAC ACT TCC TGG TTC TTT AAG TCC ATC GGA GTC* ***GTC GAC GGT ATC GAT AAG CTT***	4

*: sequence underligned corresponds to start or stop, sequence in bold **sequence annealing with plasmid**

Table XIII: List of plasmids used to make the cassettes used for yeast transformations

#	Plasmid	Plasmid size (bp)	Bacterial resistance	Modification type		Yeast selection marker	Expected length of insert* (bp)	Reference
				Term	Nature of tag			
1	pFA6a-Pgal-3HA-KanMX6	4821	Amp	N	pGAL1::3xHA-	-KanMX6	2236	(76)
2	pYM-N36	4347	Amp	N	pMet25::3XHA-	clonNAT	1892	(77)
3	pFa6a-hphNT1	4167	Amp	Gene deletion		Hph	1840	(77)
4	pBXA-PrA-SpHis5	2595	Amp	C	-PrA	-HIS5	1950-1980	(78)

*: variation depends on the length of sequence in the primer annealing with the target gene

Table XIV: PCR programs used to generate cassettes from plasmids

Plasmids 1, 4		
Temperature (°C)	**Time (min:sec)**	**# Cycles**
98	0:30	1X
98	0:05	30X
SSF1/2: 66	0:10	
72	0:30	
72	5:00	1X
4	Forever	1X

Plasmids 2, 3 (modified from Janke 2004)		
Temperature (°C)	**Time (min:sec)**	**# Cycles**
98	0:30	1X
98 [b]	1:00	10X
54	0:30	
72	1:20	
98	1:00	20X
54	0:30	
72	1:20+0:10/cycle	
4	Forever	1X

[a]: The elongation time depended on the expected length of product specified in table XVIII: iProof taq elongates 1KB/30sec.

Table XV: List of antibiotics used when manipulating yeast

Antibiotic	**Abbreviation**	**1X concentration (µg/mL)**
Geneticin	G418	200 and then 600
Noursethricine	ClonNAT	300
Hygromycin B	Hph	300

Table XVI: List of control primers used to validate yeast transformants

Name	**direction**	**Sequence**	**Salt adjusted T_m (°C)**
5'UTR NOP7	*Fwd*	*5' ACC ATA CAG GTC TTG ATA AAT*	*53.5*
5'UTR SSF1	*Fwd*	*5' AAA AAG TAG ACG AAG AAG CTC*	*56.7*
5'UTR SSF2	*Fwd*	*5' CTT CCT TTT TGG TCT TTA GTC*	*56.7*
3'N-ORF of KanMX6	*Rev*	*5' ATC GCG AGC CCA TTT ATA CCC*	*48*
3'N-ORF of hph	*Rev*	*5' CAT CAC AGT TTG CCA GTG ATA*	*58.7*
3'N-ORF SSF1/2*	*Rev*	*5' GAA GTC CTT TAC TAA TTG GTT*	*54.8*
5'C-ORF CIC1	*Fwd*	*5' TCC GAA TTG GGT TCA ATT TTC*	*55.5*
5'C-ORF SSF1/2*	*Fwd*	*5' GAA GGT CAA GGA AAA GAT GAT*	*56.7*
*5'C-ORF SSF1/2**	*Fwd*	*5' TTG GAA AGA AGA AAA GCT AGA*	*54.8*
3'UTR CIC1	*Rev*	*5' CCG AGA AAC CAA TAT TCA AAT*	*53.5*
3'UTR SSF1	*Rev*	*5' TCT GAG ATC TAC GTT TCC TTT*	*56.7*
3'UTR SSF2	*Rev*	*5' ATA TTT ACT TTG AGG TGT TCC*	*54.8*

Table XVII: Expected PCR product sizes in genomically modified and control strains

Diagnostic PCR			Control primer location*		Expected PCR product size (bp)		Nature of modification
Term	primer set	tests for	FWD	REV	If WT	if modified	
N	*1*	*SSF1 5'UTR modification*	*5'UTR SSF1*	*3'N-ORF SSF**1***/2*	*260*	*2152*	*pMet25 insertion*
	2	*SSF2 presence*	*5'UTR SSF2*	*3'N-ORF SSF**1***/2*	*629*	-	-
	3	*SSF2 ORF replacement*	*5'UTR SSF2*	*3'N-ORF of hph*	-	*935*	*gene replaced by hph gene*
	4	*NOP7 5'UTR modification*	*5'UTR NOP7*	*3'N-ORF of KanMX6*	-	*1387*	*pGal1 insertion*
C	*5*	*SSF2 modification*	*5'C-ORF SSF1/**2***	*3'UTR SSF2*	*282*	*2163*	*PrA tag*
	6	*SSF1 modification*	*5'C-ORF SSF**1***/2*	*3'UTR SSF1*	*263*	*2177*	*PrA tag*
	7	*CIC1 modification*	*5'C-ORF CIC1*	*3'UTR CIC1*	*264*	*2178*	*PrA tag*

*: Because of the high homology at the nucleotide level, most 21nt primers could anneal to a certain extent both SSF genes. However, their 5' and 3' UTR sequences are different from each other according to a blast2seq alignment.

Table XVIII : Standardized diagnostic PCR program

Temperature (°C)	Time(min:sec)	Number of cycles
95	*5:00*	*1X*
95	*0:30*	*39X*
52	*0:30*	
68	*2:30*	
68	*5:00*	*1X*
4	*Forever*	

2.4.1.1 Regulatable promoter

Following recombinant homology, the sequence upstream of the gene start site was replaced by a selection marker followed by regulatable promoter and a 3xHA tag replacing the endogenous promoter. The selection markers were KanMX6 for the Gal1 promoter and clonNAT for the Met25 promoter. Positive transformants were detected using diagnostic PCR. A 21nt-long primer annealing with the 5'UTR (*fwd*) of the gene was used. In the case of the MET25 promoter insertion, a 21nt-long primer annealing with the SSF1 ORF was used and positive transformants were expected to yield a 2152nt-long PCR product, compared to a 260nt-long PCR product for negative transformants. For the Gal1 promoter insertion, the reverse primer was 21nt-long and annealed with the resistance marker used. Only positive transformants generated a PCR product (1387nt-long).

2.4.1.2 Gene deletion

Following recombinant homology, the complete gene, including its start and stop codons, was replaced by hygromycine B resistance. To screen for positive clones, diagnostic PCR using a primer annealing in the 5'UTR of the deleted gene and another annealing within the ORF of the selection marker was performed. Only positive transformants generated a PCR product (935nt-long).

2.4.1.3 C terminal fusion

Following recombinant homology, the stop codon of the targeted gene and about 45 nucleotides after the stop codon were replaced by the PrA tag, a stop codon, and the histidine selection marker, with its start and stop codons. The remaining 3' UTR of the gene was therefore shifted downstream. To screen for positive clones, a 21nt-long primer was designed in the forward strand of the gene ORF. It was used in pair with a 21nt-long primer that annealed a region about 200nts after the endogenous stop codon of the gene. Negative transformants gave a 263-282nt-long PCR product and positive transformants gave a 2163-2178nt-long PCR product.

2.4.2 Cassette amplification and purification

The cassettes used to carry out the genomic yeast modifications were amplified from the plasmids listed in Table XIII using primers listed in Table XII. Usually, 200-500µL of PCR mix was used with the following final concentrations: 1XiProof buffer, 0.5pmol/µL of 5' and 3' primers, 200µM of each dNTP, 2% DMSO, 1ng/µL plasmid, 0.25U/µL Taq. The PCR programs used depended on the plasmid and are summarized in Table XIV.

The PCR product was cleaned prior to transformation into the yeast cells. The phenol/Chloroform/IAA clean-up procedure used is the following: the PCR reactions were topped to 450µL with water and vortexed for 30sec with 450µL of phenol/Chloroform/IAA and then spun at V_{MAX} for 2min to separate phases. To precipitate the DNA, 400µL of the aqueous phase was mixed with 40µL of a 3M NaOAc pH5.2 solution, 2µL of glycogen stock

solution (10mg/µL) and 1000µL of 100% EtOH. This mixture was then stored at -20°C from 30min to o/n and then centrifuged for 10min at 4°C, V_{MAX}. The pellet was then washed with 500µL of 70% EtOH and air-dried at RT. The pellet was then resuspended in 11µL of water of which 1µL was used for visualisation on gel and 10µL for transformation.

2.4.3 Yeast transformation

For yeast transformations, yeast cells were first made competent as follows: 50mL of yeast cells in log phase were grown to an OD_{600} of 0.6-0.8, washed with 50mL and then with 1mL of water. The cleaned cells were recovered by centrifugation at 30sec at 4000rpm and made competent by treating them with 1XTELiAc (1mM Tris-Cl, 0.1mM EDTA, 100mM LiAc pH8.0) three times (1x1mL and 2x0.5mL). The cells were finally resuspended in 500µL of 1XTELiAc and 50µL of cells were used for yeast transformation.

For the transformation, 50µL of competent cells were incubated with 10µL of cleaned PCR product, 5µL of carrier DNA and 300µL of PEG4000 (0.4g/mL PEG 4000, 1X TELiAc) for 30min at 30°C, 400rpm. The cells were then heat shocked for 15min at 42°C, pelleted, resuspended in 100µL of 1X TE and plated on appropriate plates. Single clones were streaked and validated by PCR and WB.

All working stock solutions were prepared fresh and filter sterilized using a 0.45µm filter.

2.4.4 Screening for yeast transformants

2.4.4.1 Diagnostic PCR

To screen for positive transformants, diagnostic PCRs were performed on purified chDNA (Section 2.1.5.1). Biobasic's taq DNA polymerase was used to amplify the genome according to the specifications of the product provided by the supplier. A typical 25uL PCR mix contained the following final concentration of reagents: 1X PCR buffer, 0.5pmol/µL of 5' and 3' primers, 200µM of each dNTP, 20% DMSO, 100ng/µL chDNA, 0.25U/µL Taq. The standardized diagnostic PCR program used is detailed in Table XVIII. To standardize the PCR program, the annealing temperature (T_m) was set to 52°C. Since Biobasic's taq DNA

polymerase transcribes 1kb/min at 68°C and the longest expected PCR product was of 2178bp, elongation time was set to 2min30sec. At the end of the run, 3µL of 10X loading dye was added to the mix and 3-5µL was loaded on a 1% agarose gel and run in 1X TBE for visualisation (Fig. 2.6).

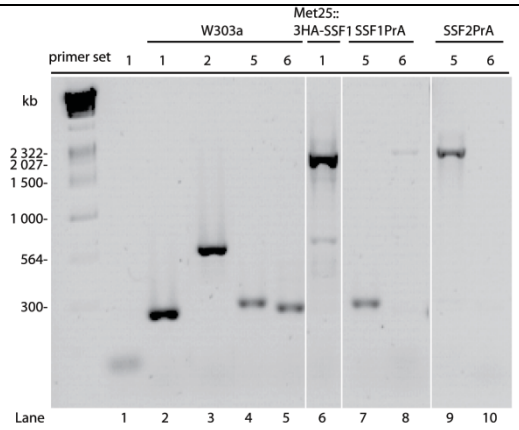

Figure 2.6: Diagnostic PCR

To validate transformants, diagnostic PCRs were performed on their purified chDNA (250ng) with sets of primers listed in Table XVI and using a standardized diagnostic PCR program (Table XVIII) Lane 1 shows where the primers migrate, W303a was used as negative control (lanes 2-5). Lanes 7-10 show that the PrA tag of either Ssf1 or Ssf2 is specific (expected sizes of amplicons are listed in Table XVII).

2.5 Growth curve

The strains were grown in 250mL of permissive media to an OD_{600} ranging between 0.2-0.6. At T_0, the cells were pelleted, washed twice with sterile water and shifted in repressive media. At each time-point, the cells were diluted with repressive media to an OD_{600} ranging between 0.2-0.6 to keep them logarithmic phase throughout the experiment. Two samples were collected at each time-point ($20OD_{600}$ and $10OD_{600}$), washed twice with ultrapure water and stored at -80°C for subsequent RNA (NB, primer extension, qRT-PCR) and protein analysis (WB). The OD_{600} was measured before and after dilution at each timepoint to calculate the dilution factor of the time-point ($DF_{tp}=DO_{before}/DO_{after}$) and the cumulative dilution factor ($DF_{cum}= DF_{tp*} DF_{cum\ previous}$). The growth curve was performed at

least in duplicate for each strain. To construct the graphs of the relative OD_{600} against time, the mean and standard deviation of the replicates' relative OD_{600} was calculated for each time-point and outliers were discarded when the standard deviation was half of the mean.

2.5.1 Serial dilution

As a rapid way to confirm that only the depletion of both SSF proteins generated a growth defect similar to other essential RiBi proteins, a serial dilution test was performed. Cells were taken from plate or from liquid culture and brought to an OD_{600} of 1 (DIL0). For the serial dilution 100µL of the previous cell dilution was mixed with 900µL of sterile water. This procedure was performed to obtain DIL-1 (1/10), -2(1/100) and -3(1/1000). To test the inducible promoter, spots of 10µL of each culture were dried on permissive and restrictive plates and grown at 30°C.

2.6 Cell harvest and cryo-lysis [78]

Cell harvest and cryo-lysis was performed as described in (78).

2.6.1 Cell harvest

Depending on the amount of material needed, 0.2-6L of cells were grown up to an OD_{600} of 0.8 and spun at 4000x*g* for 5min. The cells were then washed twice with 50mL of water. The pellet was resuspended on ice with an equal volume of resuspension buffer (1.2% PVP-40, 20mM HEPES pH 7.4, 1:100 protease inhibitor cocktail, 1:100 solution P and 1:1000 DTT) and spun twice at 2600x*g* for 15min at 4°C to completely remove the supernatant. The pellet was then passed through a syringe onto a 50mL falcon tube filled with liquid nitrogen, broken down into smaller pieces with a spatula and stored at -80°C.

2.6.2 Cryo-lysis

The noodles were placed into a metal jar filled with metal beads and pre-chilled with liquid nitrogen. The cells were cryo-lysed using a Retsch PM-100 ball mill (eight cycles of 400rpm, 1min rotation clockwise, 1min rotation counter-clockwise, 1min rotation clockwise). The jar was chilled in liquid nitrogen in between cycles. The final cell powder was stored at -80°C.

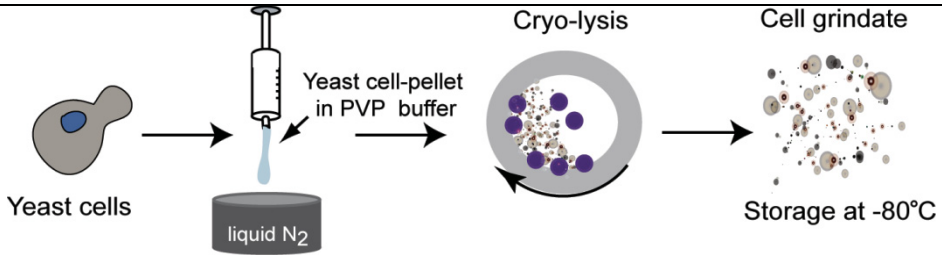

Figure 2.7: Cryolysis and storage
The cells were harvested during log phase, treated with PVP buffer, cryo-lysed and stored at -80°C. Taken from (78).

2.7 Conjugating of Dynabeads with rabbit IgG [78]

This protocol was carried out as described in (78) to obtain 160µg of rabbit IgG per mg of Dynabeads, with a final concentration of 0.15µg of beads per µL of solution. Total volumes and amounts are listed here but, to facilitate magnetic bead recovery, the mixtures were divided into four equal volumes in 15mL Falcon tubes.

To reconstitute the magnetic beads, 300mg of Dynabeads were resuspended in 16mL of a 0.1M $NaPO_4$, pH7.4 buffer by vortexing for 30sec. The solution was incubated at RT, rocking for 10min and the beads were recovered using a magnetic holder and washed with 16mL of the same buffer by vortexing (15sec).

To prepare the antibodies, 3.525mL of a 14mg/mL rabbit IgG stock was mixed with 9.850mL of 0.1M $NaPO_4$, pH7.4 and then 6.650mL of 3M NH_4SO_4 was slowly added while shaking. The solution was then filtered using a 0.22µm filter.

Once the antibody solution was ready, the beads were magnetically recovered and incubated for 18-24hrs at 30°C, rocking. The beads were then submitted to a series of washes:

- 1X 12mL of 100mM Glycine pH 2.5;
- 1X: 12mL of 10mM Tris pH8.8;
- 1X: 12mL of 100mM Triethylamine;
- 5X: 12mL of PBS 1X, rocking for 5minutes;
- 1X: 12mL of PBS 1X, 0.5% Triton X-100, rocking for 5minutes;
- 1X: 12mL of PBS 1X, 0.5% Triton X-100, rocking for 15minutes.

All the beads were then resuspended in 2mL of 1X PBS, 0.02% NaN_3 and can be stored at 4°C for up to several months.

PBS 1X, 1L: 0.26g $NaH_2PO_4*H_2O$, 1.44g $Na_2HPO_4*2H_2O$, 8.78g NaCl, final pH 7.4

2.8 Single-Step affinity purification (ssAP) [78]

Intact pre-rRNP complexes recovery was performed as described in (78). In the 96-well single step affinity purification (ssAP), a variant of the protocol was used to fit in 2mL wells in which everything was scaled down to 0.2-0.4g of cell powder.

2.8.1 ssAP and the extraction buffer

To determine the relative stability of the complexes made by Ssf1 and Ssf2 proteins, strains in which they were PrA-tagged were used to perform their single step affinity purification in a 96-well AP design detailed below, using 26 different extraction buffers with various types of salt of varying stringency and concentrations (Fig. 2.8). Some of these buffers are detailed in the results section in Figure 3.1.

Because of the relative abundance of these proteins in the cell, 0.2g of cell grindate was used for Ssf1-PrA (8150 molecules/cell) and Nop7-PrA (4530 molecules/cell) baits and 0.4g of grindate was used for Ssf2-PrA (1350 molecules/cell). The background strain (W303a) and the PrA tag expressed alone (pZPR::PrA) were used as negative controls. First, the cells were harvested and cryo-lysed using the protocol detailed in Section 2.6. For 0.2g of frozen cell grindate, 10µL of rabbit IgG conjugated Dynabeads (0.15µg/µL, Section 2.7) were pre-washed three times in 200µL of extraction buffer and resuspended in 10-15µL of

extraction buffer. The cell grindate was then thawed on ice and resuspended by pipetting in 1.8mL (for a 1:9 ratio) or 0.8mL (for a 1:4 ratio) of cold extraction buffer. The mixture was spun at 4°C, 3500rpm for 10min and the supernatant was incubated with the beads at 4°C for 30min with slow rotation. The beads were then magnetically recovered and washed three times with 250µL of extraction buffer and then incubated at RT with 250µL of last wash buffer (100mM NH_4OAc/0.1mM $MgCl_2$/0.02% Tween20) for 5min and with slow rotation. The PrA tagged protein along with its RNP complex was then eluted by incubating it twice with 250µL of elution buffer solution (500mM NH_4OAc/0.5mM EDTA) with slow rotation for 20min at RT. The eluates were pooled, dried using a speedvac compatible with organic solvents, and stored at -80°C.

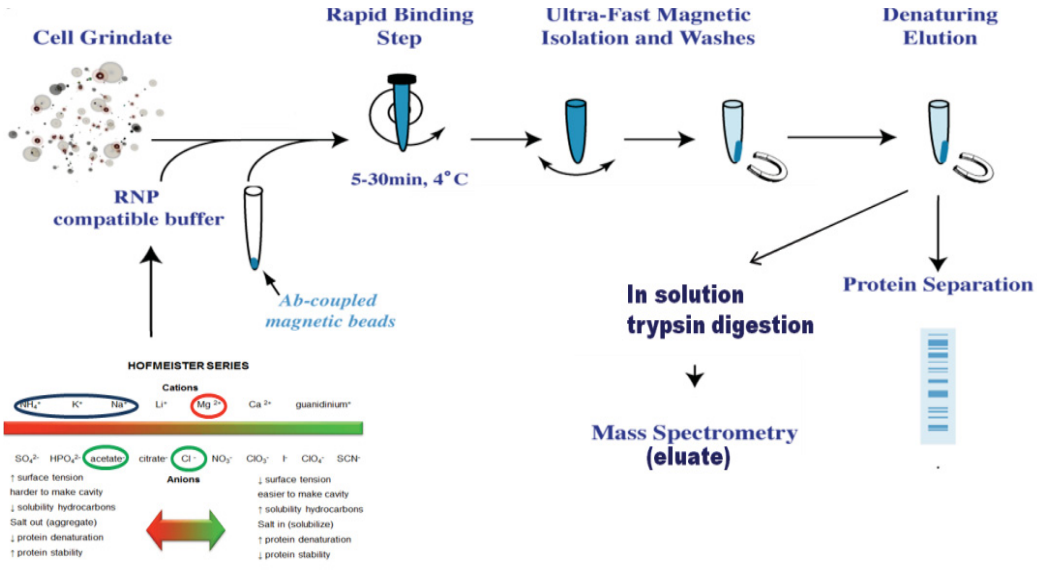

Figure 2.8:Affinity purification of intact pre-rRNP complexes.
Intact pre-rRNP complexes are recovered from cryo-lyzed log-phase cultures using a rapid single step affinity purification (ssAP) and buffers optimized for each bait protein. Adapted from (78, 79).

2.8.2 Pre-rRNP complex visualisation

The proteins were resuspended in 16µL of 1X loading dye, heated at 70°C for 10min. 8µL of the mixture was resolved using a pre-cast 4-12% Bis-Tris gel and proteins were visualized as described in (78) using a silver staining kit from invitrogen. To discriminate by eye more easily proteins belonging to the rRNPs from the background proteins, the W303a AP performed in the same buffer, which always gave a higher background than the PrA tag expressed alone, was superposed to the bait proteins AP using Photoshop.

2.9 Protease accessibility laddering [80]

For this experiment, a variant of the affinity purification protocol detailed in Section 2.8.2 was used as described in (80). For Ssf1-PrA and Nop7-PrA, 1.25g of thawed cell grindate was resuspended in TBT buffer (20mM Hepes pH 7.4, 100mM NaCl, 110mM KOAc, 0.1% Tween20, 2mM $MgCl_2$, 1:500 PIC, 1mM DTT, 1:5000 antifoam) supplemented with 1% Triton-X100 (1:9 ratio, vortex, 30sec), homogenized (polytron, 30sec) and centrifuged (15min, 2000g, 4°C). The supernatant was incubated with IgG-coupled magnetic beads for 1hr at 4°C. The beads were then submitted to five washes (1mL TBT+200mM $MgCl_2$). The beads were then resuspended in 250µL of 1X endoproteinase reaction buffer previously supplemented with 80ng of endoproteinase and 50µL aliquots were collected at timepoints 0.5, 3, 15, 75min. The reaction was stopped by adding Last Wash Buffer and incubating for 5minutes. Elution was then performed with 2x500µL of elution buffer (rock 20min at RT). Eluate was dried using a speed-vac, o/n at RT. For all previous steps, everything was doubled for *SSF2-PRA* cell grindate. The pellet was resuspended in 30µL of loading dye and 3µL was resolved on gel and immunoblotted on a PVDF membrane for PAP detection. For preliminary analysis, the amino acid sequence for each protein was compared to the proteolysis pattern obtained by the three endoproteinases. This allowed detecting the regions that were more susceptible for proteolysis (Fig. 2.9).

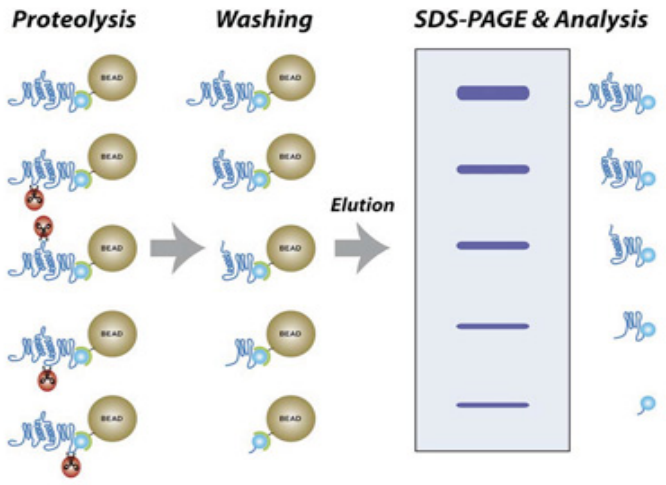

Figure 2.9 : Protease accessibility laddering (PAL) to detect exposed domains.
Using stringent buffer conditions, the PrA-tagged protein is recovered from cryolyzed cell grindate using magnetic beads and submitted to protease degradation. The PrA-recovered C-terminal end was analyzed by western blot. Figure taken from (80).

Roche endoproteinases Asp-N (catalog ID : 1 420 488 or 1 054 589, 2ug/vial), Lys-C (catalog ID : 1 420 429, 5ug/vial) and Trypsin (catalog ID : 1 521 187, 25ug/vial) were reconstituted on ice in 50uL of ultrapure water, as recommended by the supplier. Single used aliquots of 2.5uL were flash-frozen in liquid nitrogen and stored at -80°C.

To prepare the endoproteinase working stock for the PAL experiment, an aliquot of each endoproteinase was diluted with their respective 1X endoproteinase reaction buffer Asp-N (50mM Na_2PO_4 pH8.0, 0.1%SDS; 3.75µL), Lys-C (25mM Tris-Cl pH8.5, 0.1% SDS, 1mM EDTA; 11µL), Trypsin (100mM Tris-Cl pH8.5, 0.1%SDS; 64µL) to give a mix of about 16ng/µL.

2.10 qRT-PCR

To screen for any changes in mRNA levels of our proteins of interest in response to the depletion of one of them, quantitative reverse transcriptase polymerase chain reaction (qRT-PCR) was performed on cDNAs obtained using random primers (Section 2.1.8).

The primers (Table XIX) were designed to have a salt adjusted T_m close to 60°C and to generate a PCR product of 96-173bps. An additional care was taken when designing the primers to be able to discriminate between the mRNA of each of the Ssf paralogs. The

sequence tag present in some strains (HA-SSF1, SSF1-PRA, SSF2-PRA) was used to discriminate between both Ssf paralog, as one primer was designed fully or partially in this sequence. Endogenous primers for each protein were also designed and validated using PrimerBlast (endSSF1, endSSF2, endNOP7).

Table XIX: Primers designed for qRT-PCR

Primer ID		Sequence	Salt adjusted T_m (°C)
5RTPCR-SSF2PRA	Fwd	5'-AGG TCA AGG GAA AGA TGG TG	59
3RTPCR-SSF2PRA	Rev	5'- TTT GAG CTT CAC CTT CTA CTT CA	58
5RTPCR-SSF1PRA	Fwd	5'- CGA TGA GCG ATG ATG AGT CT	59
3RTPCR-SSF1PRA	Rev	5'- GCT TCA CCT TCG ACC TCA CTA	59
5RTPCR-HASSF1	Fwd	5' AAT TCA TCG GCC AAG AGA AG	59
3RTPCR-HASSF1	Rev	5'-CAC TCT GAT TAC CAT TGA CTT AGG TAT	58
5RTPCR-endSSF1	Fwd	5'- ACA GTG CCG AAT TTG CAT CG	60
3RTPCR-endSSF1	Rev	5'-ACC GGT GTT CTT TGG GAC TT	59.5
5RTPCR-endSSF2	Fwd	5'-TCT CAA ACT TCG CTG TCG CA	60
3RTPCR-endSSF2	Rev	5'- ACG TGG AGT TGG TTG CGA AT	60.5
5RTPCR-endNOP7	Fwd	5'- CAA GGG CTC TAC TGC ACC AA	60
3RT-PCRendNOP7	Rev	5'-CCC TAC CCA AAG CCC TTG TT	60
Controls			
ACT1fwd [81]	Fwd	5'-ATT ATA TGT TTA GAG GTT GCT GCT TTG G	58
ACT1rev [81]	Fwd	5'-CAA TTC GTT GTA GAA GGT ATG ATG CC	60
UBC6fwd [81]	Fwd	5'-GAT ACT TGG AAT CCT GGC TGG TCT GTC TC	69
UBC6rev [81]	Rev	5'- AAA GGG TCT TCT GTT TCA TCA CCT GTA TTT GC	66

Before attempting the experiment, the efficiency of each primer sets were tested as follows: 5µL of four different samples were mixed together (dilution 1/4) and further diluted with 60µL of water (V_{tot}=80 µL) and the same procedure was done with their corresponding negative controls (RT-). These dilutions (1/16) were considered to be dilution 1 in the qRT-PCR tests. The RT+ was further diluted in series to give dilutions 1/10, 1/100, 1/1000 and1/10 000 (10µL of previous dilution in 90µL water). For each primer set, the PCR reaction was performed in duplicate for each cDNA dilutions (1 to 1/10 000) and for RT- (Dil 1). Each reaction contained 3µL of cDNA (of varying dilutions), 5µL of SYBR Select Master Mix (2X, from Applied Biosystems) and 0.5µL of each primer set (10µM stocks). The PCR was performed in a 96-well format using ViiA7 and with the following PCR program: 50°C, 2min; 95°C, 2min and 40X (95°C, 15sec; 60°C, 1min), followed by a melting curve analysis.

The preliminary analysis showed that the primers recognized only one template, as a single peak, with the same T_m, was observed in the melting curve plot for all cDNA dilutions. Here, a representative melting curve obtained for one primer set which targets UBC6 mRNA is presented and shows a single peak (Fig 2.10A). The threshold cycle (Ct) value can be linearly correlated to the levels of target cDNA present in the sample, as demonstrated by the standard curve (Fig 2.10B). For all primer sets, R^2 of this standard curve ranged between 0.98-1. From these analyses, it was determined that the best dilution of cDNA to use for every sample was DIL1, as it gave a Ct value of about 20 cycles for all genes tested under normal conditions. For normalisation purposes, mRNA levels of actin and UBC6 were also tested for every sample. All samples were normalized against actin or UBC6 [81]. To detect mRNA level changes for a given gene, its mRNA levels at time 0 were assigned the value of 1.

A

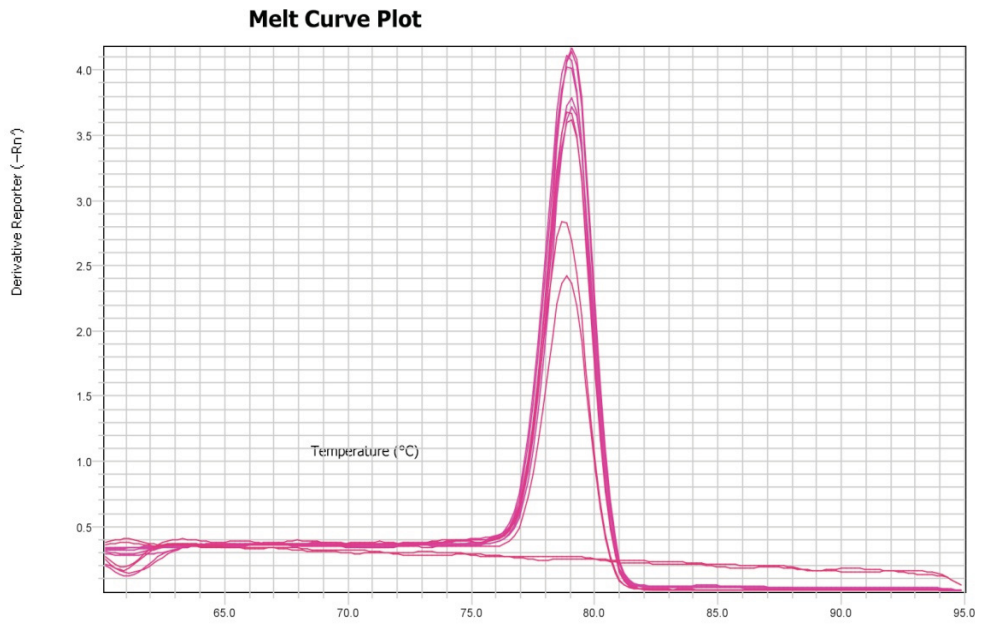

B

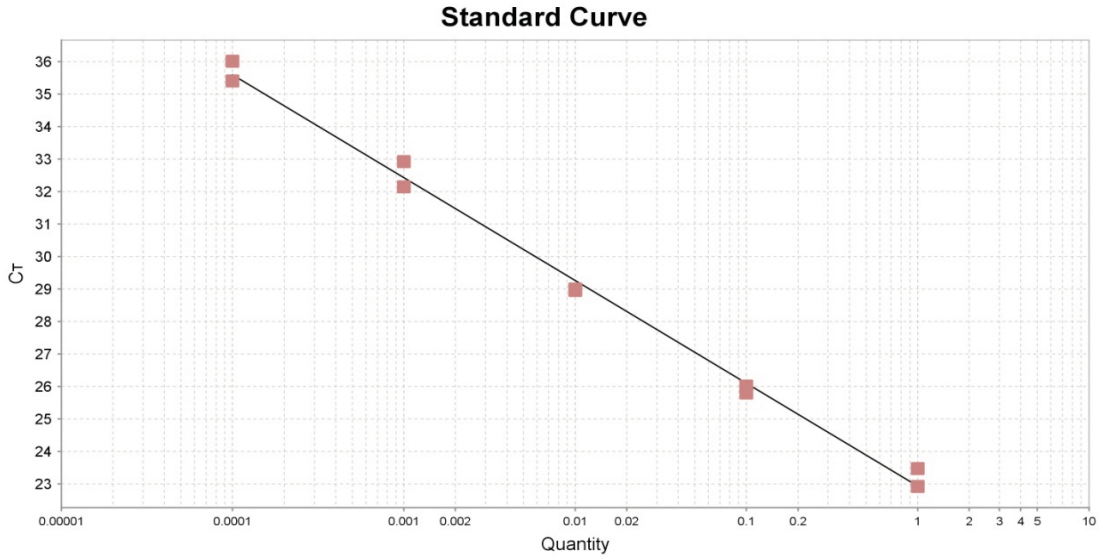

Figure 2.10: UBC6 qRT-PCR melting and standard curves

Prior to their use, each primer set was tested to validate their template specificity (melting curve) and linear correlation (R^2 = 0.98-1) between C_T values and levels of target cDNA (standard curve). Here: the UBC6 primers **(A)** generate a single narrow peak for all cDNA dilutions, which indicate that the primers are specific. **(B)** Additionally, the UBC6 primers generate C_T values which can be linearly correlated (R^2=1) with the levels of target cDNA present in a given sample.

The specificity of the endogenous primers targeting SSF1 (endSSF1) and SSF2 mRNA (endSSF2) was verified (Fig. 2.11) by testing them using the cDNA of *MET::HA-SSF1/SSF2-PRA* strain before and after shutting off the repressible promoter (depleted HA-SSF1 mRNA). Their results were compared to the primer sets overlapping with the tags (SSF2-PRA and HA-SSF1). The endSSF2 primers detected no significant change in mRNA levels after HA-SSF1 depletion (1.052), similar to what was obtained using the SSF2-PRA primers (1.016). The endSSF1 primer set detected a decrease in mRNA upon HA-SSF1 depletion (0.157), similar to what was observed with the HA-SSF1 primer set (0.051). The endogenous primers are therefore specific, as they give similar results when compared to the primer sets overlapping with the tags (SSF2-PRA and HA-SSF1).

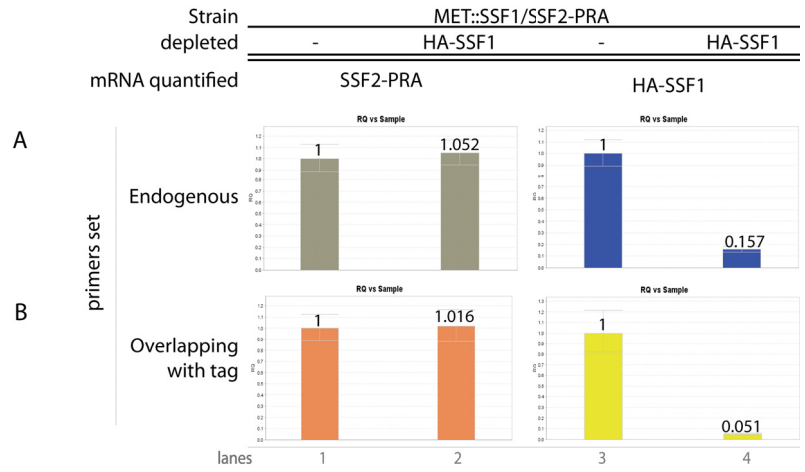

primer set	strain	MET::SSF1/SSF2-PRA	
	depletion	HA-SSF1	
	mRNA quantified	SSF2-PRA	HA-SSF1
endogenous	fold change	1,052	0,157
	significant	-	decrease
overlapping with tag	fold change	1,016	0,051
	significant	-	decrease

Figure 2.11: Endogenous primers designed for qRT-PCR can discriminate between SSF paralogs.

As SSF1 and SSF2 mRNAs are highly similar, the specificity of the primer pairs targeting their endogenous sequence needed to be verified. **(A)** The endogenous primers were tested against the cDNA of *MET::HA-SSF1/SSF2-PRA* strain, before (lanes 1 and 3) and after (lanes 2 and 4))shutting off the repressible promoter (HA-SSF1 depletion). **(B)**These gave similar results as primers overlaping with the tags (HA-SSF1 and SSF2-PRA), which confirmed their specificity.

3 Results

3.1 Generation of Yeast strains

The Ssf proteins share 94% of their sequence and are believed to be redundant in the cell. However, analysis of their BioGRID interactors has revealed that this is not the case. The first aim of this project is to determine if there are notable differences between the particles that the Ssf proteins form, as the Ssf2-particle has never been reported during log phase. For this purpose, *SSF1-PRA* and *SSF2-PRA* strains were generated to compare their particles and potentially detect subcomplexes they form by ssAP (Section 3.2). In these assays, the controls were W303a and the PRA-tag expressed alone.

Another aim is to potentially uncover the presence of parallel pathways during ribosome biogenesis involving one of the Ssf paralogs and Nop7. To alter the levels of these proteins, several strains were generated by genomically modifying haploid W303a (regulatable promoter insertion, gene deletion and C-termini tag insertion, Table XX). For this purpose, primers were designed to anneal with a genomic sequence of W303a in their 5' (45-66nts) followed by a sequence annealing (18-21nts) with a plasmid containing the modification and a resistance cassette. The generated cassette was transformed into the background strain and transformants were validated by WB and diagnostic PCR.

Combination strains were constructed to potentially uncover the presence of parallel pathways involving Nop7/Ssf1 and Ssf2 (Sections 3.3). All strains have a C-termini PRA-tagged gene that is under its own promoter. The PRA-tag is relatively small (27kDa), and has been selected for its capacity of strongly bind to IgG antibodies, a feature useful for pre-rRNP complex isolation by ssAP (Section 3.2). The PRA-tag can also be readily detected using an HRP-coupled rabbit antibody (PAP), which was useful to monitor the behavior of the tagged RiBi proteins upon depletion of Ssf1 and/or Nop7 (Section 3.3). SSF1 and NOP7 genes were put under the influence of a regulatable promoter (Met25 and Gal1 respectively) and their levels can be monitored by WB through an N-termini HA epitope (3kDa) that has been integrated into the cassette. These promoters slightly over-express the target proteins in permissive media (-methionine and GRS respectively) but this does not happen to negatively affect cell growth or progression of ribosome biogenesis. By switching media (+met and

dextrose respectively), the expression of the protein that is under the control of the regulatable promoter can be modulated. As the Ssf proteins might have a different function during ribosome biogenesis, the SSF2 gene was deleted in some strains.

Table XX: Yeast strains used in this study

Name/phenotype	Background	Genotype	Reference
W303a	-	*MAT*a {*leu2-3,112 trp1-1 can1-100 ura3-1 ade2-1 his3-11,15*}	(78)
ZPR::PRA	W303	*MAT*a {*leu2-3,112 trp1-1 can1-100 ura3-1 ade2-1 his3-11,15 YGR211W::PRA* }	(78)
SSF1-PRA	W303	*MAT*a {*leu2-3,112 trp1-1 can1-100 ura3-1 ade2-1 his3-11,15 YHR066W-PRA-SpHIS5*}	This study
SSF2-PRA	W303	*MAT*a {*leu2-3,112 trp1-1 can1-100 ura3-1 ade2-1 his3-11,15 YDR312W-PRA-SpHIS5*}	This study
NOP7-PRA	W303	*MAT*a {*leu2-3,112 trp1-1 can1-100 ura3-1 ade2-1 his3-11,15 YGR103W-PRA-SpHIS5* }	(78)
SSF2-PRA/ MET25::SSF1	W303	*MAT*a {*leu2-3,112 trp1-1 can1-100 ura3-1 ade2-1 his3-11,15 YDR312W-PRA-SpHIS5 ClonNAT-MET25::3HA-YHR066W*}	This study
CIC1-PRA/ MET25::SSF1/ ΔSSF2	W303	*MAT*a {*leu2-3,112 trp1-1 can1-100 ura3-1 ade2-1 his3-11,15 YHR052W::PRA-SpHIS5 ClonNAT-MET25::3HA-YHR066W YDR312WΔ::hph*}	This study
NOP7-PRA/ MET25::SSF1/ ΔSSF2	W303	*MAT*a {*leu2-3,112 trp1-1 can1-100 ura3-1 ade2-1 his3-11,15 YGR103W-PRA-SpHIS5 ClonNAT-MET25::3HA-YHR066W YDR312WΔ::hph*}	This study
SSF1-PRA/ GAL1::NOP7	W303	*MAT*a {*leu2-3,112 trp1-1 can1-100 ura3-1 ade2-1 his3-11,15 YHR066W-PRA-SpHIS5 KanMX6-GAL1::3HA-YGR103W*}	This study
SSF2-PRA/ GAL1::NOP7	W303	*MAT*a {*leu2-3,112 trp1-1 can1-100 ura3-1 ade2-1 his3-11,15 YDR312W-PRA-SpHIS5 KanMX6-GAL1::3HA-YGR103W*}	This study
SSF1-PRA/ GAL1::NOP7/ ΔSSF2	W303	*MAT*a {*leu2-3,112 trp1-1 can1-100 ura3-1 ade2-1 his3-11,15 YHR066W-PRA-SpHIS5 KanMX6-GAL1::3HA-YGR103W YDR312WΔ::hph*}	This study
SSF2-PRA/ GAL1::NOP7/ MET25::SSF1	W303	*MAT*a {*leu2-3,112 trp1-1 can1-100 ura3-1 ade2-1 his3-11,15 YDR312W-PRA-SpHIS5 KanMX6-GAL1::3HA-YGR103W ClonNAT-MET25::3HA-YHR066W*}	This study

All combination strains were analyzed in repressive media that is upon depletion of HA-SSF1 and/or HA-NOP7 in the presence or absence of SSF2. Each strain was tested during three independent experiments, except the *SSF1-PRA/GAL1::NOP7/ΔSSF2* strain, which was tested in duplicate only. For all strains, cell growth was monitored in repressive media for at least 20 hours as described in Section 2.5. In addition to changes in cell growth, total protein levels of the selected proteins were monitored by WB. Changes in pre-rRNA processing were monitored by NB using fluorescently labelled probes and the mature rRNAs were also detected by methylene blue staining. As premature C_2 cleavage was reported upon Nop7 depletion and also upon depletion of the SSF proteins, primer extension analysis of the C_2 and

$C_1/C_{1'}$ sites were also performed for all strains. Changes in SSF1, SSF2 and NOP7 mRNA levels were monitored by qRT-PCR (Section 3.6).

Finally, as both Ssf1 and Ssf2 potentially form homo or heterodimers, bind pre-rRNA and also bind Nop7, plasmids were constructed and the optimised conditions were determined for recombinant Ssf1, Ssf2 and Nop7 protein purification (Section 2.3). The recombinant protein will be useful for future *in vitro* interaction studies. In order to look for potential folding differences between Ssf1 and Ssf2, Ssf1-PrA and Ssf2-PrA proteins were submitted to protease accessibility laddering while they were in complex with other proteins (Section 3.7).

3.2 Ssf1 and Ssf2 form similar complexes

In order to compare Ssf1-PrA and Ssf2-PrA particles and potentially detect subcomplexes that these proteins form, ssAP (single-step affinity purification) was performed using a 96-well format. SSF1-PRA and SSF2-PRA cells were harvested and cryo-lysed. During the ssAP, the particle is recovered either intact or partially disrupted, depending on the stability of the particle and on the stringency of the buffer used during the ssAP. Since the relative stability of the complexes made by Ssf1 and Ssf2 proteins were not known, various salts were selected according to their stabilisation properties: KOAc > NH_4OAc > NaCl > NaCitrate [79, 82, 83]. In order to obtain buffers of varying stringency, these salts were used in different concentrations ranging from 100-300mM and once, $MgCl_2$ and DTT were used in low concentrations (2mM and 1mM respectively in buffer 1, TBT). The detailed composition of the buffers is detailed in Fig. 3.1C. The cell grindate was solubilised in the selected buffer and incubated with IgG-coupled magnetic metal beads [78]. The PrA tagged protein along with its intact or partially disrupted pre-rRNP complex was then eluted from the beads using NH_4OH. Proteins were separated by size (4-12% Bis-Tris) and visualized by silver staining [78]. The controls used are the background strain (W303a) and the PrA tag expressed alone under the control of the ZPR1 promoter (*ZPR::PRA*).

In general, W303a cells generated more background than ZPR::PRA; hence bands found in these two control strains were considered contaminants (Fig. 3.1B). The buffer giving the most background contained 100mM KOAc salt (Fig. 3.1A, buffer4). Neither addition of

DTT nor $MgCl_2$ had an effect on the band patterns observed (Fig. 3.1A, buffer1), which suggest that the particle stability is not affected by disruption of proteins with disulfide bonds nor by stabilizing RNA-protein interactions [78, 84]. To verify if a change in the powder to buffer ratio had an effect on the the background observed in the control strains, ssAP was performed using two powder to buffer rations (1:9 and 1:4) but this did not generate a significant change in the background for buffers #1, 2, 3 and 6.

Ssf1-PrA and Ssf2-PrA ssAPs revealed identical band patterns, which indicate that these proteins are most likely associated with similar sets of proteins. In particular, six proteins that have not yet been identified by MS repeatedly appeared in complex with each of the Ssf proteins (Fig. 3.1A). If these proteins are tightly bound to Ssf1-containing particles, then they are likely present in the proteins previously identified Ssf1 and likely enter the particle at the same time as Ssf1 (Fig. 1.7) [54, 67]. A protein of ~90kDa and two proteins appearing as a doublet at ~70kDas were continuously present, even under high-stringency conditions (buffer #6, NaCitrate 200mM) and could correspond to Dbp9, Drs1 and Nog1 [85]. The data suggest that the Ssf proteins form a stable sub-complex with these proteins. One protein of ~90kDas and two ~130kDas were repeatedly observed except when using NaCitrate-containing buffers, which are highly-stringent (buffers #3, #6 and #11). This probably indicates that these proteins are required for the sub-complex containing one of the Ssf proteins to assemble into the pre-rRNP complex and likely correspond to Dbp10, Noc1and Noc2. All of the patterns mentioned above are more strongly detected with SSF2-PRA than SSF1-PRA, indicating that the sub-complex is more stable with Ssf2. Both Ssf1 and Ssf2 associated complexes are completely disrupted in the presence of NaCitrate 300mM (buffer #11), which indicate that their interactions are less stable than other sub-complexes found during ribosome biogenesis, such as Noc1-Noc2 and Noc2-Noc3 heterodimers, which were still recovered in the low molecular weight fractions of a sucrose gradient using a buffer containing 800mM KCl [86]. The presence of a sub-complex containing Ssf1 protein is further supported by a sucrose gradient analysis which detected Ssf1-PrA in fractions of lower molecular weight than the 40S [54]. MS analysis of the Ssf particles is necessary to unambiguously identify the most abundant RiBi proteins in these particles and will be the next step.

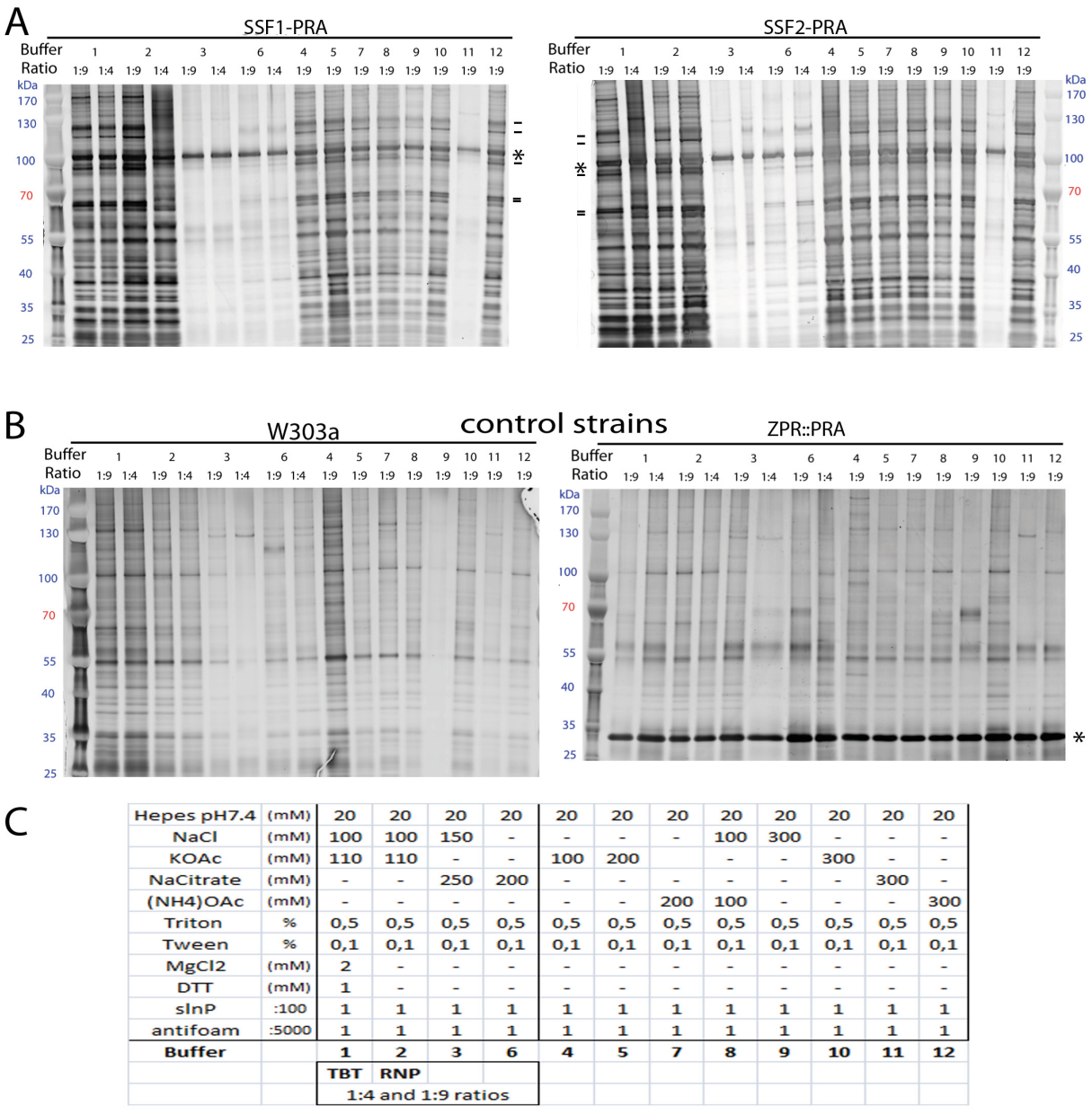

Hepes pH7.4	(mM)	20	20	20	20	20	20	20	20	20	20	20	20
NaCl	(mM)	100	100	150	-	-	-	-	100	300	-	-	-
KOAc	(mM)	110	110	-	-	100	200		-	-	300	-	-
NaCitrate	(mM)	-	-	250	200	-	-	-	-	-	-	300	-
(NH4)OAc	(mM)	-	-	-	-	-	-	200	100	-	-	-	300
Triton	%	0,5	0,5	0,5	0,5	0,5	0,5	0,5	0,5	0,5	0,5	0,5	0,5
Tween	%	0,1	0,1	0,1	0,1	0,1	0,1	0,1	0,1	0,1	0,1	0,1	0,1
MgCl2	(mM)	2	-	-	-	-	-	-	-	-	-	-	-
DTT	(mM)	1	-	-	-	-	-	-	-	-	-	-	-
sInP	:100	1	1	1	1	1	1	1	1	1	1	1	1
antifoam	:5000	1	1	1	1	1	1	1	1	1	1	1	1
Buffer		**1**	**2**	**3**	**6**	**4**	**5**	**7**	**8**	**9**	**10**	**11**	**12**
		TBT	**RNP**										
		1:4 and 1:9 ratios											

Figure 3.1: Stability of key pre-rRNP complex components

Grindate (0.25-0.5g) of cells were used. In these strains, **(A)** Ssf1 or Ssf2 was C-termini tagged (PrA) and used as bait (*) for ssAP. Recurring band patterns observed are indicated (-). **(B)** W303a and a strain expressing the PrA (*) tag alone were used as background strains. **(C)** Buffers of varying stringency were used for ssAP for each strain. For buffers #1, #2, #3 and #6, cell grindate to buffer ratio of 1:4 was also tested to verify if this change had a significant effect on background.

3.3 Ssf2 does not fully compensate for the loss of Ssf1

Initially, tetrad analysis of a diploid yeast strain lacking one copy of the SSF1 and SSF2 genes generated an inviable haploid spore, which corresponded to the one lacking both genes [49]. The other spores did not generate an obvious phenotype. In this study, a HA-SSF1-depleted strain was tested by serial dilution and the strain generated as many colonies as the wild-type strains but which were smaller, suggesting a mild growth defect (Fig. 3.2). The same phenotype was also observed in a strain slightly over-expressing HA-SSF1 in which SSF2 was deleted (data not shown). Consistent with the finding that the Ssf proteins are essential, HA-SSF1-depleted/SSF2Δ cells showed a growth defect similar to that observed upon depletion of an essential RiBi protein, like Nop7.

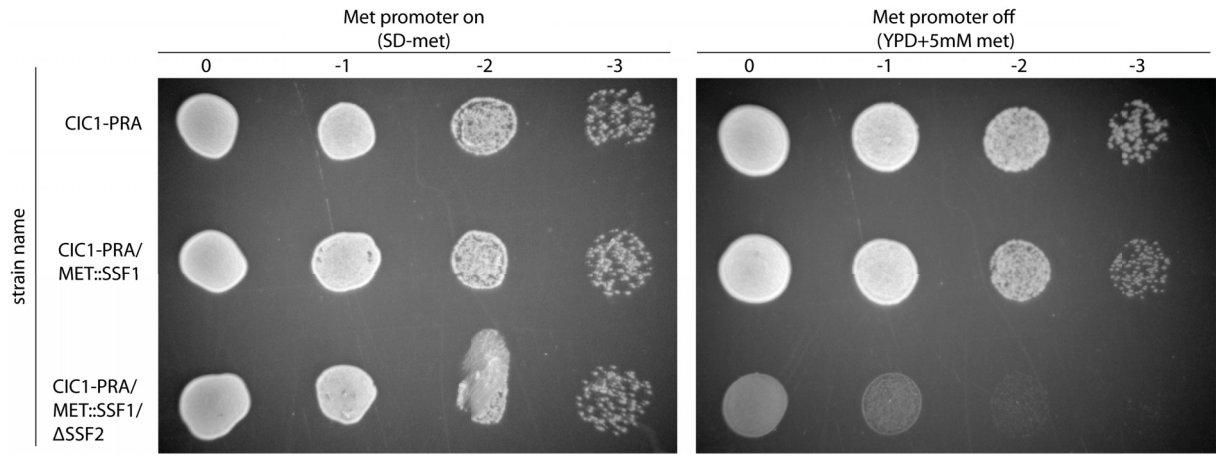

Figure 3.2: SSF1-depletion mildly affects cell growth

In permissive media, the three strains grow at a similar rate. In restrictive media, Ssf1-depleted cells show a mild growth defect while Ssf1-depleted/SSF2Δ-cells show a severe growth defect.

To further characterize this mild growth defect observed upon depletion of one of the SSF proteins, a growth curve was performed, which allows to quantify cell growth. The doubling time (Dt) of wild-type cells (WT, W303a) was of 90min (Fig. 3.3-3.5A). The precursors detected by NB in W303a were: 27SA (both $27SA_2$ and $27SA_3$) and 27SB, 23S, 20S, A_3-C_2, 7S, 6S; to a lesser extent, $27SA_2$ and non-detectable levels of A_2-C_2 (Fig. 3.3-3.5D, lanes 1-2). Primer extension using a probe annealing to the 5' coding region of the 25S

allowed the amplification of part of the ITS2. For W303a, this analysis showed no primer extension stop at the C_2 site and a normal $C_{1'}$ and C_1 stops, which indicates normal 5' processing of 25S (Fig. 3.3-3.5F lanes 1-2). The levels of mature rRNAs did not change (25S, 18S 5.8S and 5S). These were detected by using probes targeting their 5' (Fig. 3.3-3.5D lanes 1-2) and also by staining the membrane with methylene blue (Fig. 3.3-3.5E lanes 1-2). Staining also detected tRNAs, which could serve as a loading control, since 5S rRNA has been shown to decrease upon depletion of the Ssf paralogs.

HA-Ssf1 protein, was no longer detected after 6 hours of growing in repressive media (YPD+met) for the three strains tested, which indirectly confirmed repression of the HA-SSF1 gene. The Dt of HA-SSF1-depleted cells in which Ssf2 was present was of 120min (*MET::SSF1/SSF2-PRA*, Fig. 3.3A). Analysis of total protein showed that total Ssf2-PrA levels increased in these strains, which may indicated the existence of a compensatory mechanism (Fig. 3.3B lanes 3-6). However, this increase in Ssf2 was not sufficient to maintain ribosome biogenesis, which, at least partially, may explain the mild decrease in cell growth. Accumulation of 35S precursor and 23S and A_3-C_2 pre-rRNA indicate that ribosome biogenesis was mildly affected in this strain (Fig. 3.3D lanes 3-4). The levels of other intermediates and mature rRNAs did not seem to change and primer extension showed no stop at the C_2 site as well as normal $C_{1'}$ and C_1 stops (Fig. 3.3D-F lanes 3-4).

Two ΔSSF2 populations were also tested (*MET::SSF1/ΔSSF2/CIC1-PRA* and *MET::SSF1/ΔSSF2/NOP7-PRA*). In permissive media (t0), pre-rRNA analysis of these strains showed an accumulation of 35S (Fig. 3.3D lanes 5 and 7), indicating that slightly over-expressed levels of Ssf1 cannot fully compensate for the loss of Ssf2. In repressive media, the Dt of each population was of 168 and 180min respectively, a significant decrease in cell growth characteristic of the depletion of an essential RiBi gene, like Nop7 (Fig. 3.4A). As the depletion phenotype observed upon depletion of both of the Ssf proteins has been reported by Fatica *et al*, NB analysis and primer extension of the pre-rRNAs for these strains would corroborate their depletion phenotype. Therefore, an accumulation of 35S pre-rRNA and a reduction in $27SA_2$, 27SB, 20S, 7S, 6S precursors is expected, as well as a premature C_2 cleavage (primer extension), a reduction of all mature rRNAs, including 5S, and accumulation of aberrant pre-rRNAs (23S, 5'ETS-D, A_2-C_2) [54]. However, the background strains used in the previous study is W3031a, a strain sensitive to oxidative stress because of mutations in the

YBP1 gene. Therefore, it would be normal to observe slight differences in pre-rRNA processing, but the background strain used in this study (W303a) is expected to be more fit.

Upon HA-SSF1 depletion, *MET::SSF1/ΔSSF2/CIC1-PRA* showed a slight accumulation of 35S, concomitant with a decrease in $27SA_2$, 27SAs and 27SBs, 20S, 7S, 6S precursors, as previously reported (Fig. 3.3D lane 6). A premature C_2 cleavage was detected using primer extension as well as a mild decrease in $C_{1'}$ and C_1 stops, which indicate that the ITS2 processing from the C_2 cleavage site to the mature end of the 5'-25SrRNA is delayed (Fig. 3.3F lane 6). The 23S (5'ETS-A_3) pre-rRNA was still visible but decreased and this was concomitant with the appearance of a 22S (A_0-A_3) precursor, which indicate that A_0 site-processing is delayed but still occurring in the absence of the Ssf proteins (Fig. 3.3D lane 6). The probe required for 5'ETS-D pre-rRNA detection was not available at the time the probing was performed. Aberrant A_2-C_2 pre-rRNA could not be detected before or after depletion, which highlights a difference in pre-rRNA processing between W3031a and W303a. Instead, A_3-C_2 pre-rRNA accumulated, which indicate a premature C_2 cleavage is occurring, since it would be normally cleaved after complete ITS1 processing (Fig. 3.3D lane6). A decrease in all mature rRNAs, including the 5S, was detected by NB and methylene blue staining, confirming that depletion of the Ssf proteins induces a decrease in all mature rRNAs (Fig 3.3 D-E lanes 5-6). The same phenotype was observed for *MET::SSF1/ΔSSF2/NOP7-PRA*.

3.3.1 Nop7 levels are affected by Ssf protein levels

Using an antibody against endogenous Nop7, it was possible to detect constant levels of Nop7 in wild-type cells. However, endogenous levels of Nop7 could not be detected in the *MET::SSF1/SSF2-PRA* strain or in the *CIC1-PRA/MET::SSF1/ΔSSF2* strain, which suggest that Nop7 levels are decreased in these strains. Alternatively, this could also be explained in limitations of the WB analysis. However, analysis of the levels of Nop7-PrA in the third strain showed that the Nop7 protein levels decreased in the absence on the Ssf proteins, whereas Cic1-PrA protein levels, another RiBi protein, did not change (Fig. 3.3B lanes 7-11). Taken together, this data therefore contradicts the hypothesis that Nop7 and Ssf2 are not genetically linked and suggests that the levels of Nop7 are correlated to the cellular levels both Ssf

proteins. Additional analysis of other strains will help determine if the contrary is also valid (Section 3.5).

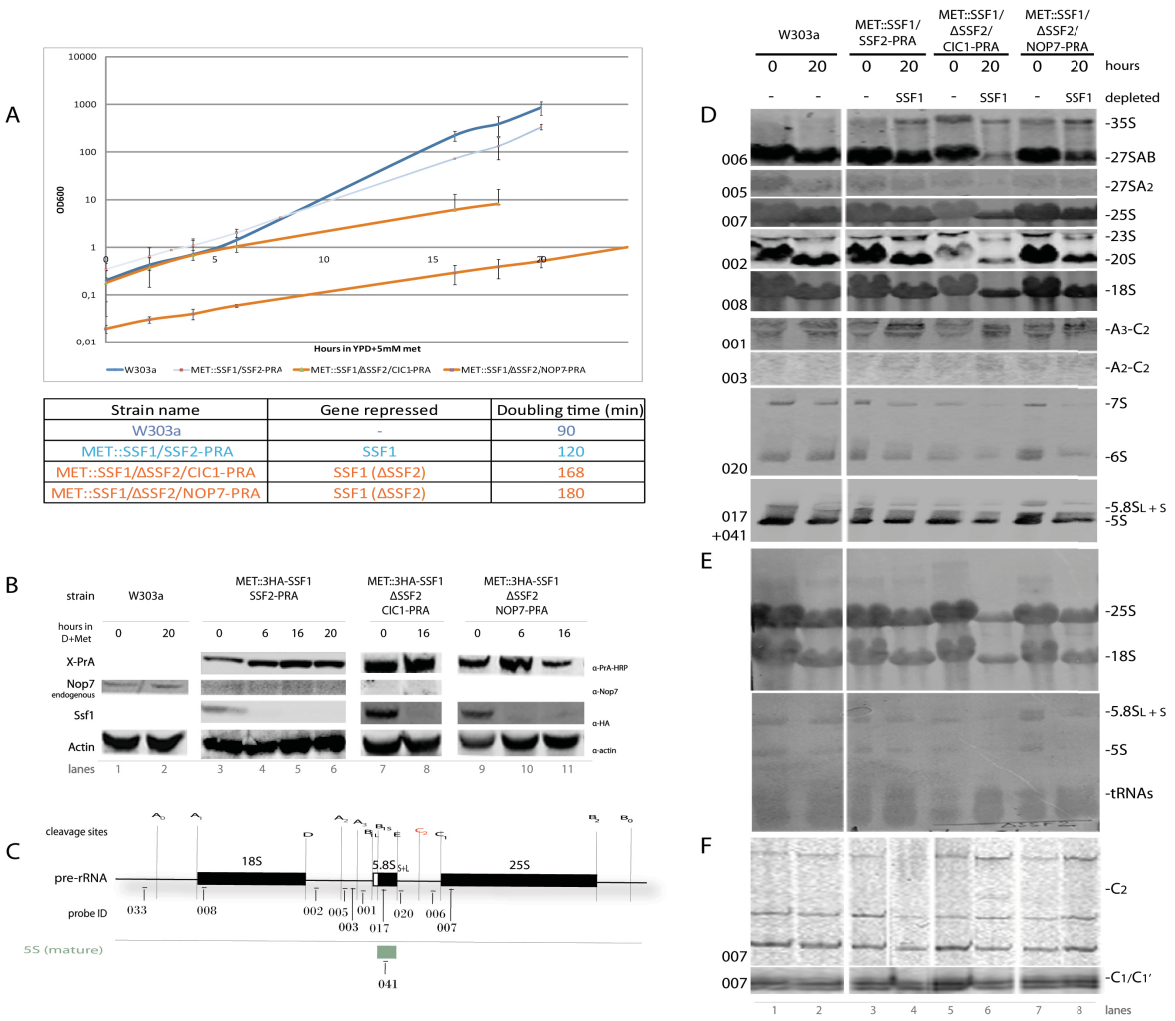

Strain name	Gene repressed	Doubling time (min)
W303a	-	90
MET::SSF1/SSF2-PRA	SSF1	120
MET::SSF1/ΔSSF2/CIC1-PRA	SSF1 (ΔSSF2)	168
MET::SSF1/ΔSSF2/NOP7-PRA	SSF1 (ΔSSF2)	180

Figure 3.3 : Ssf2 does not fully compensate for the loss of Ssf1

Depletion of HA-SSF1 was performed by switching cells in repressive media (YPD+5mM met). **(A)** Cell growth was monitored for these cells in the presence (light blue) or absence of Ssf2 (orange). **(B)** Levels of Ssf2 were assayed for several timepoints. Ssf1 depletion was confirmed by WB and actin was used as loading control. Total protein levels of Ssf2, the antibodies used for WB analysis are indicated at the right. **(C)** Using fluorescent probes, **(D)** total RNAs were analyzed by NB. **(E)** The most abundant RNAs were also detected using methylene blue staining. **(F)** Using 1µg of RNA, primer extension was performed to detect changes C_2 and $C_1/C_{1'}$ site-processing.

3.4 Nop7 and Ssf1 belong to a similar maturation route

As demonstrated in the previous section, Ssf2 is upregulated in the absence of Ssf1, and depletion of both Ssf proteins downregulate the levels of Nop7. A strain was constructed in which HA-Nop7 and HA-Ssf1 levels could be independently regulated by changing media to dextrose or adding methionine respectively.

Prior to repressing HA-NOP7 and/or HA-SSF1 genes, *GAL::NOP7/MET::SSF1/SSF2-PRA* cells showed normal pre-rRNA processing phenotype, except for a mild increase in 35S, which show that the slight overexpression of HA-Ssf1 mildly affects the levels of its paralog, Ssf2, which performs a function that cannot be fully compensated for by Ssf1 (Fig. 3.4D-F lanes 1-3).

This strain allowed testing if HA-Nop7 depletion affects the levels of Ssf2-PrA, when Ssf1 levels are stably regulated by means of a regulatable promoter. Under these conditions, cellular Dt increased to 180min (Fig. 3.4A), which corroborates the growth phenotype defect previously reported in Nop7-depleted cells [36]. Upon HA-Nop7 depletion, HA-Ssf1 levels did not notably change, which was partially expected since the transcription of the gene was controlled by the Met25 promoter. Ssf2-PrA levels decreased, confirming that Ssf2 and Nop7 are genetically linked (Fig. 3.4B lanes 1-2). The strain used in the previously reported study used a variant of S288C, which differs from W303a in that it cannot form pseudohyphae and has a mutated HAP1 gene, which alters normal processes occurring in the mitochondria. Therefore, slight changes in pre-rRNA processing are expected between the previously reported results and the ones obtained in this study. Furthermore, pre-rRNA processing should also be modified because the levels of the Ssf proteins are altered under these conditions and these were found associated with histone modifiers of opposite function. Ssf1 was found associated with Eaf7 a histone acetylase and acetyltransferases open DNA while Ssf2 has been associated with deacetylases Rpd3 and Hda1 and these should close chromatin [55].

HA-NOP7-depleted cells showed a strong accumulation of 35S, premature C_2-site processing and a reduction in 27SA/27SB, 7S and 6S pre-rRNA (Fig. 3.4D and F lanes 3-4), which is consistent with previous results [36]. However, instead of observing an accumulation of aberrant 23S (5'ETS-A_3) pre-rRNA, this precursor decreased and a lower molecular weight precursor, probably 22S (A_0-A_3), was observed (Fig. 3.4D lanes 3-4), which suggest that under

these conditions A_0 processing can still occur. A reduction in 25S, 18S, 5S and 5.8S rRNA was detected by NB and methylene blue staining but problems with the gel resolution did not allow discriminating between short and long forms of 5.8S rRNA (Fig. 3.4D-E). These results suggest that, in addition to the effect of Nop7 depletion, this phenotype is also resulting from the altered levels of the Ssf proteins. For instance, as Ssf2 can be found in affinity purifications of histone deacetylases, while Ssf1 can be found associated with histone acetylases, the resulting levels of these proteins for this strain under these conditions could have a role in closing rDNA repeats and reducing transcription.

If Nop7 and Ssf1 belong to a same maturation route, as hypothesised, their simultaneous depletion should result in an increase of cellular Dt from 90 to 180min, as observed upon Nop7 depletion. Indeed, cellular Dt increased to 180min and WB analysis revealed increased Ssf2-PrA levels (Fig. 3.4A). During NB analysis, no 35S, 27SA/27SB, $27SA_2$ precursors were detected (Fig. 3.4D lane 6). Levels of 23S were not detected but there was a slight accumulation of 22S and 20S (A_1-A_2) pre-rRNA, which suggest that A_0, A_1 and A_3 processing can occur under these conditions. No change in A_2-C_2 and A_3-C_2 levels were detected, which suggest that these pre-rRNAs are still normally processed (Fig. 3.4D lane 6). However, premature C_2-site processing was detected by primer extension and was concomitant with undetectable levels of 7S and 6S pre-rRNA, suggesting that these precursors are rapidly processed or even degraded under these conditions, as the levels or 5.8S rRNA were nearly non detectable by NB and non detectable by methylene blue staining (Fig. 3.4D-F lane 6). Lower levels of mature rRNAs were detected, including 5S rRNA by NB and methylene blue staining (Fig. 3.4D-E lane 6), which suggest that overall transcription was also affected upon depletion of Nop7 and Ssf1. Together, these data suggest that Nop7 and Ssf1 are genetically linked and function in a similar maturation route, as hypothesised.

3.4.1 Ssf2-PrA levels are inversely correlated to Nop7 and Ssf1

If Nop7 and Ssf2 are not genetically linked, no change in Ssf2-PrA levels is expected upon HA-Nop7 depletion. After 16 hours of repressing HA-NOP7 gene transcription (Gal1 promoter shut-off in SD-met), HA-Nop7 protein levels were no longer detected, indirectly confirming the repression of the gene transcription, and HA-Ssf1 protein levels detected did

not change, as its gene was under the expression of a regulatable promoter that was kept on (Fig. 3.4B lanes 1-2). Unexpectedly, Ssf2-PrA levels decreased under these conditions, which imply that its protein levels can be correlated to Nop7 proteins levels. In the same strain, depletion of HA-Ssf1 increased Ssf2-PrA levels (Fig. 3.4B lanes 1 and 3), which corroborates that was previously observed in the *MET::SSF1/SSF2-PRA* strain (Fig. 3.3A and B lanes 4-6). If Ssf2 is inversely regulated by Nop7 and Ssf1 depletions, then simultaneous repression of both HA-SSF1 and HA-NOP7 genes would show intermediate levels of Ssf2. WB analysis revealed that this is the case and therefore show that Nop7 and Ssf1 protein levels inversely correlate to the levels of Ssf2. This contradicts the hypothesis that Nop7 and Ssf2 are not genetically linked.

3.4.2 HA-Nop7 levels unexpectedly increase upon depletion of HA-Ssf1 in the presence of Ssf2

After 24 hours of repressing HA-SSF1 gene transcription (Met25 promoter shut-off in GRS+met), HA-Ssf1 levels were no longer detected, Ssf2-PrA levels increased cellular Dt was of 120min (Fig. 3.4A and B lanes 1 and 3). This phenotype is identical to the one observed upon HA-Ssf1 depletion in the MET::SSF1/SSF2-PRA strain and further corroborates that Ssf2 cannot fully compensate for the loss of HA-Ssf1 (Fig. 3.3 lanes 3-6). As the HA-NOP7 gene is under the Gal promoter, the HA-Nop7 levels are slightly higher than in wild-type cells, which is expected. As these conditions were tested in the same WB and actin levels are similar, the HA-Nop7 levels should be the same before and after depletion of HA-Ssf1 (Fig. 3.4B lanes 1 and 3). Unexpectedly, HA-Nop7 levels increased, which contradicts the observation in the *MET::SSF1/SSF2-PRA* strain, where Nop7 levels were undetectable, and was concomitant with a mild accumulation of 35S and 23S pre-rRNA (Fig. 3.3B lanes 3-6). HA-Ssf1 depletion delays pre-rRNA processing and is most likely responsible for the 35S pre-rRNA accumulation observed (Fig. 3.4D lane 5). As Nop7 has been associated with 27SAB processing, its increase should result in faster processing of 27SAB precursors [36]. This phenotype is indeed observed in these cells and is concomitant with premature C_2 site cleavage, as observed by primer extension (Fig. 3.4D and F), which suggest that the C_2 site is

partially unprotected when HA-Ssf1 is absent but HA-Nop7 and Ssf2-PrA are increased. The levels of the other precursors and mature rRNAs did not notably change (Fig. 3.4D and E). This data therefore suggests that the increase in HA-Nop7 levels observed by WB is real and qRT-PCR analysis of its mRNA levels should determine if the cell achieves this by stabilising its mRNA or rather by increasing its translation rate or stabilising the protein. These results are presented and discussed in Section 3.6.

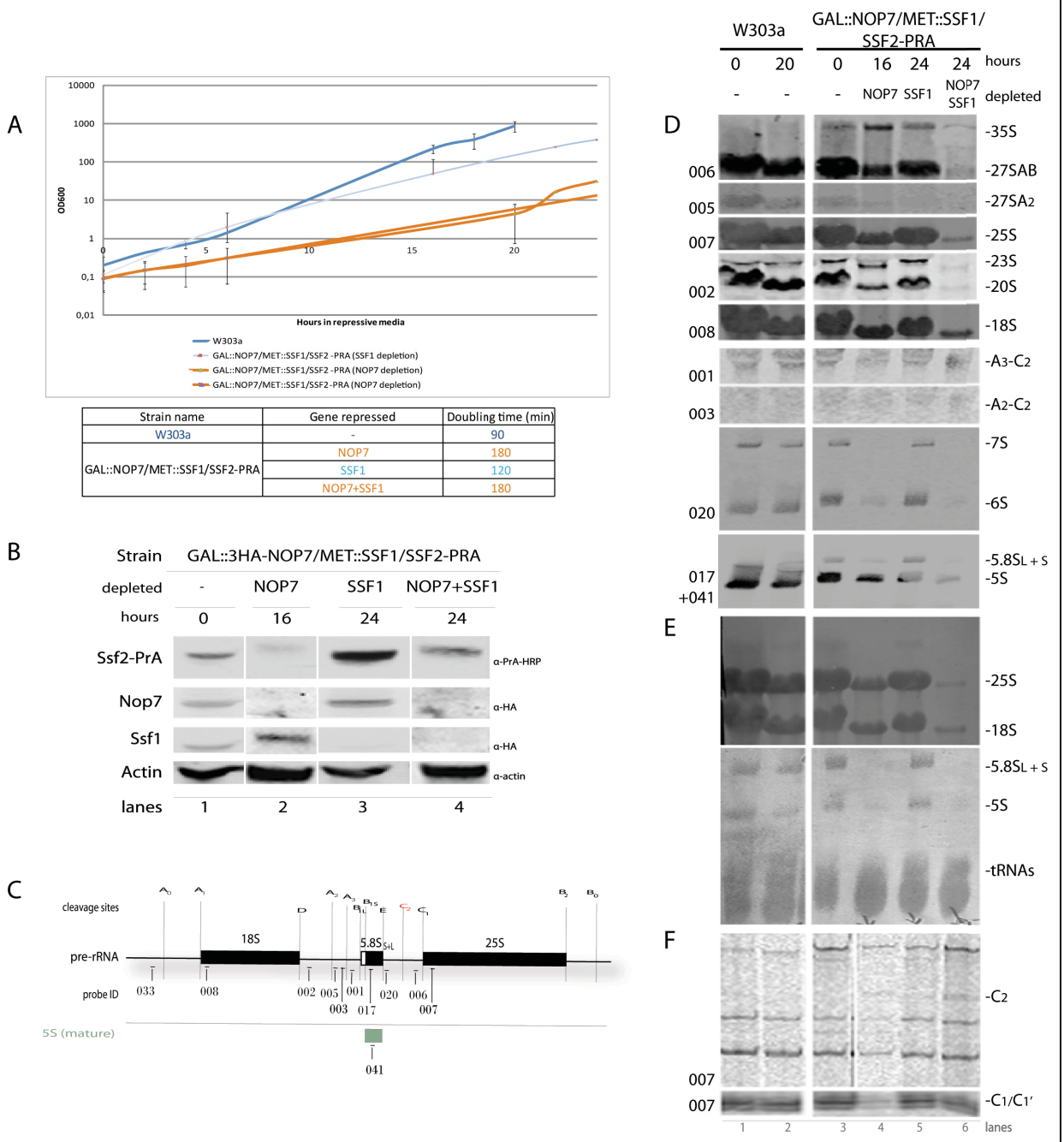

Strain name	Gene repressed	Doubling time (min)
W303a	-	90
GAL::NOP7/MET::SSF1/SSF2-PRA	NOP7	180
	SSF1	120
	NOP7+SSF1	180

Figure 3.4: Ssf1 and Nop7 belong to a similar maturation route

Depletion of HA-SSF1 and/or HA-NOP7 was performed by switching cells in repressive media (SD-met, GRS+5mM met or YPD+5mM met). **(A)** Cell growth was monitored upon depletion of HA-Nop7 (orange), HA-Ssf1 (light blue), and simultaneous depletion of both proteins (orange). **(B)** Levels of HA-Ssf1, HA-Nop7 and Ssf2-PrA were assayed for each condition by WB and actin was used as loading

control. The antibodies used for WB analysis are indicated at the right. **(C)** Using fluorescent probes, **(D)** total RNAs were analyzed by NB. **(E)** The most abundant RNAs were also detected using methylene blue staining. **(F)** Using 1µg of RNA, primer extension was performed to detect changes C_2 and $C_1/C_{1'}$ site-processing.

3.5 Nop7 depletion in the absence of Ssf2 may generate aberrant ribosomes and severely impair cell growth

First, in order to further support the finding that Nop7 levels affect both Ssf1 and Ssf2 protein levels, Nop7 was depleted in two strains in which both Ssf proteins were present and regulated by their endogenous promoters. Depletion of Nop7 was validated by WB and the Dt was of 180min in both strains (Fig. 3.5A and B lanes 1-8). In the first strain, Ssf1-PrA levels decreased over time and the same was observed for Ssf2-PrA in the second strain. These results therefore further validate that Nop7 levels are correlated to the levels of both Ssf proteins.

As previously demonstrated, Nop7 and Ssf1 most likely function in a same maturation route. Unexpectedly, the levels of Ssf proteins are correlated to Nop7 levels and the contrary is also valid, which links Ssf2 with Nop7. However, it is still possible that Ssf2 functions in a parallel LSU maturation pathway, independent of Ssf1 and Nop7. In order to test this hypothesis, HA-Nop7 was depleted in a strain in which Ssf1 was C-termini PrA-tagged and SSF2 was deleted from the genome. In restrictive media, the Dt of NOP7-depleted/SSF2Δ-cells was of 372min (Fig. 3.5A). At time 0, the levels of Ssf1-PrA were significantly lower in this strain compared to the other strain in which Ssf2 was still present (Fig. 3.5B lanes 1 and 9). Previously, it was observed that Ssf2-PrA levels increased as a response to Ssf1 depletion (Figs. 3.3 lanes 3-6 and 3.4B lanes 1 and 3) but the the contrary does not seem to be the case. This therefore suggests that the levels of the Ssf proteins are regulated in the cell through independent mechanisms. Upon Nop7 depletion, the levels of Ssf1-PrA increase and then decrease only in SSF2Δ-cells (Fig. 3.5B lanes 9-12).

Prior to HA-Nop7 depletion, *GAL::NOP7/SSF1-PRA/ΔSSF2* cells show a pre-rRNA processing phenotype comparable to WT (Fig. 3.5D-F lanes 1-3) except for a mild accumulation of 35S pre-rRNA that was also observed in other strains in which Ssf2 was deleted (Fig. 3.3D lanes 5 and7).

Upon depletion of Nop7 and Ssf2, pre-rRNA processing defects would be expected to resemble features of both phenotypes (Table I). However, after HA-NOP7 depletion, 35S pre-rRNA levels did not change, 18S and 5S levels dramatically decreased and no other pre-rRNA or mature rRNA could be detected by NB (Fig. 3.5D lane4). Primer extension using a probe that hybridized within the 5' end of mature 25S rRNA (007) did unfortunately not reveal any accumulation of premature cleavage of the C_2-site (Fig. 3.5F lane4). Methylene blue staining showed strong accumulation rRNAs that were slightly lower in molecular weight than 25S, 18Sand 5S (Fig. 3.5E lane4).

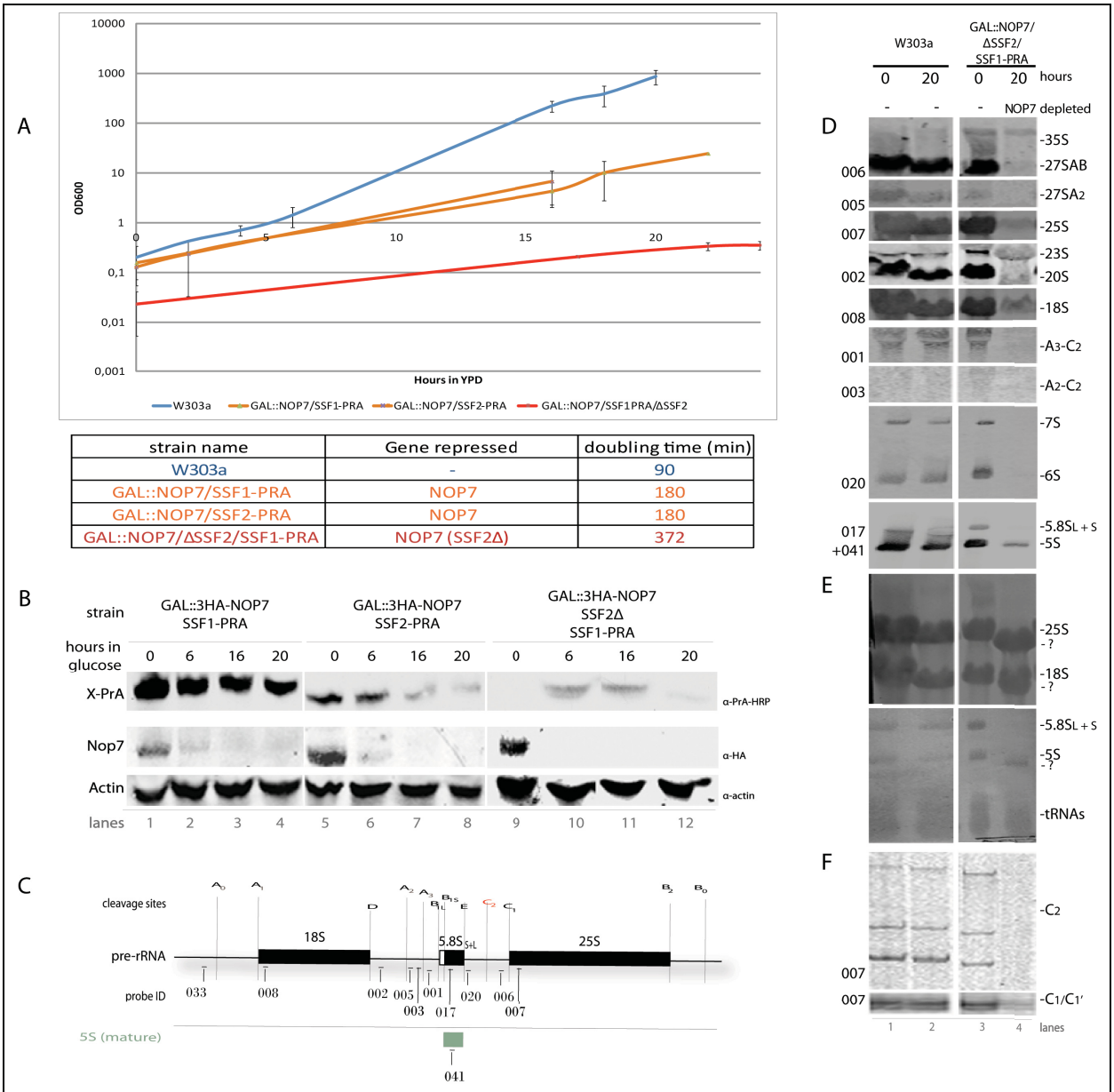

strain name	Gene repressed	doubling time (min)
W303a	-	90
GAL::NOP7/SSF1-PRA	NOP7	180
GAL::NOP7/SSF2-PRA	NOP7	180
GAL::NOP7/ΔSSF2/SSF1-PRA	NOP7 (SSF2Δ)	372

Figure 3.5: Ssf2 belongs to a parallel LSU maturation pathway independent of Nop7 and Ssf1

Depletion of HA-NOP7 was performed by growing cells in repressive media (YPD). **(A)** Cell growth was monitored upon depletion of HA-Nop7 (orange, red). **(B)** Levels of HA-Nop7, Ssf1-PrA and Ssf2-PrA were assayed by WB and actin was used as loading control. The antibodies used for WB analysis are indicated at the right. **(C)** Using fluorescent probes, **(D)** total RNAs were analyzed by NB. **(E)** The most abundant RNAs were also detected using methylene blue staining. **(F)** Using 1µg of RNA, primer extension was performed to detect changes C_2 and $C_1/C_{1'}$ site-processing.

3.6 The cell regulates differently the levels of Ssf2 and Nop7

3.6.1 Upon depletion of Ssf1 or both Ssf proteins, Nop7 mRNA is stabilized and its translation rate is modulated

As previously shown, Nop7 protein levels unexpectedly decreased upon depletion of Ssf1 or in the absence of the Ssf proteins (Fig. 3.3B lanes 1-11). It is therefore valid to ask whether regulation of Nop7 is performed transcriptionally, post-transcriptionally or both. Upon depletion of Ssf1, both in presence (Fig. 3.6A lanes 1-2) and absence of Ssf2 (Fig. 3.6B lanes 1-4), the mRNA levels of Nop7 significantly increased. Because the decrease in Nop7 protein is not concomitant with a decrease in its mRNA, then post-transcriptional mechanisms exist that degrade Nop7 protein. Alternatively this could also be explained by a decreased affinity of its transcript with the translational machinery. The increase in NOP7 mRNA levels could be explained by increased transcriptional rate or is stabilised under these conditions. Using the Gal regulatable promoter, NOP7 gene transcription was kept constant upon HA-Ssf1 depletion (Fig. 3.6A lane 5). Under these conditions, there was an increase in its mRNA, which suggests that the increase in NOP7 mRNA levels results from an increase in its stabilisation. Although NOP7 mRNA levels always increased, its protein levels either decreased (Fig. 3.3B lanes 1-11) or increased (Fig. 3.4B lanes 1 and 3). This data is therefore consistent with the supposition that altering the levels of at least one of the Ssf proteins generates NOP7 mRNA stabilisation with changes in its translational rate and/or protein stability.

3.6.2 Upon depletion of Ssf1 or Nop7+Ssf1 proteins, Ssf2 protein levels change, its mRNA levels remains stable and its translation rate is modulated

As Ssf2 proteins levels are upregulated in the absence of Ssf1 and downregulated in the absence of Nop7, analysis of its mRNA levels could provide further insight on the mechanisms the cell used to regulated Ssf2 protein levels. Upon depletion of Ssf1, the mRNA levels of Ssf2 did not significantly change, suggesting that the protein levels of Ssf2 result from the stabilisation of the protein or from increased translation rate of its transcript (Fig. 3.6A lanes 1-2). Depletion of Nop7 or both Nop7 and Ssf1 protein levels also did not significantly change the mRNA levels of SSF2, which further support this idea. In this strain, Ssf1 depletion, resulted in an increase in both Ssf2 and Nop7 protein levels and the levels of SSF2 mRNA significantly decreased (0.588-fold, Fig. 3.6A lanes 3 and 5).

Upon Nop7 depletion, the SSF1 gene was under the expression of Met25 promoter and both levels of mRNA and protein remained constant (Figs. 3.6A lane 4 and 3.4B lanes 1-2 respectively). This implies that if the levels of mRNA change, it is most probably caused by a change in transcriptional rate of the gene. In another strain, Nop7-depleted/ Ssf2Δ cells increased the levels of SSF1 mRNA (1.521-fold increase, Fig. 3.6B lane 5-6). This increase was however concomitant with significantly lower levels of Ssf1 proteins that fluctuated over time (Fig. 3.6B lanes 9-12). In order to better understand if the fluctuation of Ssf1 protein observed is linked to a change in its mRNA, a timepoint analysis of SSF1 mRNA will be required for this strain.

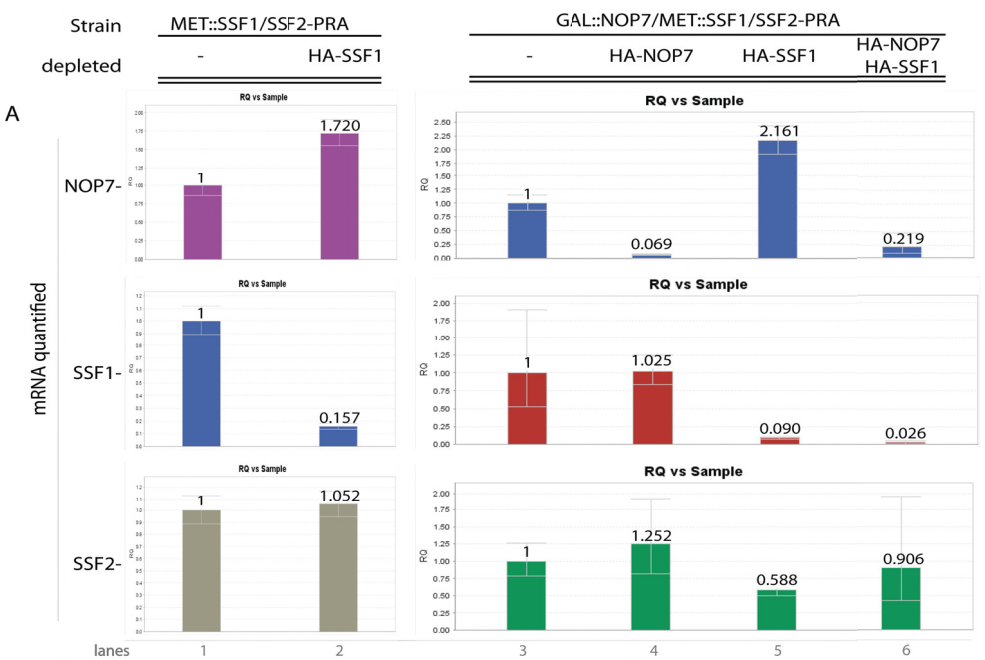

mRNA quantified	strain depletion	MET::SSF1/SSF2-PRA SSF1	GAL::NOP7/MET::SSF1/SSF2-PRA NOP7	SSF1	NOP7+ SSF1
NOP7	fold change	1,720	0,069	2,161	0,219
	significant	increase	decrease	increase	decrease
SSF1	fold change	0,157	1,025	0,090	0,026
	significant	decrease	-	decrease	decrease
SSF2	fold change	1,052	1,252	0,588	0,906
	significant	-	-	decrease	-

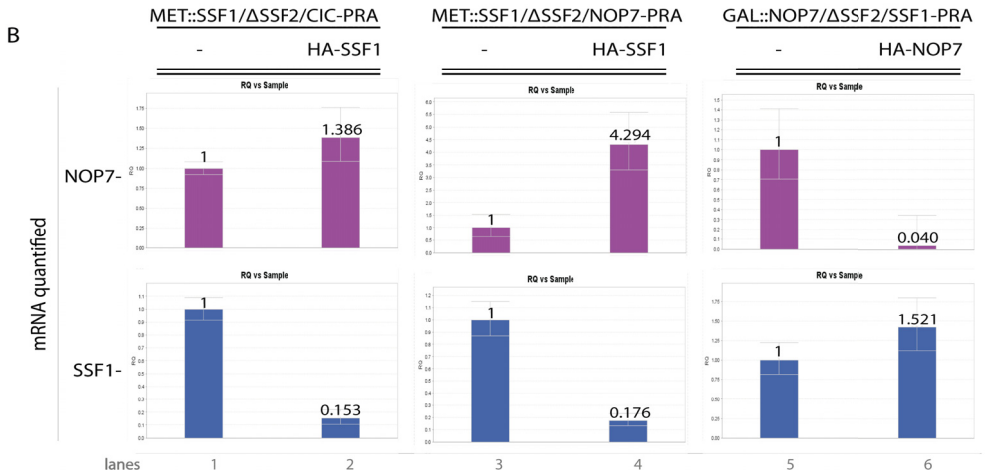

mRNA quantified	strain depletion	MET::SSF1/ΔSSF2/ CIC1-PRA SSF1	MET::SSF1/ΔSSF2/ NOP7-PRA SSF1	GAL::NOP7/ΔSSF2/ SSF1-PRA SSF1
NOP7	fold change	1,386	4,294	0,040
	significant	increase	increase	decrease
SSF1	fold change	0,153	0,176	1,521
	significant	decrease	decrease	increase

Figure 3.6: qRT-PCR analysis of NOP7, SSF1 and SSF2 mRNA levels

For each strain, cells in log phase were collected in the presence or absence of Ssf1 and or Nop7, regulated by means of distinct regulatable promoters. Using random primers and reverse transcriptase II, cDNAs were created from total RNA extracts. Primer sets specifically targeting unique endogenous sequences of key mRNAs were used for RT-PCR. Results were normalised against actin or UBC6, which are expected to remain constant. Assays in which Ssf2 is **(A)** present or **(B)** absent.

3.7 Structural changes of Ssf1, Ssf2 and Nop7

In an attempt to discern potential protein folding differences between Ssf1 and Ssf2, a protease accessibility laddering (PAL) assay was performed as per (80). Depending if the protein is alone or in complex, protein folding changes are expected and can be associated with changes in the accessibility of specific amino acids in the protein sequence when degraded using limited protease activity [87-89]. The PAL assay can also confirm fold recognitions and sequence structures [80]. The PAL assay was also chosen because the cell grindate of log phase strains with either Ssf1, Ssf2 or Nop7 C-terminally tagged (PrA) were already available in the lab. The tagged protein is recovered in its natively folded state using single-step affinity purification (ssAP) and it can be recovered alone or in complex, depending on the buffers stringency and the stability of the complexes it forms with other proteins. Limited proteolysis is then used to target exposed surface loops and domain-linking segments. The resulting C terminal PrA tagged fragments of the protein can then be tracked by western blot (Fig. 2.9) [80]. For each sample, three different endoproteinases targeting one or two amino acids were used: Asp-N (D, aspartic acid), Lys-C (K, lysine) and trypsin (K, lysine and R, arginine), which helped locate the reacting amino acids. By comparing changes in proteolytic cleavages when the protein is alone or in complex, structural changes can be inferred and the exact location of the amino acid sequence can be identified by Edman sequencing [80].

As a preliminary step, NOP7-PRA, SSF1-PRA and SSF2-PRA strains were submitted to limited proteolysis using a low stringency buffer (20 mM K/HEPES pH 7.4, 110 mM KOAc, 2 mM $MgCl_2$, 0.1% Tween 20, 1 mM DTT, 1:500 protease inhibitor cocktail) [80]. The exposed regions of the Nop7 protein, when it is in complex with other proteins, can be approximated to regions located between its known domains (Fig. 3.7A). When they are in complex, both Ssf

proteins fold similarly and the exposed regions were approximated to regions located between domains (Fig. 3.7B). The The Ssf proteins show a similar pattern, consistent with the finding that the Ssf proteins are most likely associated with similar sets of proteins (Section 3.2). Cleavage patterns of the Ssf and Nop7 proteins when they are in complex with other RiBi factors under normal cellular conditions have been identified in this study.

A

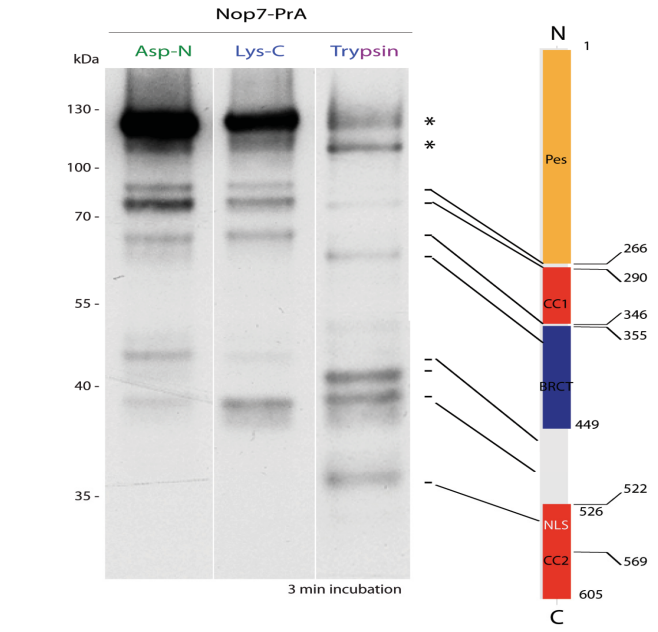

B

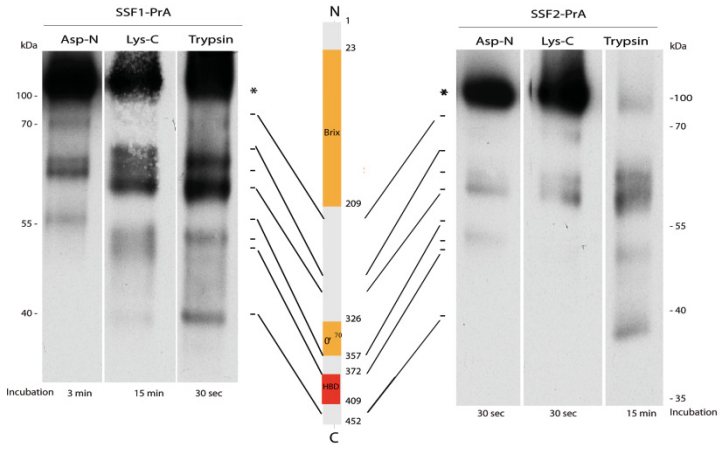

Figure 3.7: Exposed domains of key proteins when in complex.

Using stringent buffer conditions, the PrA-tagged protein is recovered from cryolyzed cell grindate using magnetic beads and submitted to protease degradation (*: full length). The PrA-recovered C-terminal end was analyzed by western blot. Nop7 **(A)** and Ssf **(B)** proteins domains constructed according to information taken from (54), (52) and (1).

4 Discussion and perspectives

4.1 Ssf1 and Ssf2 form similar pre-rRNP particles and subcomplexes

In the cell, Ssf1 is six times more abundant than its paralog, Ssf2. The Ssf1 affinity purification complex has previously been reported during log phase and contains many LSU RiBi factors, consistent with its role during ribosome biogenesis. Both paralogs can potentially heterodimerize with each other, although Ssf1 particles do not seem to contain Ssf2 under normal conditions [54]. Moreover, Ssf2 has been found in particles in which Ssf1 is absent, like the Arx1 particle [90]. Therefore, taken together, this data suggests that both proteins associate with distinct particles during ribosome biogenesis. However, analysis of the Ssf1 and Ssf2 associated complexes has revealed that both paralogs form similar pre-rRNP complexes under normal growing conditions (Fig. 3.2 A, all buffers except #3, #6 and #11).

Above 60kDa, six proteins consistently observed in higher abundance are probably always found in particles containing Ssf1 or Ssf2 (Fig. 3.1). It is therefore very likely that those six proteins are Dbp9, Dbp10, Drs1, Noc1, Noc2 and Nog1, as they are present in the previously reported Ssf1-particle and match the corresponding molecular weights [54]. Also, if the particles are nearly identical, then Ssf1-particles are very likely to also contain Rrp15 (LSU RiBi factor) and Nop53 (pre-90S RiBi factor) proteins, as Ssf2 has been shown to directly interact with Ssf2 [54, 60]. Unfortunately, both RiBi are expected to run below the 60kDa region, which showed high background. MS analysis will therefore be necessary to determine whether these proteins are found in both complexes, or not.

Significant disruption of the particles revealed that three of the components previously observed in high abundance were still associated with the bait proteins and are likely Dbp9, Drs1 and Nog1, as these RiBi proteins are predicted to enter the LSU maturing particle nearly at the same time as Ssf1 and could represent a subcomplex (Fig. 3.2 A, buffer #6) [85].. Previously, this type of observation has proven to be effective in identifying proteins that enter the pre-rRNP particle as subcomplexes, as is the case of Rpf2, Rrs1, Rpl5 and Rpl11 [17]. Ssf1 was previously detected in fractions of lower molecular weight than the 40S subunit during a sucrose gradient analysis, which further supports that this protein belongs to a yet unidentified subcomplex [54]. A sucrose gradient separation coupled to ssAP of the fractions of lower

molecular weight than the 40S sub-unit followed by MS analysis would allow the identification of these proteins as this method proved effective in identifying the Nop7-Erb1-Ytm1 subcomplex [1]. Once unambiguously identified, *in vitro* studies could be performed in order to validate their interaction.

It is tempting to speculate that the other highly abundant proteins, likely Dbp10, Noc1 and Noc2, are required for the entry of the tetrameric subcomplex into the pre-60S particle (Fig. 1.2) [85]. However, if the proteins are not Dbp10, Noc1 and Noc2, then it is possible that these proteins are enriched in the particle because they associate earlier with the pre-60S and leave later than the Ssf proteins. In this latter scenario, the disappearance of these proteins in buffers of higher stringency would reflect that they are not in close proximity with the Ssf proteins in the pre-60S particles. Identification of these proteins by MS together with the data already available for the RiBi proteins will provide further insight.

Ssf1 and Ssf2 differ in charge at only nine amino acids and yet Ssf2 appeared to make stronger interactions with the above mentioned proteins (Figs. 1.4 and 3.1). It is therefore likely that the nature of amino acids 281, 282, 290, 299, 300, 316, 411, 413 and 427 in Ssf2 stabilize protein-protein. In order to verify this hypothesis, PCR-induced mutations could be performed on one paralog to change these amino acids and verify if a change in the stability of the associated subcomplex can be observed. In the short-term, MS analysis will readily identify these components and also distinguish background from real interactors below 60kDa, since some patterns are also conserved between the Ssf1 and Ssf2 particles in this region; however, these bands are most likely r-proteins in both ssAPs.

4.2 Nop7, Ssf1 and Ssf2 proteins are genetically linked

Thorough analysis of data available prior to this study, lead to the hypothesis that Nop7 and Ssf1 were genetically linked and function in the main LSU maturation pathway, whereas Nop7 and Ssf2 were not genetically linked. Moreover, it was hypothesized during this study that Ssf2 functioned in a parallel, unreported pathway. In order to uncover the presence of parallel maturation pathways during ribosome biogenesis using Nop7, Ssf1 and Ssf2, one or two of these proteins were modulated, and changes in cell growth, total protein and mRNA levels (for some key factors) and pre-rRNA processing were monitored. Results concur with

the likely presence of parallel pathways independently involving Ssf1 or Ssf2 (Section 3.5). Results also suggest that Nop7 is genetically linked with Ssf1 but, also with Ssf2, contrary to what was previously expected. This study also uncovered an unreported phenotype observed upon Ssf2 and Nop7 depletion, which raises several questions that will be addressed in this section and will require further investigation.

A heat map that summarizes all phenotypes observed in this study is listed in Table XXI. Phenotypes were divided in three; (**A**) in the first section, Ssf1 depletion in the presence of Ssf2 was observed with endogenous or slightly overexpressed Nop7 protein. (**B**) In the second section, the growth phenotype previously reported in SSF1-depleted/SSF2Δ cells was corroborated in two strains [54]. The growth phenotype previously reported in Nop7-depleted cells was almost identical to the phenotype observed in cells Nop7-depleted but slightly overexpressed Ssf1-protein [36]. (**C**) Finally, Nop7 depletion in Ssf1-depleted or Ssf2Δ cells was assayed. In all cases, depletion of the targeted protein and its mRNA levels were validated by WB and qRT-PCR, respectively.

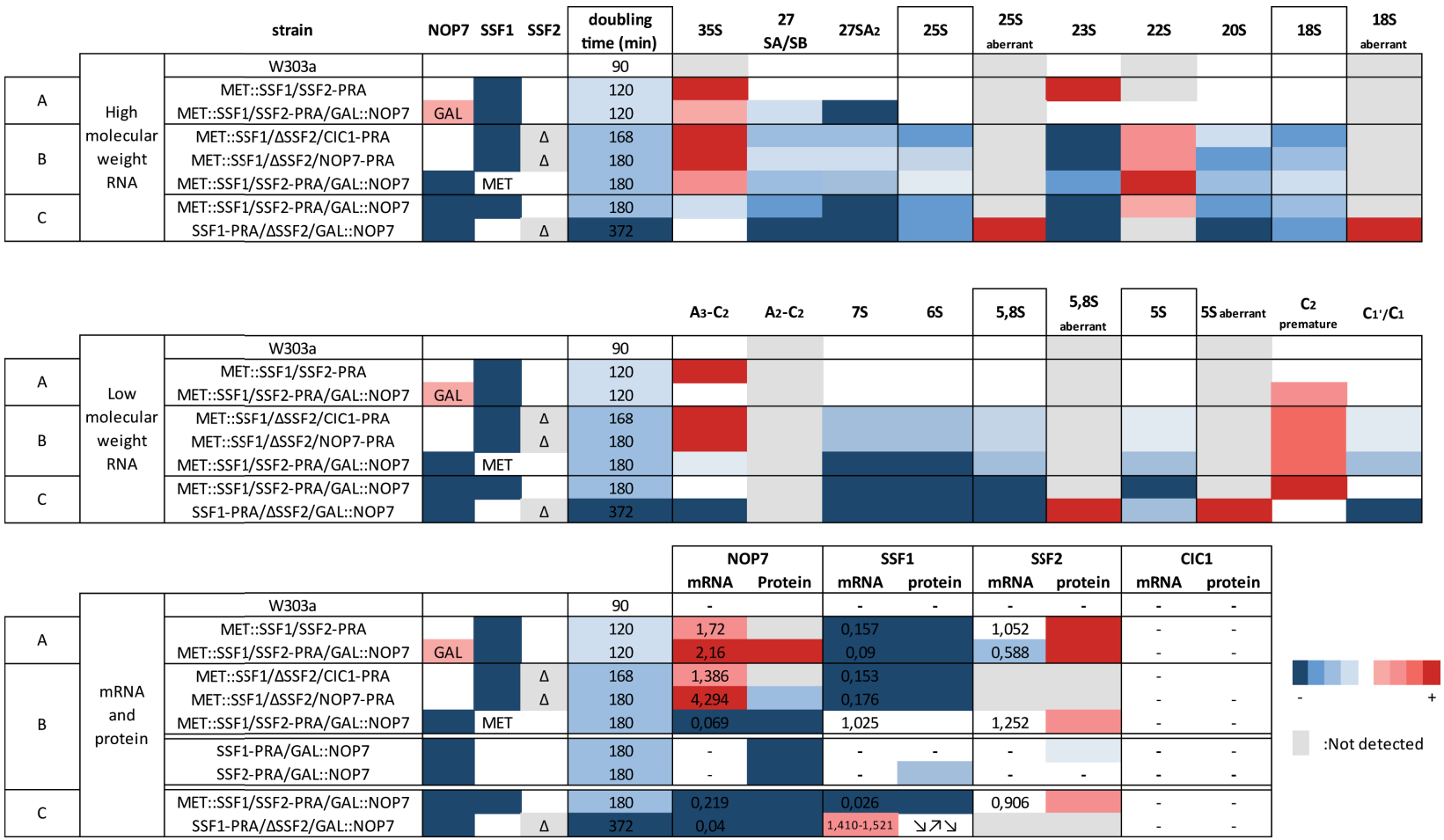

Table XXI : Summary of the phenotypes observed

To summarize the phenotypes observed (cell growth, pre-rRNA, mRNA, protein levels), a heat map was constructed for all the strains tested. **(A):** depletion of Ssf1 only. **(B)** Absence of both Ssf proteins. **(C)** Depletion of Nop7 under different cellular contexts.

4.2.1 Comparison between reported and observed phenotypes is limited because of the choice of the background strain

As background strain W303a was used in this study. The previously reported Nop7-depletion phenotype was reported in S288C-derived cells, which differs from W303a in that it cannot form pseudohyphae and has a mutated HAP1 gene, which alters normal processes occurring in the mitochondria [36]. The depletion phenotype observed upon depletion of the Ssf proteins was reported in W303-1a cells, which are W303a cells sensitive to oxidative stress due to further mutations in the YBP1 gene [54]. Therefore, strain variability has to be considered and could account for some differences observed during pre-rRNA processing. However, because W303a is less genetically modified than S288C and W3031a, it is expected to be the most fit.

Another improvement in the NB assays would be to independently probe for 5S and 5.8S rRNA, instead of simultaneously. Because these rRNAs are very close in size (5S: 121bases, $5.8S_L$: 160bases, and $5.8S_s$: 154bases), the 5S signal was very strong and it did not allow discrimination between the $5.8S_S$ and $5.8S_L$ forms of rRNAs. Ideally a separate gel of lower polyacrylamide content (6% instead of 8%) and for a longer period of time should be run to resolve $5.8S_S$ and $5.8S_L$ rRNAs. Primer extension analysis could also be performed.

Upon depletion of the Ssf proteins, A_0 and A_1 cleavages are expected to be severely delayed and to occur after ITS1 processing is completed, leading to an accumulation of aberrant 5' ETS-D pre-rRNA [54]. However, with the probes used in this study, this aberrant form of pre-RNA could not be detected. Additional analyses could be performed using a probe targeting the 5'ETS of pre-rRNA (033). This, however, would most likely detect the accumulation of this pre-rRNA only in the cases where both Ssf paralogs have been deleted, as reported previously [54]. Therefore, using this probe is not expected to alter the conclusions of this study.

4.2.2 Ssf1 depletion cannot be fully compensated for by Ssf2

Previous tetrad dissection studies have reported that the presence of one Ssf paralogs is sufficient for cell viability [49]. Since Ssf1 and Ssf2 are required during the mating response and cell budding, deletion of both proteins impairs cell division, particularly during meiosis,

and cells arrest in G1 while no obvious phenotype was observed in cells lacking Ssf1 [49, 54]. The current study shows a mild growth defect in SSF1-depleted cells (Dt: 120min, Table XXIA) which is likely explained by a slower processing of 35S pre-rRNA, indicating slowerpre-90S particle formation despite increased levels of Ssf2. Also, aberrant precursors indicated a mild processing delay of A_0, A_1 and A_2 sites (23S: 5'ETS-A_3) concomitant with the mild increase in premature C_2 cleavage (A_3-C_2). As deletion of one single endonuclease does not seem to greatly affect A_0, A_1 or A_2 processing, it has been proposed that several endonucleases can ensure these pre-rRNA processing events to take place. Endonucleases required during ribosome biogenesis include Rnt1 (A_0, A_2), Rcl1 (A_2), RNase MRP (A_0, A_1, A_2, A_3) [4-6, 8]. In addition to endonucleases, U3 snoRNPs have also been reported to have the capacity to bind and cleave at A_0, A_1 and A_2 sites [76, 91]. The pre-rRNA precursors accumulating in the absence of Ssf1 point towards a mild delay in U3-dependent cleavages (A_0-A_2). It would therefore be of interest to verify if the Ssf2-particle contains the components of the U3-snoRNP complex, which include Sof1, Mpp10, Rrp9, Lcp5 and whether or not these change upon depletion of Ssf1 [76, 91]. Alternatively, the delay could also be explained by lower activity of the Imp3 protein, which is necessary for the recruitment of U3-snoRNP complex on the pre-rRNA concomitant with a longer occupancy of the Imp/Brix-family member Imp4, which has been reported to bind to U3 RNA, and promote its release from pre-rRNA [76, 91].

A delay in A_0-A_2 cleavages should result in a premature A_3 cleavage, generating 23S and 27SA_3 pre-rRNA, the latter of which was not shown in this assay. However, the presence of an A_3-C_2 precursor suggests that 27SA_3 is further prematurely cleaved at C_2, which should also generate 26S' (C_2-B_0). Presence of this precursor was not assayed in this study but could be detected using a probe hybridizing within the 3'ETS2. Taken together, these results indicate that Ssf1 depletion, and hence function, of Ssf1 cannot be fully compensated for by Ssf2, despite a clearly increased level.

4.2.2.1 The effect of Ssf1 depletion depends on the cellular level of other RiBi proteins

Ssf1 depletion was also performed in another strain where Nop7 was slightly overexpressed (MET::SSF1/SSF2-PRA/GAL::NOP7, SSF1-depletion, Table XXIA).

The growth phenotype observed in this strain is nearly identical as with MET::SSF1/SSF2-PRA cells. However, no 23S aberrant pre-rRNA was detected in these cells, and therefore the phenotype cannot be explained by a delay in U3-dependent cleavages [10]. Therefore, accumulation of the 35S pre-rRNA in these cells could fit a scenario in which mechanisms up regulating 35S pre-rRNA transcriptional rate and creating a mild accumulation of this precursor. As both Ssf proteins were found in the particles of histone modifiers, the second scenario is plausible but would require further investigation. For example, AP-MS could be performed to assay changes in the Sdc1, Swr1, Eaf7, Rpd3 and Hda1-containing particles caused by the modulation of the Ssf proteins (Fig. 1.7A) [55, 56].

In this strain, GAL::NOP7 mRNA levels unexpectedly increased upon Ssf1 depletion.. Since Nop7 is an important scaffold protein required for 27S pre-rRNA processing, its increased levels likely accounts for decreased levels of 27SA/SB and $27SA_2$ pre-rRNA of these precursors observed in this strain. However, a decrease in these pre-rRNAs could also be caused by an accumulation of $27SA_3$ precursor. The levels of this pre-rRNA can be verified by probing between the A_3 and B_1 sites (probe 001) and, alternatively, by primer extension analysis. If no change or a decrease in $27SA_3$ precursor is confirmed, then the phenotype would fit this scenario. Higher levels of Nop7 may increase the processing rate of 27S precursors, which, along with Ssf1 depletion, could generate less stable pre-rRNP complexes and a few of these complexes do not completely protect their C_2-site.

According to results presented in this study, Ssf2 is part of both Nop7-dependent and independent pathways (Section 3.5). Therefore, the Nop7/Erb1/Ytm1 complex is likely required in both common and parallel pathways involving Ssf2 under these conditions. It would therefore be if interest to i) identify the proteins present and the ones disappearing from the Ssf2-particle upon Nop7-depletion these conditions and ii) PRA-tag a protein not associated to Ssf2-containing particles in a MET::SSF1/GAL::NOP7 background.

Together, this data further reiterates that Ssf1 and Ssf2 proteins cannot fully compensate for the loss of one another. Furthermore, it suggests that accumulation of different precursors at steady-state levels depend on the available levels of specific RiBi proteins.

4.2.3 Nop7 is genetically linked with both Ssf proteins

Pre-rRNA processing defects associated with NOP7-depleted and SSF1-depleted/SSF2Δ cells were previously reported and have been successfully reproduced in this study (Tables I and XXIB) [36, 54]. As the absence of Ssf proteins affects early events that occur co-transcriptionally and can potentially associate with histone modifiers (Fig. 1.7A), it would be interesting to verify if rDNA transcription rates are altered in SSF1-depleted/SSF2Δ cells by performing either a Miller spread or psoralen assay.

What seems clear from whole cell protein analyses is that absence of both Ssf proteins correlated with a decrease in Nop7, but not Cic1. The Cic1 protein is a RiBi protein binding within ITS2, close to the Nop7 binding site [12]. It has been shown to interact with Nop7 (protein-fragment complementation assay) in at least one particle, and finally, it is part of both the Ssf1 and Nop7 associated complexes while is not likely to physically interact with the Ssf proteins [12, 54]. Furthermore, Ssf1 and Ssf2 protein levels decrease upon Nop7 depletion. This data therefore adds weight to Nop7 being genetically linked with Ssf1 and, unexpectedly, also with Ssf2.

Previously, it has been observed that depletion of one component of the Nop7-Erb1-Ytm1 trimeric complex affects the total protein levels of the two other components without altering other RiBi proteins present in the same pre-60S particle [39]. However, under normal conditions, the Nop7 associated particle was found to contain only Ssf1, suggesting that Nop7 has higher affinity for Ssf1, which may change when Ssf1 is absent, and Ssf2 is present in higher levels. This will be validated in future characterization of these interactions *in vitro* and *ex vivo*.

4.2.4 Nop7/Ssf1 and Ssf2 can be part of parallel pathways

Because of an observed correlation between the levels of Nop7, Ssf1 and Ssf2, NOP7 depletion was assayed i) when SSF1 was slightly overexpressed (MET::SSF1, promoter *on*) or; ii) depleted (MET::SSF1, promoter *off*); and, iii) when SSF2 was deleted. The doubling time (Dt) of NOP7-depleted cells was not affected (180min) upon alteration of Ssf1 proteins

levels (by either overexpression or depletion) while the Dt of NOP7-depleted/SSF2Δ cells nearly doubled (372min).

4.2.4.1 Altering the levels of the Ssf proteins can reduce the number of open rDNA

In this study, a reduction of 5S rRNA was observed in SSF1-depleted/SSF2Δ-cells, as previously reported [54]. In addition, an unambiguous reduction in 5S rRNA was observed in GAL::NOP7/MET::SSF1/SSF2-PRA cells but only upon the simultaneous depletion of Nop7 and Ssf1 (Fig. 3.4D-E lane6). Unlike an Ssf1-depletion, Nop7 depletion was shown to correlate with a drop in Ssf2 (Figs 3.3B lanes 3-6 and 3.5B lanes 5-8). Consequently, the simultaneous depletion of Nop7 and Ssf1 resulted in a moderate increase in Ssf2 (Fig. 3.4B). As the main maturation pathway was blocked under these conditions (Nop7 depletion), it is logical to imagine LSU ribosome biogenesis being driven by a larger proportion of Ssf2-containing particles lacking Nop7 and Ssf1. As 5S rRNA is not transcribed by RNA pol I but is located between rDNA repeats, its reduction is likely caused by a reduction in the number of open rDNA repeats, which is dependent on the activity of chromatin remodelling factors. Ssf1 and Ssf2 potentially associate with chromatin modifiers; it is therefore very likely that Ssf2 is not abundant enough in these cells to perform every one of its cellular functions. In is therefore highly probable that, Ssf2 fails to associate with Rpd3 and Hda1, or other chromatin modifiers, resulting in a decresase in the number of open rDNA repeats (Fig 1.7A). As transcription of the four rRNA genes is tightly correlated through TORC1, a decrease in transcription rate of RNA pol I, assayed by a Miller spread, could indirectly explain the reduction in 5S rRNA and will be performed.

4.2.4.2 Nop7 and Ssf1 depletion

It was previously reported that upon Nop7 depletion a switch to the minor pathway, that makes $5.8S_L$-containing ribosomes, occurs [36]. It has also been reported that Nop7 binds to 5'-25S rRNA, and yet its depletion, or that of both Nop7 and Ssf1 simultaneously, does not result in 'de-protection' of this region, as (Table XXI C) [12]. This data supports the existence of an alternative pathway along which at least another RiBi factor that can bind pre-rRNA is

able to ensure the protection of this region and will be likely be found enriched in the Ssf2-containign particles upon Ssf1+Nop7 depletion.

4.2.4.3 Absence of Nop7 and Ssf2 generate a dominant negative mutant with severely impaired cell growth

The effect of Nop7-depletion in the absence of Ssf2 was assayed in *GAL::NOP7/SSF1-PRA/ΔSSF2* cells (Fig. 3.5B lanes 9-12). From what was observed in previous strains, at time 0, Ssf1 should compensate for the absence of Ssf2, and its levels should be increased or at least wild-type. Unexpectedly, Ssf1 protein levels were almost non-detectable at time 0, which suggests that in the absence of Ssf2 and the minor overexpression of Nop7, Ssf1 becomes dispensable. This results therefore implies that there is at least one pathway in which ribosome maturation occurs independent on Ssf1 and Ssf2 and the presence of Nop7. Upon Nop7 depletion, cellular doubling time was of 372min (roughly 6 hours) and Ssf1 levels slightly increased (6 and 16 hours), and could be caused by increased number of cells delayed during formation of the bud tip, where Ssf1 is likely needed [30]. Information of such fluctuations has been overlooked in the literature. Changes in RiBi protein levels of as a response to depletion of another RiBi protein, if available, include only two time points (levels before and after depletion). Moreover, this information is often limited to proteins known to form stable complexes during ribosome biogenesis, as the Nop7/Ytm1/Erb1 complex, while RPs are used as controls [39].

When grown in media repressing the *NOP7* gene, cells showed a dominant negative phenotype for growth: its Dt increased to 372min. As Nop7 depletion can account for doubling the normal Dt, the additional 182min can be explained only by the absence of Ssf2. Therefore, taken together, this indicates that Ssf2 functions in an alternative pathway, independent of Nop7.

4.2.4.3.1 Slow growing cells, fast pre-rRNA processing and aberrant ribosomes

With the exception of modest levels of 35S, 22S, 18S and 5S, no other precursor or mature form of rRNA accumulated, pointing towards unusually fast pre-rRNA processing (Table XXI C). Methylene blue staining detected highly abundant, lower molecular weight

forms of 25S, 18S were undetected with probes targeting their 5' coding regions (5'18S+115bases = probe 008; 5'25S+135 bases = probe 007).

During ribosome biogenesis, Nop7 binds to the 5' region of 25S rRNA[12] The Ssf proteins likely bind to ITS1 and participate in the formation of ITS1-5' 5.8S base pairing structure required to preventing hairpin structure formation [11, 12, 53]. Results therefore suggests that Nop7 and the Ssf pair therefore likely protect 5' ends of 25S and 5.8S rRNA during ribosome biogenesis from 5'→3' degradation and imply that there exists at least one protein which can bind the 5' regions of the 25S in particles devoid of Nop7. Presence of likely 5'trimmed 18S rRNA in Nop7-depleted/SSF2Δ cells also suggest that the Ssf proteins might have a role in stabilising RNA-protein, protein-protein interactions or both in pre-90S particles which will protect the 5' region of 18S rRNA.

Results could reflect that there exists a small, nearly undetectable pool of normal ribosomes while there is a trong accunmulation of pre-rRNA degradation products In the past, pre-rRNA degradation products have been detected upon depletion of RiBi proteins, giving specific degradation patterns but this was not observed in this study (Fig. 3.5D) [92]. Degradation of aberrant pre-rRNA usually occurs very fast and degradation products can be probed upon depletion of exosome components or exonucleases (e.g Rrp17 and Rat1) but neither Nop7, Ssf1 nor Ssf2 are knwon or predicted exonucleases [7, 93]. A scenario in which NOP7-depleted/SSFΔ cells produce aberrant ribosomes which are inefficient in mRNA translation could explain the highly impaired cell growth observed. In either scenario, polysome gradient analysis coupled with RNA analysis of the collected fractions would address these questions.

4.2.5 Nop7/Ssf1, Ssf2 and parallel pathways during ribosome biogenesis

Previously it had been shown that pre-90S processing events can occur via two alternative pathways [31]. However, the study was focused on pre-90S and pre-40S particles, and no study so far has shown whether the LSU can also be processed by alternative pathways. What is known, however, are all the components required to incorporate the 5S

rRNA, which is mediated, as previously mentioned, by Rpf2 and timed to coincide with C_2 processing [17].

Is it possible that early associations dictate the downstream pre-rRNA processing events that will generate $5.8S_S$ or $5.8S_L$-containing ribosomes? This possibility will be explored in this subsection, taking into account the results obtained during this study, and should be further supported by performing additional NB probing, primer extension (ITS1) and MS analysis of the bait proteins for all the strains tested in this study (permissive and restrictive conditions). In some strains, especially in the case of *GAL::NOP7/ΔSSF2/SSF1-PRA*, pulse-chase analysis should be performed.

4.2.5.1 There exists a LSU maturation pathway dependent on Ssf1/Ssf2 heterodimer

As demonstrated in this study, the Ssf proteins associate within similar complexes under normal cellular conditions. This study has also shown that the Ssf proteins cannot fully compensate for the loss of each other, and that this is due to the fact that they do not function along the same but parallel pathways. It is tempting to speculate that the Ssf proteins can only homodimerize, however, Ssf1 is one result in a search for physical and genetic interactions of Ssf2 [30]. Thus, this possibility cannot be ruled out with the available data but it could suggest that Ssf1/Ssf2 heterodimer is relatively rare under normal conditions, since the Ssf1 particle does not contain Ssf2 [54]. *In vitro* studies (solution binding assay) will have to be performed to ultimately explore either possibility.

4.2.5.2 The $5.8S_S$ pathway is mostly Ssf1/Nop7 dependent

Upon Nop7 depletion, cells switch to producing high levels of $5.8S_L$-containing ribosomes, which are normally the result of a less preferred RiBi pathway. Cells lacking both Ssf proteins generate less ribosomes overall, possibly due to a drop in transcription, yet the ratio of $5.8S_S$ to $5.8S_L$ does not change, suggesting that these proteins are involved in events upstream of both pathways leading to the different forms of 5.8SrRNAs.

Early pre-90S processing events can occur via two alternative pathways, one of which is Rrp5 (Noc1/Noc2)/UTP-C dependent [31]. Both Nop7 and Ssf1 proteins most likely follow this pathway as both of their particles (Fig 1.8A) contain Noc1/Noc2 heterodimer and Nop7-containing particles also include Rrp5. From what has been published, and the data obtained during this study, it can be speculated that Nop7 is likely genetically linked to both Ssf proteins but that it is most often found with Ssf1, as Nop7 normally only binds with Ssf1 in its homodimeric form. This scenario would explain why Ssf2 is not part of Nop7 associated complexes [37]. However, even if Ssf2 is not part of the Rrp5-dependent pre-90S pathway, it can, albeit to a lesser extent, be associated with B_{1S} processing through its direct interaction with Rrp15, a protein required for B_{1S} processing, which is also not part of Nop7 associated complexes. Upon Nop7 depletion, both Ssf protein levels drop but are still detectable. It is therefore possible that B_{1S} processing still occurs in these cells through Ssf2-Rrp15-containing particles as well as Ssf1-containing particles. What is certain is that, Nop7-depleted cells are able to successfully protect the 5'ends of rRNA, through a yet unidentified mechanism, as no overly exonucleolytically processed 5' forms of 25S, 18S and 5S rRNAs could be detected.

4.2.5.3 Ssf2 is probably linked to the U3 snoRNP/Bms1-dependent pre-90S pathway

The Rpf2 particle is the only one that has been reported to contain the Ssf2 protein [17]. Why has Ssf2 not been reported in other particles? This could be due to previous detection limitations in MS analysis in addition to the low abundance of the protein. Another reason could be that Ssf2 is involved in the pre-90S pathway, which is U3 snoRNP/Bms1 dependent. Ssf1 and Nop7 particles contain all Noc1/Noc2 and members of the Imp/Brix superfamily (Brx1, Ssf1, Rpf1, and Rpf2) except Imp4 and Ssf2 [51, 52]. As previously mentioned, pre-90S processing events can also occur through a pathway that is U3 snoRNP/Bms1 dependent and requires Imp3 and Imp4 RiBi factors [31]. Imp3 has been reported to recruit U3 RNA on the pre-rRNA and Imp4 (Imp4/Brix family) has been reported to bind to U3 RNA, and promote its release from pre-rRNA [76]. U3-RNA plays a role in correct processing of A_0 to A_2 sites. If Ssf2 is involved in this pathway, then MS analysis of its particle under at least some of the conditions tested during this study should identify U3 snoRNP components or Bms1 as well as

other components usually attributed to pre-90S or early pre-40S maturation. If Ssf2 does belong into this pathway, then it was most likely ruled out as background in pre-90S and pre-40S studies due to its high similarity with Ssf1, which was associated with pre-60S maturation.

4.2.5.4 Ribosome biogenesis devoid of A_3-cluster factors

In the field, some believe that pre-60S maturation is split from pre-40S maturation and others believe that it can be coupled. Results from this study suggest that Nop7/Ssf1 and Ssf2 might play a role in stabilizing the RiBi factors required for 5' protection of 18S, 5.8S and 25S rRNAs and therefore implies that particles exist in which the LSU and SSU RiBi factors are partially stabilizing each other in the pre-90S particle. In one scenario, in which Nop7 is depleted, this stabilizing role might be compensated by particles lacking A_3-cluster ribosomes, as defined by Granneman *et al* (2011). These particles most probably contain Ssf2 and other factors that are able to bind pre-rRNA within the ITS1 and ITS2 regions. These proteins are also stabilizing a second structure later during LSU pre-rRNA processing that will ensure the protection of the 5S rRNA. Upon depletion of both Ssf2 and Nop7, the stabilization role required during both of these cases cannot be efficiently compensated by the presence of Ssf1 alone, and the 5' of the rRNAs become unprotected.

4.2.6 Regulating protein levels

Another aspect of the dynamics of the RiBi proteins is regulation of their protein levels. A qRT-PCR analysis of the mRNA coupled with whole-protein extract analysis could determine on how the cell specifically regulates its protein levels. Overall, this analysis indicates that the cell uses different mechanisms for regulating the levels or a RiBi protein, and those depend on the cellular context.

4.2.6.1 SSF2 is mostly post-transcriptionally regulated

In the *MET::SSF1/SSF2-PRA*, the protein levels of Ssf2 increased but its mRNA levels remained constant (1.052-fold). In the *MET::SSF1/SSF2-PRA/GAL::NOP7* strain, when Ssf1 was depleted and Nop7 protein levels increased, Ssf2 protein levels increased, yet its mRNA levels decreased (0.588-fold). In all other cases studied in the same strain, which is upon Nop7 depletion or Nop7+Ssf1 depletion, the mRNA levels did not significantly change (1.252-fold and 0.906-fold), whilst the protein levels respectively decreased and increased. However, these results were analyzed in triplicate and generated high variability and should therefore be repeated. From the data available, it can be concluded that SSF2 mRNA stability and/or transcription can be altered, depending on the cellular context; Ssf2 protein levels can also be modulated by stabilizing the protein, or changing its translation rate.

4.2.6.2 NOP7 mRNA can be stabilized

In the *MET::SSF1/SSF2-PRA* strain, Nop7 protein levels were not detectable but its mRNA levels were significantly increased (1.72-fold). Upon Ssf1 depletion in the *MET::SSF1/SSF2-PRA/GAL::NOP7* strain, there was an increase in Nop7 mRNA levels (2.161X) and protein, which could also be attributed to its expression being driven from a Gal-promoter. In the *MET::SSF1/ΔSSF2/CIC1-PRA* strain, endogenous Nop7 protein levels were not detectable although its mRNA levels significantly increased (1.386-fold). The *MET::SSF1/ΔSSF2/NOP7-PRA* strain further corroborated that Nop7 protein levels decreases even if its mRNA levels increased (4.294-fold). Because the NOP7 gene was under the control of a regulatable promoter and the mRNA levels increased, this data suggests that Nop7 mRNA transcription rate is not altered in response to a stress, but its mRNA becomes stabilized. This explains the increase of NOP7 mRNA in all cases. Because Nop7 protein usually decreased, either the protein is degraded faster or is less translated. Why its mRNA is not targeted for degradation, has to be determined.

4.2.6.3 Ssf1 regulation needs to be further studied

Ssf1 mRNA levels were assayed in two strains. In the first strain, there was no change in Ssf1 mRNA (1.025-fold) and protein levels upon Nop7 depletion (*MET::SSF1/SSF2-PRA/GAL::NOP7*), when Ssf2 was present. In the second strain, Ssf2 protein was completely absent, Nop7 was depleted and the Ssf1 gene was under its endogenous promoter (*GAL::NOP7/SSF1-PRA/ΔSSF2*). Under these conditions, Ssf1 protein levels fluctuated significantly (Table XXIC). At the last timepoint observed, Ssf1 protein levels were nearly non-detectable, whilst its mRNA levels were increased (1.5-fold). Because Ssf1 protein levels unexpectedly fluctuated in the absence of Ssf2, its mRNA levels should be assayed under the same conditions but in the presence of Ssf2 protein (*GAL::NOP7/SSF1-PRA*) before drawing any conclusions.

4.3 Dissecting structural changes in Ssf1, Ssf2 and Nop7

Using the buffer for complex purification detailed in (80), cleavage patterns of the Ssf1, Ssf2 and Nop7 proteins when they are in complex with other RiBi factors have been identified in this study. The exposed regions corresponded to regions located between domains (Fig. 3.7A and B). The Ssf proteins show a similar pattern, consistent with the finding that they are most likely associated with similar sets of proteins (Section 3.2).

Because of the nature of the proteins and the strength of the association it forms with other RiBi proteins, the stringency of the buffer required to recover a RiBi protein alone changes and needs to be individually validated. The ssAP buffer condition that is stringent enough to completely disrupt complexes formed by the Ssf proteins (20mM Hepes pH 7.4, 300mM NaCitrate, 0.5% Triton, 0.1% Tween 20, 1:100 solution P) has been identified in this study and will allow to detect possible changes in Ssf1 and Ssf2 protein folding when they are alone. Nop7 forms a tight trimeric sub-complex with Erb1 and Ytm1. The buffers detailed in Section 3.2 were not stringent enough to recover Nop7-PrA as a single protein (data not shown). Further investigation is necessary to identify a ssAP buffer stringent enough to completely disrupt Nop7-PrA pre-rRNP complexes.

It is possible to recover endogenously-folded bait protein alone, without associated proteins, by coupling ssAP with a highly stringent buffer. Alternatively, association with endogenous Nop7 protein recovered in this fashion could be tested using recombinant Ssf1 or Ssf2 protein, and if an interaction is detected, limited protease accessibility assay on this complex could provide further information on changes in Nop7 protein folding upon binding with the Ssf proteins. The same could be performed using Ssf1 or Ssf2 as bait proteins and recombinant Nop7.

4.4 Nop7 likely interacts directly with Ssf1

Previously it has been reported that Ssf1 and Nop7 directly interact with each other during *Xenopus laevis* pronephros development, independently of ribosome biogenesis (Ssf2 has not been tested) [47]. The possibility of them physically interacting with each other during yeast ribosome biogenesis was supported by the accumulation of a common, aberrant pre-rRNA (26S) upon their independent depletion, suggesting premature C_2 cleavage in both cases (Fig. 1.7) [36, 54].

Several aspects of the Ssf proteins need to be validated by *in vitro* studies, such as their capacity to bind rRNA through their family conserved ó70-like motif, and their capacity to homo- and/or heterodimerize with each other, through their predicted homo/hetero-binding domain (Fig. 1.4). Furthermore, the potential interaction of Ssf1 with Nop7 also needs to be validated *in vitro.* Given the high similarity to Ssf1, a potential interaction of Ssf2 with Nop7 also needs to be addressed. During this study, the plasmids required to generate recombinant proteins were cloned and the conditions for the expression of recombinant Nop7, Ssf1 and Ssf2 were optimized (Table XI and Figs. 2.3-2.4) and will allow *in vitro* solution binding studies to test for these protein-protein interactions. The capacity of the Ssf proteins to bind RNA will also be tested since they are believed to protect, though binding, the 5' coding region of 5.8S during $27SA_3$ 5'→3' trimming of ITS1, thus slowing the activity of the exonuclease (Rat1 or Rrp17) [7, 12, 53].

5 Conclusion

The Ssf1 and Ssf2 proteins have been implied to fulfil redundant functions in the cell and during ribosome biogenesis. This work supports this observation to some extent, as it highlights that, under normal conditions, both paralogs can make identical pre-rRNP particles. However, analysis of the stability of these particles using buffers of different stringency during ssAP suggests that Ssf2-PrA containing complexes may be more stable. Disruption of the affinity purified particles using higher stringency buffers revealed that at least three proteins, likely Dbp9, Drs1 and Nog1 strongly affinity purify with the bait proteins and likely represent a subcomplex.

Although cellular levels of Ssf2-PrA increased upon SSF1-depletion, this works provides evidence that the Ssf proteins cannot entirely compensate for the loss of each other, as pre-rRNA processing was mildly delayed in SSF1-depleted cells. The pre-rRNA processing defects previously reported for both Nop7-depleted and SSF1-depleted/SSF2Δ cells were corroborated [36, 54]. This work also provides evidence that Ssf1 and Ssf2 levels are correlated to the levels of Nop7 and are genetically linked. The Ssf1 and Nop7 proteins might be required, under normal conditions, in the major pre-rRNA maturation pathway, which is further reinforced by the fact that they are found in particles associated with tagged Nop7 and Ssf1. Nop7 depletion, when Ssf1 was overexpressed, and generated a pre-rRNA depletion phenotype reminiscent of the depletion phenotype observed in the absence of both Ssf proteins. Simultaneous depletion of Nop7 and Ssf1 in the presence of Ssf2 also and generated less ribosomes, as shown by Northern blot analysis. The pre-rRNA depletion phenotype observed here was reminiscent of the one observed upon depletion of both Ssf proteins, in which transcription and early processing appears delayed.

In clear contrast, simultaneous absence of Nop7 and Ssf2 in the presence of Ssf1 showed a dominant negative growth phenotype with a strong accumulation of what appears to be overly exonucleolytically processed 5' forms of 25S, 18S and 5S rRNAs and no 5.8S rRNA. To this date, such depletion phenotype has never been reported and implies that there exists an early particle that requires the presence of Nop7/Ssf1 or Ssf2 to correctly stabilize RiBi proteins required for 5' protection of rRNA coding regions. In fact is was previously suggested that Ssf1 would fulfil such a role for 25S and 5.8S, however it appears that Ssf1 alone is not sufficient for the protection of 5'ends of pre-rRNAs. These results also imply that

under these conditions, incorporation of 5S rRNA in the pre-60S particle is possible but that this rRNA becomes unprotected and at least partially degraded, a phenotype never previously observed. Further analysis of the Northern blots generated as well as additional assays will allow a more detailed analysis of this phenotype and its origins. Moreover, performing ssAP coupled with MS/MS will allow screening for any pre-rRNP particle changes in all the strains and conditions tested in this study.

While cellular Ssf2 protein levels varied, its mRNA levels remained relatively stable in four of the five conditions it was tested, which suggests that it is mostly post-transcriptionally regulated. This clearly contrasts with the cellular regulation of Nop7 protein. In three of the four cases studied, Nop7 protein levels appeared decreased and in the fourth case, the gene was steadily transcribed under the Gal1 promoter and WB analysis showed a clear increase in Nop7 protein upon Ssf1 depletion. In the four cases, Nop7 mRNA increased, which suggest that NOP7 mRNA stabilisation.

Taken together, these results strongly suggest that the Ssf paralogs function in fact along separate parallel maturation pathways during yeast ribosome biogenesis, and are not, as previously thought, interchangeable. These findings highlight the relevance to further characterise these proteins *in vitro*. RNA binding and solution binding assays can be performed in the future, as recombinant proteins have been generated in this study. As other paralogs, such as for example Fpr3 and Fpr4, are believed to play also a functionally redundant role during ribosome biogenesis, results presented in this study raise the question as to whether these proteins as well as others are truly functional homologues, or fulfil functional different tasks along different branches of the pathway or under certain circumstances. Better understanding the binding partners of such paralogs could provide a good starting point for new studies. In ribosome biogenesis of higher eukaryotes there are 74 RiBi proteins which have no homolog in yeast and which include several paralogs or proteins submitted to alternative splicing [(94)]. The present study suggests that these paralogs can be used as tools to gain better understanding of the additional layers of complexity observed during ribosome biogenesis in these cells and may finally lead to an understanding of why so many proteins are involved in this intricate pathway.

Bibliography

1. Du YC, Stillman B. Yph1p, an ORC-interacting protein: potential links between cell proliferation control, DNA replication, and ribosome biogenesis. Cell. 2002;109(7):835-48. Epub 2002/07/12.
2. Dez C, Tollervey D. Ribosome synthesis meets the cell cycle. Current opinion in microbiology. 2004;7(6):631-7. Epub 2004/11/24.
3. Albert B, Leger-Silvestre I, Normand C, Ostermaier MK, Perez-Fernandez J, Panov KI, et al. RNA polymerase I-specific subunits promote polymerase clustering to enhance the rRNA gene transcription cycle. The Journal of cell biology. 2011;192(2):277-93. Epub 2011/01/26.
4. Venema J, Tollervey D. Ribosome synthesis in Saccharomyces cerevisiae. Annual review of genetics. 1999;33:261-311. Epub 2000/02/26.
5. Elela SA, Igel H, Ares M, Jr. RNase III cleaves eukaryotic preribosomal RNA at a U3 snoRNP-dependent site. Cell. 1996;85(1):115-24. Epub 1996/04/05.
6. Lindahl L, Bommankanti A, Li X, Hayden L, Jones A, Khan M, et al. RNase MRP is required for entry of 35S precursor rRNA into the canonical processing pathway. RNA. 2009;15(7):1407-16. Epub 2009/05/26.
7. Oeffinger M, Zenklusen D, Ferguson A, Wei KE, El Hage A, Tollervey D, et al. Rrp17p is a eukaryotic exonuclease required for 5' end processing of Pre-60S ribosomal RNA. Molecular cell. 2009;36(5):768-81. Epub 2009/12/17.
8. Sloan KE, Mattijssen S, Lebaron S, Tollervey D, Pruijn GJ, Watkins NJ. Both endonucleolytic and exonucleolytic cleavage mediate ITS1 removal during human ribosomal RNA processing. The Journal of cell biology. 2013;200(5):577-88. Epub 2013/02/27.
9. Granneman S, Baserga SJ. Ribosome biogenesis: of knobs and RNA processing. Experimental Cell Research. 2004;296(1):43-50.
10. Gallagher JE, Dunbar DA, Granneman S, Mitchell BM, Osheim Y, Beyer AL, et al. RNA polymerase I transcription and pre-rRNA processing are linked by specific SSU processome components. Genes & development. 2004;18(20):2506-17. Epub 2004/10/19.
11. Yeh LC, Thweatt R, Lee JC. Internal transcribed spacer 1 of the yeast precursor ribosomal RNA. Higher order structure and common structural motifs. Biochemistry. 1990;29(25):5911-8. Epub 1990/06/26.
12. Granneman S, Petfalski E, Tollervey D. A cluster of ribosome synthesis factors regulate pre-rRNA folding and 5.8S rRNA maturation by the Rat1 exonuclease. The EMBO journal. 2011;30(19):4006-19. Epub 2011/08/04.
13. Henry Y, Wood H, Morrissey JP, Petfalski E, Kearsey S, Tollervey D. The 5' end of yeast 5.8S rRNA is generated by exonucleases from an upstream cleavage site. The EMBO journal. 1994;13(10):2452-63. Epub 1994/05/15.
14. Cote CA, Peculis BA. Role of the ITS2-proximal stem and evidence for indirect recognition of processing sites in pre-rRNA processing in yeast. Nucleic acids research. 2001;29(10):2106-16. Epub 2001/05/23.
15. van Nues RW, Rientjes JM, Morre SA, Mollee E, Planta RJ, Venema J, et al. Evolutionarily conserved structural elements are critical for processing of Internal Transcribed

Spacer 2 from Saccharomyces cerevisiae precursor ribosomal RNA. Journal of molecular biology. 1995;250(1):24-36. Epub 1995/06/30.
16. Dembowski JA, Ramesh M, McManus CJ, Woolford JL, Jr. Identification of the binding site of Rlp7 on assembling 60S ribosomal subunits in Saccharomyces cerevisiae. RNA. 2013. Epub 2013/10/17.
17. Zhang J, Harnpicharnchai P, Jakovljevic J, Tang L, Guo Y, Oeffinger M, et al. Assembly factors Rpf2 and Rrs1 recruit 5S rRNA and ribosomal proteins rpL5 and rpL11 into nascent ribosomes. Genes & development. 2007;21(20):2580-92. Epub 2007/10/17.
18. Lebreton A, Saveanu C, Decourty L, Rain JC, Jacquier A, Fromont-Racine M. A functional network involved in the recycling of nucleocytoplasmic pre-60S factors. The Journal of cell biology. 2006;173(3):349-60. Epub 2006/05/03.
19. Claypool JA, French SL, Johzuka K, Eliason K, Vu L, Dodd JA, et al. Tor pathway regulates Rrn3p-dependent recruitment of yeast RNA polymerase I to the promoter but does not participate in alteration of the number of active genes. Molecular biology of the cell. 2004;15(2):946-56. Epub 2003/11/05.
20. Wittner M, Hamperl S, Stockl U, Seufert W, Tschochner H, Milkereit P, et al. Establishment and maintenance of alternative chromatin states at a multicopy gene locus. Cell. 2011;145(4):543-54. Epub 2011/05/14.
21. Keener J, Josaitis CA, Dodd JA, Nomura M. Reconstitution of yeast RNA polymerase I transcription in vitro from purified components. TATA-binding protein is not required for basal transcription. The Journal of biological chemistry. 1998;273(50):33795-802. Epub 1998/12/05.
22. Beckouet F, Labarre-Mariotte S, Albert B, Imazawa Y, Werner M, Gadal O, et al. Two RNA polymerase I subunits control the binding and release of Rrn3 during transcription. Molecular and cellular biology. 2008;28(5):1596-605. Epub 2007/12/19.
23. Aprikian P, Moorefield B, Reeder RH. New model for the yeast RNA polymerase I transcription cycle. Molecular and cellular biology. 2001;21(15):4847-55. Epub 2001/07/05.
24. Albert B, Perez-Fernandez J, Leger-Silvestre I, Gadal O. Regulation of ribosomal RNA production by RNA polymerase I: does elongation come first? Genetics research international. 2012;2012:276948. Epub 2012/05/09.
25. Perez-Fernandez J, Martin-Marcos P, Dosil M. Elucidation of the assembly events required for the recruitment of Utp20, Imp4 and Bms1 onto nascent pre-ribosomes. Nucleic acids research. 2011;39(18):8105-21. Epub 2011/07/05.
26. Jack K, Bellodi C, Landry DM, Niederer RO, Meskauskas A, Musalgaonkar S, et al. rRNA pseudouridylation defects affect ribosomal ligand binding and translational fidelity from yeast to human cells. Molecular cell. 2011;44(4):660-6. Epub 2011/11/22.
27. Nguyen-Lefebvre AT, Leprun G, Morin V, Vinuelas J, Coute Y, Madjar JJ, et al. V-erbA generates ribosomes devoid of RPL11 and regulates translational activity in avian erythroid progenitors. Oncogene. 2013. Epub 2013/04/09.
28. Komili S, Farny NG, Roth FP, Silver PA. Functional specificity among ribosomal proteins regulates gene expression. Cell. 2007;131(3):557-71. Epub 2007/11/06.
29. Zebarjadian Y, King T, Fournier MJ, Clarke L, Carbon J. Point mutations in yeast CBF5 can abolish in vivo pseudouridylation of rRNA. Molecular and cellular biology. 1999;19(11):7461-72. Epub 1999/10/19.

30. Cherry JM, Hong EL, Amundsen C, Balakrishnan R, Binkley G, Chan ET, et al. Saccharomyces Genome Database: the genomics resource of budding yeast. Nucleic acids research. 2012;40(Database issue):D700-5. Epub 2011/11/24.
31. Perez-Fernandez J, Roman A, De Las Rivas J, Bustelo XR, Dosil M. The 90S preribosome is a multimodular structure that is assembled through a hierarchical mechanism. Molecular and cellular biology. 2007;27(15):5414-29. Epub 2007/05/23.
32. Warner JR. Nascent ribosomes. Cell. 2001;107(2):133-6. Epub 2001/10/24.
33. Henras AK, Soudet J, Gerus M, Lebaron S, Caizergues-Ferrer M, Mougin A, et al. The post-transcriptional steps of eukaryotic ribosome biogenesis. Cellular and molecular life sciences : CMLS. 2008;65(15):2334-59. Epub 2008/04/15.
34. Kaberdina AC, Szaflarski W, Nierhaus KH, Moll I. An unexpected type of ribosomes induced by kasugamycin: a look into ancestral times of protein synthesis? Molecular cell. 2009;33(2):227-36. Epub 2009/02/04.
35. Kinoshita Y, Jarell AD, Flaman JM, Foltz G, Schuster J, Sopher BL, et al. Pescadillo, a novel cell cycle regulatory protein abnormally expressed in malignant cells. The Journal of biological chemistry. 2001;276(9):6656-65. Epub 2000/11/10.
36. Oeffinger M, Leung A, Lamond A, Tollervey D. Yeast Pescadillo is required for multiple activities during 60S ribosomal subunit synthesis. RNA. 2002;8(5):626-36. Epub 2002/05/23.
37. Oeffinger M. Nop7-associated proteins during log phase. Unpublished; 2012.
38. Krogan NJ, Peng WT, Cagney G, Robinson MD, Haw R, Zhong G, et al. High-definition macromolecular composition of yeast RNA-processing complexes. Molecular cell. 2004;13(2):225-39. Epub 2004/02/05.
39. Tang L, Sahasranaman A, Jakovljevic J, Schleifman E, Woolford JL, Jr. Interactions among Ytm1, Erb1, and Nop7 required for assembly of the Nop7-subcomplex in yeast preribosomes. Molecular biology of the cell. 2008;19(7):2844-56. Epub 2008/05/02.
40. Adams CC, Jakovljevic J, Roman J, Harnpicharnchai P, Woolford JL, Jr. Saccharomyces cerevisiae nucleolar protein Nop7p is necessary for biogenesis of 60S ribosomal subunits. RNA. 2002;8(2):150-65. Epub 2002/03/26.
41. Xie W, Feng Q, Su Y, Dong B, Wu J, Meng L, et al. Transcriptional regulation of PES1 expression by c-Jun in colon cancer. PloS one. 2012;7(7):e42253. Epub 2012/08/04.
42. Cheng L, Li J, Han Y, Lin J, Niu C, Zhou Z, et al. PES1 promotes breast cancer by differentially regulating ERalpha and ERbeta. The Journal of clinical investigation. 2012;122(8):2857-70. Epub 2012/07/24.
43. Li J, Yu L, Zhang H, Wu J, Yuan J, Li X, et al. Down-regulation of pescadillo inhibits proliferation and tumorigenicity of breast cancer cells. Cancer science. 2009;100(12):2255-60. Epub 2009/09/22.
44. Xie W, Qu L, Meng L, Liu C, Wu J, Shou C. PES1 regulates sensitivity of colorectal cancer cells to anticancer drugs. Biochemical and biophysical research communications. 2013;431(3):460-5. Epub 2013/01/22.
45. Bork P, Hofmann K, Bucher P, Neuwald AF, Altschul SF, Koonin EV. A superfamily of conserved domains in DNA damage-responsive cell cycle checkpoint proteins. FASEB journal : official publication of the Federation of American Societies for Experimental Biology. 1997;11(1):68-76. Epub 1997/01/01.

46. Matsumoto S, Yahara I. YTM1, a suppressor of beta-tubulin mutation, encodes a novel microtubule-interacting protein and is essential for G1/S transition in Saccharomyces cerevisiae. Unpublished1997.
47. Tecza A, Bugner V, Kuhl M, Kuhl SJ. Pescadillo homologue 1 and Peter Pan function during Xenopus laevis pronephros development. Biology of the cell / under the auspices of the European Cell Biology Organization. 2011;103(10):483-98. Epub 2011/07/21.
48. Holzel M, Rohrmoser M, Schlee M, Grimm T, Harasim T, Malamoussi A, et al. Mammalian WDR12 is a novel member of the Pes1-Bop1 complex and is required for ribosome biogenesis and cell proliferation. The Journal of cell biology. 2005;170(3):367-78. Epub 2005/07/27.
49. Yu Y, Hirsch JP. An essential gene pair in Saccharomyces cerevisiae with a potential role in mating. DNA and cell biology. 1995;14(5):411-8. Epub 1995/05/01.
50. Kim J, Hirsch JP. A nucleolar protein that affects mating efficiency in Saccharomyces cerevisiae by altering the morphological response to pheromone. Genetics. 1998;149(2):795-805. Epub 1998/06/11.
51. Bogengruber E, Briza P, Doppler E, Wimmer H, Koller L, Fasiolo F, et al. Functional analysis in yeast of the Brix protein superfamily involved in the biogenesis of ribosomes. FEMS yeast research. 2003;3(1):35-43. Epub 2003/04/19.
52. Eisenhaber F, Wechselberger C, Kreil G. The Brix domain protein family -- a key to the ribosomal biogenesis pathway? Trends Biochem Sci. 2001;26(6):345-7. Epub 2001/06/19.
53. Wehner KA, Baserga SJ. The sigma(70)-like motif: a eukaryotic RNA binding domain unique to a superfamily of proteins required for ribosome biogenesis. Molecular cell. 2002;9(2):329-39. Epub 2002/02/28.
54. Fatica A, Cronshaw AD, Dlakic M, Tollervey D. Ssf1p prevents premature processing of an early pre-60S ribosomal particle. Molecular cell. 2002;9(2):341-51. Epub 2002/02/28.
55. Chatr-Aryamontri A, Breitkreutz BJ, Heinicke S, Boucher L, Winter A, Stark C, et al. The BioGRID interaction database: 2013 update. Nucleic acids research. 2013;41(Database issue):D816-23. Epub 2012/12/04.
56. Kaluarachchi Duffy S, Friesen H, Baryshnikova A, Lambert JP, Chong YT, Figeys D, et al. Exploring the yeast acetylome using functional genomics. Cell. 2012;149(4):936-48. Epub 2012/05/15.
57. Gray JV, Petsko GA, Johnston GC, Ringe D, Singer RA, Werner-Washburne M. "Sleeping beauty": quiescence in Saccharomyces cerevisiae. Microbiology and molecular biology reviews : MMBR. 2004;68(2):187-206. Epub 2004/06/10.
58. Martinez MJ, Roy S, Archuletta AB, Wentzell PD, Anna-Arriola SS, Rodriguez AL, et al. Genomic analysis of stationary-phase and exit in Saccharomyces cerevisiae: gene expression and identification of novel essential genes. Molecular biology of the cell. 2004;15(12):5295-305. Epub 2004/10/01.
59. Catala M, Tremblay M, Samson E, Conconi A, Abou Elela S. Deletion of Rnt1p alters the proportion of open versus closed rRNA gene repeats in yeast. Molecular and cellular biology. 2008;28(2):619-29. Epub 2007/11/10.
60. Wang Y, Zhang X, Zhang H, Lu Y, Huang H, Dong X, et al. Coiled-coil networking shapes cell molecular machinery. Molecular biology of the cell. 2012;23(19):3911-22. Epub 2012/08/10.

61. Suarez-Huerta N, Boeynaems JM, Communi D. Cloning, genomic organization, and tissue distribution of human Ssf-1. Biochemical and biophysical research communications. 2000;275(1):37-42. Epub 2000/08/17.
62. Bugner V, Tecza A, Gessert S, Kuhl M. Peter Pan functions independently of its role in ribosome biogenesis during early eye and craniofacial cartilage development in Xenopus laevis. Development. 2011;138(11):2369-78. Epub 2011/05/12.
63. Communi D, Suarez-Huerta N, Dussossoy D, Savi P, Boeynaems JM. Cotranscription and intergenic splicing of human P2Y11 and SSF1 genes. The Journal of biological chemistry. 2001;276(19):16561-6. Epub 2001/03/30.
64. Naji S, Ambrus G, Cimermancic P, Reyes JR, Johnson JR, Filbrandt R, et al. Host cell interactome of HIV-1 Rev includes RNA helicases involved in multiple facets of virus production. Molecular & cellular proteomics : MCP. 2012;11(4):M111 015313. Epub 2011/12/17.
65. Askjaer P, Jensen TH, Nilsson J, Englmeier L, Kjems J. The specificity of the CRM1-Rev nuclear export signal interaction is mediated by RanGTP. The Journal of biological chemistry. 1998;273(50):33414-22. Epub 1998/12/05.
66. Daugeron MC, Kressler D, Linder P. Dbp9p, a putative ATP-dependent RNA helicase involved in 60S-ribosomal-subunit biogenesis, functionally interacts with Dbp6p. RNA. 2001;7(9):1317-34. Epub 2001/09/22.
67. Gavin AC, Bosche M, Krause R, Grandi P, Marzioch M, Bauer A, et al. Functional organization of the yeast proteome by systematic analysis of protein complexes. Nature. 2002;415(6868):141-7. Epub 2002/01/24.
68. Collins SR, Miller KM, Maas NL, Roguev A, Fillingham J, Chu CS, et al. Functional dissection of protein complexes involved in yeast chromosome biology using a genetic interaction map. Nature. 2007;446(7137):806-10. Epub 2007/02/23.
69. Wilmes GM, Bergkessel M, Bandyopadhyay S, Shales M, Braberg H, Cagney G, et al. A genetic interaction map of RNA-processing factors reveals links between Sem1/Dss1-containing complexes and mRNA export and splicing. Molecular cell. 2008;32(5):735-46. Epub 2008/12/09.
70. Gilmore JM, Sardiu ME, Venkatesh S, Stutzman B, Peak A, Seidel CW, et al. Characterization of a highly conserved histone related protein, Ydl156w, and its functional associations using quantitative proteomic analyses. Molecular & cellular proteomics : MCP. 2012;11(4):M111 011544. Epub 2011/12/27.
71. Costanzo M, Baryshnikova A, Bellay J, Kim Y, Spear ED, Sevier CS, et al. The genetic landscape of a cell. Science. 2010;327(5964):425-31. Epub 2010/01/23.
72. Kushnirov VV. Rapid and reliable protein extraction from yeast. Yeast. 2000;16(9):857-60. Epub 2000/06/22.
73. Bellemer C, Chabosseau P, Gallardo F, Gleizes PE, Stahl G. Genetic interactions show the importance of rRNA modification machinery for the role of Rps15p during ribosome biogenesis in S. cerevisiae. PloS one. 2010;5(5):e10472. Epub 2010/05/11.
74. Mansour FH, Pestov DG. Separation of long RNA by agarose-formaldehyde gel electrophoresis. Analytical biochemistry. 2013;441(1):18-20. Epub 2013/06/27.
75. Ying BW, Fourmy D, Yoshizawa S. Substitution of the use of radioactivity by fluorescence for biochemical studies of RNA. RNA. 2007;13(11):2042-50. Epub 2007/09/13.

76. Longtine MS, McKenzie A, 3rd, Demarini DJ, Shah NG, Wach A, Brachat A, et al. Additional modules for versatile and economical PCR-based gene deletion and modification in Saccharomyces cerevisiae. Yeast. 1998;14(10):953-61. Epub 1998/08/26.
77. Janke C, Magiera MM, Rathfelder N, Taxis C, Reber S, Maekawa H, et al. A versatile toolbox for PCR-based tagging of yeast genes: new fluorescent proteins, more markers and promoter substitution cassettes. Yeast. 2004;21(11):947-62. Epub 2004/08/31.
78. Oeffinger M, Wei KE, Rogers R, DeGrasse JA, Chait BT, Aitchison JD, et al. Comprehensive analysis of diverse ribonucleoprotein complexes. Nature methods. 2007;4(11):951-6. Epub 2007/10/09.
79. Zhang Y, Cremer PS. Interactions between macromolecules and ions: The Hofmeister series. Current opinion in chemical biology. 2006;10(6):658-63. Epub 2006/10/13.
80. Dokudovskaya S, Williams R, Devos D, Sali A, Chait BT, Rout MP. Protease accessibility laddering: a proteomic tool for probing protein structure. Structure. 2006;14(4):653-60. Epub 2006/04/18.
81. Teste MA, Duquenne M, Francois JM, Parrou JL. Validation of reference genes for quantitative expression analysis by real-time RT-PCR in Saccharomyces cerevisiae. BMC molecular biology. 2009;10:99. Epub 2009/10/31.
82. Bondos SE, Bicknell A. Detection and prevention of protein aggregation before, during, and after purification. Analytical biochemistry. 2003;316(2):223-31. Epub 2003/04/25.
83. Damodaran S, Kinsella JE. Dissociation of nucleoprotein complexes by chaotropic salts. FEBS letters. 1983;158(1):53-7. Epub 1983/07/11.
84. Meyer AE, Hoover LA, Craig EA. The cytosolic J-protein, Jjj1, and Rei1 function in the removal of the pre-60 S subunit factor Arx1. The Journal of biological chemistry. 2010;285(2):961-8. Epub 2009/11/11.
85. Kressler D, Hurt E, Bassler J. Driving ribosome assembly. Biochimica et biophysica acta. 2010;1803(6):673-83. Epub 2009/11/03.
86. Milkereit P, Gadal O, Podtelejnikov A, Trumtel S, Gas N, Petfalski E, et al. Maturation and intranuclear transport of pre-ribosomes requires Noc proteins. Cell. 2001;105(4):499-509. Epub 2001/05/24.
87. Underbakke ES, Zhu Y, Kiessling LL. Protein footprinting in a complex milieu: identifying the interaction surfaces of the chemotaxis adaptor protein CheW. Journal of molecular biology. 2011;409(4):483-95. Epub 2011/04/06.
88. Fernandez-Martinez J, Phillips J, Sekedat MD, Diaz-Avalos R, Velazquez-Muriel J, Franke JD, et al. Structure-function mapping of a heptameric module in the nuclear pore complex. The Journal of cell biology. 2012;196(4):419-34. Epub 2012/02/15.
89. Dokudovskaya S, Waharte F, Schlessinger A, Pieper U, Devos DP, Cristea IM, et al. A conserved coatomer-related complex containing Sec13 and Seh1 dynamically associates with the vacuole in Saccharomyces cerevisiae. Molecular & cellular proteomics : MCP. 2011;10(6):M110 006478. Epub 2011/04/02.
90. Krogan NJ, Cagney G, Yu H, Zhong G, Guo X, Ignatchenko A, et al. Global landscape of protein complexes in the yeast Saccharomyces cerevisiae. Nature. 2006;440(7084):637-43. Epub 2006/03/24.
91. Venema J, Vos HR, Faber AW, van Venrooij WJ, Raue HA. Yeast Rrp9p is an evolutionarily conserved U3 snoRNP protein essential for early pre-rRNA processing cleavages and requires box C for its association. RNA. 2000;6(11):1660-71. Epub 2000/12/06.

92. Kufel J, Allmang C, Petfalski E, Beggs J, Tollervey D. Lsm Proteins are required for normal processing and stability of ribosomal RNAs. The Journal of biological chemistry. 2003;278(4):2147-56. Epub 2002/11/20.
93. Allmang C, Mitchell P, Petfalski E, Tollervey D. Degradation of ribosomal RNA precursors by the exosome. Nucleic acids research. 2000;28(8):1684-91. Epub 2000/03/29.
94. Tafforeau L, Zorbas C, Langhendries JL, Mullineux ST, Stamatopoulou V, Mullier R, et al. The Complexity of Human Ribosome Biogenesis Revealed by Systematic Nucleolar Screening of Pre-rRNA Processing Factors. Molecular cell. 2013;51(4):539-51. Epub 2013/08/27.